Characterizing Walking Variability in the Real World Using Wearable Sensors

by

Loubna Baroudi

A dissertation submitted in partial fulfillment
of the requirements for the degree of
Doctor of Philosophy
(Mechanical Engineering)
in the University of Michigan
2023

Doctoral Committee:

Professor Kira Barton, Co-Chair
Associate Professor K. Alex Shorter, Co-Chair
Assistant Professor Stephen M. Cain, West Virginia University
Professor Natalie Colabianchi
Associate Professor Mark W. Newman

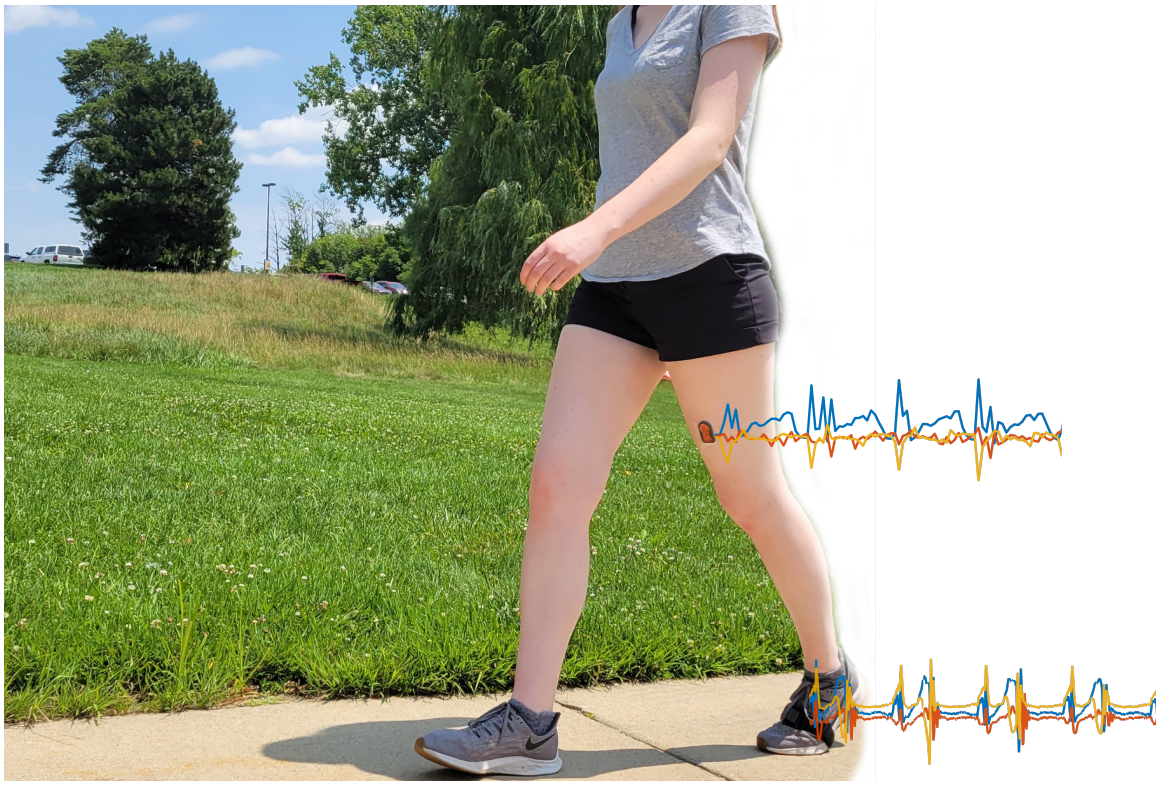

Loubna Baroudi
lbaroudi@umich.edu
ORCID iD: 0000-0002-3065-6196

© Loubna Baroudi 2023

DEDICATION

To my family.

ACKNOWLEDGMENTS

My journey to the University of Michigan started with a rejection email, to which I replied. I asked for advice, with the idea that I would try to apply again the following year. To my surprise, the chair of the department at the time reviewed my application and changed my admission letter. And just like that, with a one-sentence email, I was going to move from Paris to Ann Arbor.

When I arrived in Michigan, I had never done research but was curious about it. There were many emails getting sent out about research opportunities and I reached out to Stephen Cain. After we met, he offered me the opportunity to work on a project with two other professors: Alex Shorter and Kira Barton. This is where my acknowledgments should start. I thank Stephen for trusting me and bringing me onto this project that I have grown to love. I have learned so much from you and I always looked up to you as being a great researcher. I am grateful that you stayed by my side even when you left for another university. Alex, I have always been fascinated by the number of research ideas you have. Your mind is incredibly creative and I have always tried to be inspired in that way. Most importantly, you care about your students. I know that you were always making sure I was having fun and I was being proud of myself. Kira, you were the one who sat me down and convinced me to do a Ph.D. You are a strong woman who inspires me to have a great career and go for the things I want. You have always brought a unique perspective to the different projects we have worked on. Overall, having the three of you as my advisors has made my experience a million times richer, and I thank you for that. I also thank Mark Newman for being part of most of the projects I have worked on and always giving strong feedback. It was great to have you be part of my committee. Finally, I thank Natalie Colabianchi for being on my committee. You have a great eye for detail and I am grateful that you took the time to help me make my dissertation work better.

During these five years, I was part of a great lab and I learned about so many different research topics (mostly about e-jet printing...). It was great to share my time and space with amazing lab mates. Outside of the lab, I also had another advisor/instructor, James Power. You trained me to become a great pilot, and it is thanks to you that I got my license and grew to love aviation. I thank all the people who climbed on the tiny club airplanes with me and trusted me to take them up in the Michigan sky. I made many friends here that made my experience so incredible. I also managed to keep many friends back home, and I am grateful they kept up with me, even 4,000mi away.

I met the love of my life here, Henry. I never thought when I landed in Michigan in 2018, that I would meet someone like you two years later. Our adventures are only starting but they have been so fantastic already. There is nothing like coming back home to you and Stassi. Even in the hard times, I knew that I had succeeded in one thing by being with you. Orchard street will always be the place you asked me to marry you. I am sad to leave our home, but I am more excited about the idea of finding a new one with you soon. In a way, you and your family are my home here. Your family has welcomed me in the warmest way, and my love for them is ever-growing.

Finally, I want to thank my family. Last year, Nayl was born and it is like the greatest ray of sunshine entered in our home and hearts. Marwan and Nabil, I am proud to be your little sister. You have been so supportive of my research and there was nothing like coming back to France after not seeing you for a while. Maman, je me rappellerai toujours du jour où on s'est quitté à l'aéroport. On a beaucoup pleuré... On s'est appelé tous les jours depuis que je suis partie. Tu as toujours été près de moi, ta voix au téléphone est l'un des meilleurs moments de ma journée. Merci d'être une Maman incroyable. Papa, you have been another advisor to me. Following every single one of my projects, giving me advice, and always being so pragmatic about the things that I found difficult. You have inspired me to be a great researcher and I hope you are proud I followed in your footsteps. I love you all.

TABLE OF CONTENTS

DEDICATION ii

ACKNOWLEDGMENTS iii

LIST OF FIGURES viii

LIST OF TABLES xiii

LIST OF APPENDICES xv

LIST OF ACRONYMS xvi

ABSTRACT xvii

CHAPTER

1 Introduction 1

1.1 Motivation & Background 1
1.1.1 Walking for Health 1
1.1.2 Walking as Measured in the Laboratory Setting 2
1.1.3 Walking as Measured in the Real World 3
1.1.4 Measuring Real-world Context 4
1.2 Dissertation Contributions 6
1.2.1 Aim 1: Walking economy in the real world 6
1.2.2 Aim 2: Estimating and characterizing walking speed in the real world using a single-point accelerometer 8
1.2.3 Aim 3: Classifying and characterizing indoor and outdoor walks in the real world using a single-point accelerometer 9
1.3 Research Impact 10
1.4 Dissertation Outline 10

2 Understanding the Influence of Context on Real-World Walking Energetics 11

2.1 Motivation 11
2.2 Methods 13
2.2.1 Experimental Protocol 13
2.2.2 Data Processing 17
2.2.3 Statistical Analysis 21

2.3 Results . . . 22
2.3.1 Real-world Walking Behavior . . . 22
2.3.2 In-lab Cost of Transport Models . . . 23
2.3.3 Steady-state Walking and Context . . . 24
2.3.4 Cost of Transport Minimization and Walking Speed Variability . . . 25
2.4 Discussion . . . 29
2.5 Conclusion . . . 33

3 Estimating Walking Speed Using an Accelerometer Only . . . 35

3.1 Motivation . . . 35
3.2 Methods . . . 38
3.2.1 Subjects . . . 38
3.2.2 Instruments . . . 39
3.2.3 Subject-specific Model Derivation . . . 42
3.2.4 Model Evaluation . . . 43
3.2.5 Statistical Analysis . . . 44
3.2.6 Model Correction . . . 46
3.2.7 Week-Long quantification of the Walking Activity . . . 46
3.3 Results . . . 48
3.3.1 Mapping from Stride Frequency to Stride Speed . . . 48
3.3.2 Quantification of the Walking Speed Estimate Error . . . 49
3.3.3 A Week in the Life of Subject 1 . . . 52
3.4 Discussion . . . 53
3.5 Conclusion . . . 58

4 Characterizing Walking Speed Variability Using an Accelerometer Only . . . 60

4.1 Motivation . . . 60
4.2 Methods . . . 61
4.2.1 Subjects . . . 61
4.2.2 Long-term Free-living Measurements . . . 61
4.2.3 Statistical Analysis . . . 64
4.3 Results . . . 66
4.3.1 Real-world data pre-processing . . . 66
4.3.2 Walking Periods Classification . . . 66
4.3.3 Walking Period Characteristics . . . 66
4.3.4 Influence of Period Continuity and Duration on Walking Speed . . . 67
4.4 Discussion . . . 71
4.5 Conclusion . . . 74

5 Classifying Context Using an Accelerometer Only . . . 76

5.1 Motivation . . . 76
5.2 Methods . . . 79
5.2.1 Overview . . . 79
5.2.2 Datasets . . . 80
5.2.3 Classification Algorithm Development . . . 81

5.2.4 Outdoor versus Indoor Walking Analysis 85
5.3 Results 87
5.3.1 Classification Algorithm Evaluation 87
5.3.2 Model Classifications on Mixed Walking Periods 90
5.3.3 Characterization of Indoor versus Outdoor Walking Periods 91
5.4 Discussion 91
5.5 Conclusion 94

6 Conclusions and Future Directions 96

6.1 Contributions 97
6.2 Opportunities for Future Work 99
6.3 Broader Impact 101

APPENDICES 103

BIBLIOGRAPHY 118

LIST OF FIGURES

FIGURE

1.1 **Dissertation Overview** — This Figure presents the 3 aims in my dissertation with their associated dataset and research questions. 6

2.1 **Data Collection and Processing** — (A) Data collection combined a week of data collection in the real world and an in-lab treadmill walking task. (B) Data processing methods were used to combine the different sensor streams to obtain stride speed profiles in the real world with associated contexts, and a map of cost of transport vs. stride speed in the lab. (C) The activPAL labels were used to isolate walking periods in the IMU signal in the real world. From these walking periods, we obtained steady-state walking speed profiles. Subsequently, we collected indirect calorimetry data at a range of speeds on the treadmill. Then, we built subject-specific models of cost of transport vs. speed to identify the energetically optimal speed range for each individual. The energetically optimal speed range is defined as the minimum cost of transport, plus 10% of that minimum value (shaded region). Finally, we observed the overlap between that range and real-world speeds. 17

2.2 **Steady-state identification flowchart** — The algorithm and the cutoff choices are detailed in Appendix A.3 (CV: Coefficient of Variation) 18

2.3 **Walking periods duration and their proportion of steady-state strides** — Relationship between walking period duration and percentage of steady-state strides within a walking period — (A) Each dot corresponds to a walking period. The different colors are for each context. (B) We binned all walking periods by their bout duration and looked at the percentages of steady-state strides within a walking period for each bin. (C) We binned all walking periods by their percentage of steady-state strides and looked at the walking period durations for each bin. 23

2.4 **Energetic optimality for steady-state strides in each context** — (A) Proportion of steady-state strides for each context for all participants with the associated proportion of strides within the energetically optimal speed range. The darker part of each bar represents the proportion of strides with speeds within the energetically optimal range. For instance, we read that the context Pleasure represents approximately 35% of the data and that a little more than half of the strides have a stride speed within the energetically optimal speed range. (B) Distribution of stride speed subtracted by the subject-specific speed at the minimum cost of transport for all subjects in each context. Each shaded area represents the shape of the distribution, and the horizontal lines mark the mean. For instance, we read that participants walked on average $0.35m \cdot s^{-1}$ faster than their energetically optimal when commuting. 24

2.5 **Steady-state stride speed distributions and proportion of energetically optimal strides for each context** — Each shaded area represents the shape of the distribution of stride speed subtracted by the speed at the minimum cost of transport for the different contexts for a subject, with the horizontal line for the mean. The energetically optimal speed range is centered around 0 and represented by the grey boxes. The percentages are the proportion of speeds within the energetically optimal speed range. Some individuals had no data for a given context. 28

3.1 **Data Processing** —- Data extraction and pre-processing from the synchronized activPAL (AP) and the IMU. A representative window of 4 strides illustrates the preprocessing of the raw data from both sensors. The AP is worn on the thigh, and the accessible raw data is from the embedded 3-axis accelerometer. The x-axis signal, which is from the sensor-axis that is aligned with the thigh and is positive in the inferior direction, is smoothed and a peak detection (threshold in red-dotted line) method enables the detection of each stride. For the IMU, raw data from the embedded 3-axis accelerometer and gyroscope are processed using a continuous wavelet transform to detect gait events; foot velocity and position are then calculated using a ZUPT algorithm. 40

3.2 **Experimental flow chart** — **(A)** We start by deriving the parameters a and b of the power model using data collected from the IMU worn on the foot during the designed Metronome Walk. **(B)** To verify the accuracy of the model and validate the identified parameters, each subject performs a long unsupervised walk in the real world wearing both the activPAL (AP) on the thigh and the IMU on the foot. The error between the estimated speed from the AP and the speed extracted from the IMU is then analyzed. If the error is not clinically acceptable (Coverage probability with boundaries $\pm 0.2m \cdot s^{-1}$ $CP_{0.2} > 0.95$), the model is adjusted by finding new parameters a' and b'. **(C)** Once the model is validated, we can proceed to a longer observation with the AP only. 47

3.3 **Subject 4 analysis** — **(A)** Subject-specific data-driven map from stride frequency to stride speed built from the metronome walk. Each cloud of points corresponds to an imposed stride frequency. **(B)** Bland Altman analysis of the residuals with mean difference, limits of agreement, and their confidence intervals (CI). 49

3.4 **Distribution of residuals** — The violin plot enables the visualization of the distribution of the error for each subject with $\pm 0.1m \cdot s^{-1}$ (black-dotted line) and $\pm 0.2m \cdot s^{-1}$ (grey-dotted line) bands. Each shaded area represents the shape of the distribution of residuals for a particular subject. 50

3.5 **Model Correction** — **(A)** Observation of the metronome walk fitted curve ($a = 2.050$ and $b = 0.335$) against the corrected power model ($a' = 2.266$ and $b' = 0.399$) for Subject 2. **(B)** Bland Altman analyses for the original and **(C)** corrected models with mean differences, limits of agreements, and their confidence intervals (CI). 52

3.6 **Week Analysis** — **(A)** Analysis of the distribution of all stride speed values collected over a week for one subject. **(B)** Observation of the evolution of walking speed in a week. Each point corresponds to the average of the values of stride speed in a quasi-steady-state walking bout as defined in Methods. **(C)** A closer look at the values of stride speed on a particular day, shaded in yellow in the figure above. Each point corresponds to the average of three strides. 53

3.7 **Subjects' models and their parameters — (A)** Parameters a and b from each subjects power model and their 95% confidence intervals. **(B)** Fitted lines for all subjects and visualization of the effects of variations of the parameters a and b. Females are represented with solid lines and males with dashed lines. 55
3.8 **Distributions of estimated and true speed** — Distributions of the estimated speeds from the AP using the built models, and of the true speeds calculated from the IMU. Gaussian curves were fitted to each distribution and the mean and standard deviation for each curve are given. 57

4.1 **Characterization of a Walking Period — (A)** Raw acceleration data and activity state were used to parameterize stepping periods. **(B)** To identify a stepping period 5 strides windows were first defined. A decision tree classified each window as either walking, running, or other. **(C)** Finally, we evaluate the percentage of 5-stride windows labeled as walking within each stepping period to determine walking period. 65
4.2 **Stride speed distribution across walking modes — (A)** Map of the different walking modes based on their duration and continuity. Each point represents a walking period, containing at least 5 strides. The distribution of duration and continuity are on the left and top of the figure respectively. **(B)** Distribution of stride speed over the different walking modes for all subjects. Each shaded area represents the shape of the distribution for a mode, with the horizontal line representing the mean. **(C)** Distribution of stride speed over the different walking modes for 6 representative subjects. Each shaded area represents the shape of the distribution for a mode, with the horizontal line representing the mean. Stride speed normalized by leg length can be found on the right y-axis. 70
4.3 **Stride speed distribution for all data and for data from Mode 4 and Mode 5** — Histograms for four representative subjects **(A)** and for all subjects **(B)** representing the distribution of stride speed values for all data and for data from Mode 4 and Mode 5. The dashed lines illustrate the mean of each distribution. 71

5.1 **Data Collection and Processing Overview — (A)** Dataset A was collected over 7 days on 20 participants, using an accelerometer, self-report, and GPS data from the participants' phones. Dataset B was collected over 14 days on 15 participants using an accelerometer. **(B)** The walking periods from dataset A were labeled using the GPS and self-report data. Walking periods labeled exclusively indoor or outdoor were used to train, validate, and test a classification model. The walking periods labeled mixed (e.g., inside and outside), as well as all the unlabeled walking periods from dataset A and B were classified using the model to characterize indoor versus outdoor walks. . . 79
5.2 **Classification Model** — We extracted walking periods from the accelerometer that we then labeled using self-report and GPS data. We extracted features from the accelerometer data and the stride detection. Labeled walking periods were then split into training, validation, and testing set. We trained and validated two different learning algorithms, Random Forest and Ensemble SVM, using a leave-one-participant-out scheme. This led to 15 trained models that were then tested on the 5 remaining untouched participants' data. The best-performing model was chosen for the rest of the analyses. 81

5.3 **Data Labeling using GPS and self-report data** — We show here 3 examples for walking periods labeled indoor, outdoor, and both indoor and outdoor. The GPS sampling was variable and dependent to the type of phone used. The text in quotations corresponds to the participant's self-report. 82
5.4 **Feature Importance using Feature Permutation** — Decrease in model accuracy for each shuffled feature. The error bars represent standard deviation. 88
5.5 **Analysis of Walks labeled both Indoor and Outdoor** — (A) GPS and self-report data is shown for a sample of walks labeled indoor only, outdoor only, mostly indoor, and mostly outdoor by the researcher (from left to right). The mixed walking periods highlighted here are likely to be mislabeled. The sampling rate of the GPS data is variable and depends on the participant's phone type. (B) Principal component analysis for walking periods labeled indoor, outdoor, mostly indoor, and mostly outdoor by the researcher. (C) Principal component analysis with the mixed walking periods labeled by the model. We can see that the majority of mostly indoor walks are labeled indoor and vice versa, and that the walking periods that were likely mislabeled by the researcher are likely correctly labeled by the model. 90
5.6 **Indoor and Outdoor Walking Periods Duration and Continuity** — Relationship between walking period duration and continuity — (A) Each dot corresponds to a walking period. (B) and (C) We binned all walking periods by their context and looked at their durations and continuity. 92
5.7 **Stride Speed for Walking Periods Indoor vs. Outdoor** — Distribution of stride speeds for all participants grouped by context. Each shaded area represents the shape of the distribution, and the horizontal lines mark the mean. 93

A.1 **Enforcing Walking Strategy** — Power model mapping stride length to stride speed for both the real-world and the in-lab data collection. Each dot represents the average for a given trial on the treadmill and the error bars represent the standard deviation for both stride speed and stride length. We chose to not show the real-world data points to not crowd the plots. 108
A.2 **Sensitivity Analysis** — Variation of the percentage of steady-state strides based on changes in the parameters CV_{length} (A), CV_{speed} (B), and $cos(\theta)$ (B) for a given subject. 109
A.3 **In-lab Walk for Validation** — (A) Representative track for S7 during a controlled in-lab walk where participants walked back and forth in a hallway. (B) Parameters variation associated with the track. The green line represents the chosen threshold for each parameter. 109

B.1 **Extraction of Walking Periods** — **(A)** From each 5-stride window, an ensemble of 44 features was extracted. **(B)** We applied a principal component analysis to the matrix of features. Then, an unsupervised clustering method was used to isolate the different point clouds. Each point corresponds to a 5-stride window. Using heart rate **(B - a))** and the labels obtained from the runners **(B - b))**, we confirmed the nature of the clusters as walking, running, and others. **(C)** Then, we built a decision tree using the labels from our clustering. Finally, the tree was used to classify each 5-stride window. 115

B.2 **Performance Evaluation** — Plot of the percentage of data labeled run being removed against the different values of lambda. Each line represents a runner. We observed the highest percentage of data labeled run being removed for the tree built with Subject 14's data, at a value of λ of 77%, noted by a red dashed line on the zoomed subplot. . . 116

LIST OF TABLES

TABLE

2.1 **Sensor specifications** — We extracted walking using the activPAL and derived stride parameters using the IMU. 14
2.2 **Walking periods characterization** — There are variations between contexts in the number of strides and walking periods, as well as the proportion of steady-state within a walking period. Contexts with longer walking periods tend to have less walking periods, but more strides and steady-state strides. 22
2.3 **Linear Mixed Model Coefficients** 25
2.4 **Subject-specific data** — Each participant had a different economical speed range, leading to varied proportions of economical walking speeds in the real world for the different contexts. For each context, participants displayed different walking strategies as well. 27

3.1 **Subject Information** 38
3.2 **Goodness of fit** - Analysis of the goodness of fit of the power model built during the Metronome Walk for each subject. (CI: Confidence interval; RMSE: Root mean square error) 48
3.3 **Bland-Altman Analysis** — Bland & Altman plot statistics for all subjects. μ and σ correspond to the mean and standard deviation respectively. 50
3.4 **Measures of Agreement** — Coverage probabilities (CP) for the boundaries 0.1, 0.2, and $0.3m \cdot s^{-1}$ and concordance correlation coefficient (CCC) with its confidence interval (CI) 51

4.1 **Sensor specifications** 62
4.2 **Walking periods and associated parameters** — Number of walking period N for each participant and all participants with number of strides analyzed n, average μ and standard deviation σ of period duration, period continuity, and stride speed. 68
4.3 **Stride speed for each mode** — Number of stride speed values N, average μ, and standard deviation σ of stride speed within each mode for each participant and all participants. The '-' notation means the subject did not present any walking period in this mode. 69

5.1 **Datasets details** 80
5.2 **Model Validation with All Features** 88
5.3 **Model Validation with Biomechanics Features** 89

5.4 **Model Choice** — Results of the 15 models with the 5-participant test set. Each model corresponds to the models trained and validated with the leave-one-participant-out scheme using the Random Forest algorithm with the biomechanics features set as shown in Table 5.3. Model 13 performs the best. 89

C.1 **List of Features** 117

LIST OF APPENDICES

A Chapter 2 - Supplementary Material **103**

B Chapter 4 - Supplementary Material **110**

C Chapter 5 - Supplementary Material **117**

LIST OF ACRONYMS

AIC Akaike Information Criterion

AUC Area Under the ROC Curve

AP activPAL

CCC Concordance Correlation Coefficient

CI Confidence Interval

CP Coverage Probability

CV Coefficient of Variation

CWT Continuous Wavelet Transform

DBSCAN Density-Based Spatial Clustering of Application with Noise

EMA Ecological Momentary Assessment

GPS Global Positioning System

HAR Human Activity Recognition

IMU Inertial Measurement Unit

MEMS Micro-electromechanical systems

MLM Multi-Level Model

PCA Principal Component Analysis

RMSE Root Mean Square Error

SVM Support Vector Machine

ZUPT Zero-velocity Update

ABSTRACT

The walking movement of an individual is a window into their health. Both physical and mental illnesses can alter the way someone walks. As such, the analysis of walking gait is essential for understanding an individual's health status and mobility. Developments in measurement tools available in laboratory settings have enabled high-resolution, accurate, and comprehensive assessments of human movement. Researchers have established important relationships between key aspects of human walking and various health issues. However, the laboratory environment naturally places constraints on the types and variety of movements that can be measured; labs are not infinite in size, are indoors, and data collections are limited in time. As a result, researchers can only capture a small sample of the highly variable movement that people are capable of and exhibit when walking in the real world. This restricted view can result in decisions that aren't fully informed, as they are based on a mere fraction of available data. Thoroughly capturing the variability in movement patterns is essential to grasp the complete spectrum of an individual's abilities and performance. Doing so enables a more comprehensive understanding of health statuses and facilitates the delivery of better, more tailored care.

The rapid advancement of wearable sensing technologies offers new possibilities for data collection outside the laboratory setting and in the real world. Wearable sensors of different types, sizes, and body placements exist and are accessible for the measurement of walking in unconstrained environments with little to no supervision. Real-world data is rich and can provide information that is not available in laboratory settings, such as habits or physical activity levels. However, walking in the real world is highly variable, involving a large variety of contexts. The movement patterns required to navigate the different scenarios of everyday life are diverse and can be complex. As such, interpreting the data collected in the real world using wearable sensors can be challenging.

This dissertation proposes several frameworks that leverage real-world data collected from wearable sensors to address these challenges and further our understanding of how humans walk. Specifically, we collected datasets over multiple timescales and with different sensor suites to develop methods for analyzing walking variability in the real world. We identified various contextual factors that significantly impact human walking movement and energetics, and offer a new perspective on walking economy that complements previous findings established in the laboratory setting.

Additionally, we demonstrate how a reduced sensor set, a single low-resolution accelerometer, can be utilized to characterize the variability of walking in the real world, by identifying parameters that can be used to parse the data in a meaningful way. We also built a framework able to accurately classify walking context using the same reduced sensor set.

This work aims to facilitate and promote the use of wearable sensors for the study of human walking biomechanics in the real world. It demonstrates how capturing the variability in walking patterns can be an advantage, potentially providing insight into an individual's capabilities and health. The proposed methods have the potential to be extended to clinical populations and utilized by clinicians to aid their decision-making.

CHAPTER 1

Introduction

1.1 Motivation & Background

1.1.1 Walking for Health

The study of human movement biomechanics is essential in healthcare for the prevention, diagnosis, treatment, and overall management of various health issues [1, 2]. In particular, walking is a fundamental human motion, integral to most individuals' daily life, that has been intensely studied for centuries [3–5]. It is a natural movement that does not require any specific equipment or skills and that has diverse benefits for both the body and mind [6–9]. Walking is a milestone in human development and typically occurs around the age of one. As an individual grows, their gait changes and there are numerous factors that can influence this evolution. Health status is one of the main causes of change in walking patterns. As such, the characterization of an individual's locomotion can be a gateway to insights into a person's health. Researchers have identified gait parameters that have significant correlations with changes in health. For example, a decline in walking speed can be associated with different health issues, including cardiovascular disease, neurodegenerative disease, and frailty. Changes in gait can also be used for the early detection of disorders. Parkinson's disease is a neurodegenerative condition that has greatly benefited from the study of evolution in gait analysis. In fact, changes in speed and balance when walking are often early signs of such an ailment. Overall, the study of human walking is critical for our understanding of health and well-being. As such, there are numerous methods that can be used to

analyze gait in the laboratory/clinical setting. Yet, these methods lack a systematic approach to understanding and characterizing walking in the real world.

1.1.2 Walking as Measured in the Laboratory Setting

Clinicians use a wide variety of tests to assess patients' locomotion [10]. Among these, the six-minute walk test is one of the most commonly used assessments that offers a straightforward method to estimate an individual's walking speed while simultaneously observing their walking performance [11]. During the test, walking speed is calculated based on the relationship between distance traveled, time taken, and speed. Often, time is captured using a stopwatch while the distance is measured by using a predetermined length of the walking path or using a measuring wheel. However, the quantification of gait during these tests presents a number of limitations. Clinical tests often vary in their duration, distance, and instructions, which can result in different walking characteristics for the same individual across different types of tests or clinics [12–14]. Additionally, different results can be found for the same individual from one day to the next even when undergoing the same test [15, 16]. The measurement tools used in these studies are often rudimentary — for example, a stopwatch — and can result in large measurement errors.

Research labs and a growing number of clinics are becoming equipped with more advanced measurement technologies. Motion capture is one of the most accurate tools available to quantify human kinematics [17–19]. It can be complemented with force plates installed on a treadmill or an instrumented walkway to measure kinetics as well. Thanks to these measurement tools, researchers have been able to model many aspects of human walking and discover some of the underlying mechanisms of gait. One of the central principles of walking states that people prefer to move in ways that minimize their energy consumption. Studies conducted in the lab have shown that individuals will converge towards gait patterns that minimize energetic cost by modifying different aspects of their gait, including step width, step height, or arm swing [20–25].

However, researchers have identified factors that hinder people from walking naturally in clinical

and laboratory settings. For instance, the ”white-coat effect” is defined as a change in behavior due to the awareness of being observed by doctors [26–28]. This phenomenon can result in a misleading characterization of an individual’s walking performance [29, 30]. Moreover, the controlled environment of a laboratory or clinic cannot replicate the large variability in the environment encountered when walking in the real world. For instance, individuals often have a purpose when ambulating in their daily lives, which might lead to different behaviors that are difficult to simulate in the confines of the laboratory. As such, it is unclear whether results found in the lab directly translate to the real world. Overall, these fundamental limitations highlight the importance of considering real-world measurements of human locomotion for a better representation of human behavior and performance.

1.1.3 Walking as Measured in the Real World

With the advancements of micro-electromechanical systems (MEMS), motion sensors have undergone remarkable transformations, becoming compact, lightweight, and affordable. High-resolution inertial measurement units (IMUs) are now embedded in mobile phones, smartwatches, and various wearable devices, enabling the measurement of real-world movements [31, 32]. Researchers are increasingly capitalizing on these technological innovations to complement in-lab assessments of walking behavior with continuous long-term monitoring. Smartwatches, for instance, are now commonly used for measuring daily physical activity levels [33, 34]. These devices have proven valuable in evaluating mobility, but also in designing interventions and evaluating their efficacy. Simple metrics, like daily step count, have shown strong correlations with diverse health issues, including cardiovascular diseases and mental health issues [35–37]. However, as stated earlier, more advanced kinematics metrics can also be essential health indicators, like walking speed. As such, novel methods have emerged, utilizing high-resolution sensors, to achieve more precise quantification of individual gait patterns. For example, foot-worn IMUs can provide accurate estimates of walking speed by using the physics of the movement

of the foot when walking [38–41]. Importantly, these high-resolution datasets of walking biomechanics in natural environments demonstrate a superior ability to distinguish between healthy and pathological gait when compared to traditional in-lab studies [42, 43]. Moreover, the real-world setting offers a richness in the variability of movement patterns, with walks on different terrains, weather conditions, and many other contexts. Capturing this variability is essential to fully understanding an individual's health and is at the foundation of precision medicine. Such variability not only reveals an individual's capabilities but also highlights their limitations. Furthermore, it can be instrumental in distinguishing between different populations or individual characteristics. However, this variability and the unsupervised nature of real-world datasets collected with wearable sensors can pose challenges when it comes to their analysis and interpretation.

1.1.4 Measuring Real-world Context

As individuals walk through diverse environments, moving from one location to another and with different purposes, it is important to gain a deeper understanding of the influence of these contextual changes on walking behavior. Researchers have integrated other measurement channels in addition to wearable sensors to try and capture this contextual information. Cameras have emerged as a direct measurement tool, allowing researchers to capture valuable information about daily-life contexts [44, 45]. Images and videos can provide insights into factors influencing locomotion, such as activity type, location, and terrain characteristics (e.g., slope gradient, type). Advanced computer vision techniques have been developed to accurately and automatically analyze video data. Often, these techniques are combined with data from wearable sensors to offer a multi-dimensional analysis of movement. Self-reporting is another direct approach to gathering contextual information on an individual's daily activities. For instance, Ecological Momentary Assessment (EMA) is a real-time self-report method that allows individuals to provide contextual information related to specific events that can influence their mobility [46, 47]. GPS data, obtained from mobile phones or dedicated devices, represents another measurement channel

that effectively enhances the contextual understanding of real-world movements. In an innovative study, Wang et al. leveraged the repetitive nature of daily routines and utilized GPS data to identify frequently-repeated paths of an individual [48]. They demonstrated how using only these paths, as opposed to all strides, resulted in reduced variability in spatiotemporal gait parameters (e.g., stride length, stride speed, stride width, foot clearance). In another study, Kim et al. also utilized GPS data to compare the mobility of lower-body amputees in areas close to their homes versus those farther away [49]. These methods have highlighted the significance of contextual factors and their influence on real-world walking. However, collecting data from numerous measurement channels can be challenging and unrealistic for long-term monitoring, as it may impact individual compliance.

There are ways to infer contextual information from wearable sensors only. Even simple characteristics of a walk, such as its duration, can have significant impacts on someone's gait patterns. Researchers have found that longer walking bouts tend to contain information that better discriminates between clinical and healthy populations [42, 50]. Additionally, the way someone moves during a walking bout can be indicative of different contextual factors. For example, Hu et al. showed that data from a single IMU placed on the lower back could be used to effectively differentiate flat and uneven terrain, as well as to categorize participants' age group [51]. Individual emotions are another contextual factor associated with gait. Researchers have been able to successfully classify a person's emotional state by measuring the way they walked using accelerometer-based wearable devices [52, 53]. This area of research is promising for the diagnosis and treatment of mental health. However, the majority of studies that develop methods for the identification of real-world context using wearable sensors leverage synthetic datasets, generated in supervised and controlled environments. This raises concerns regarding the ecological validity of the findings and the performance of these methods when deployed in real-world settings.

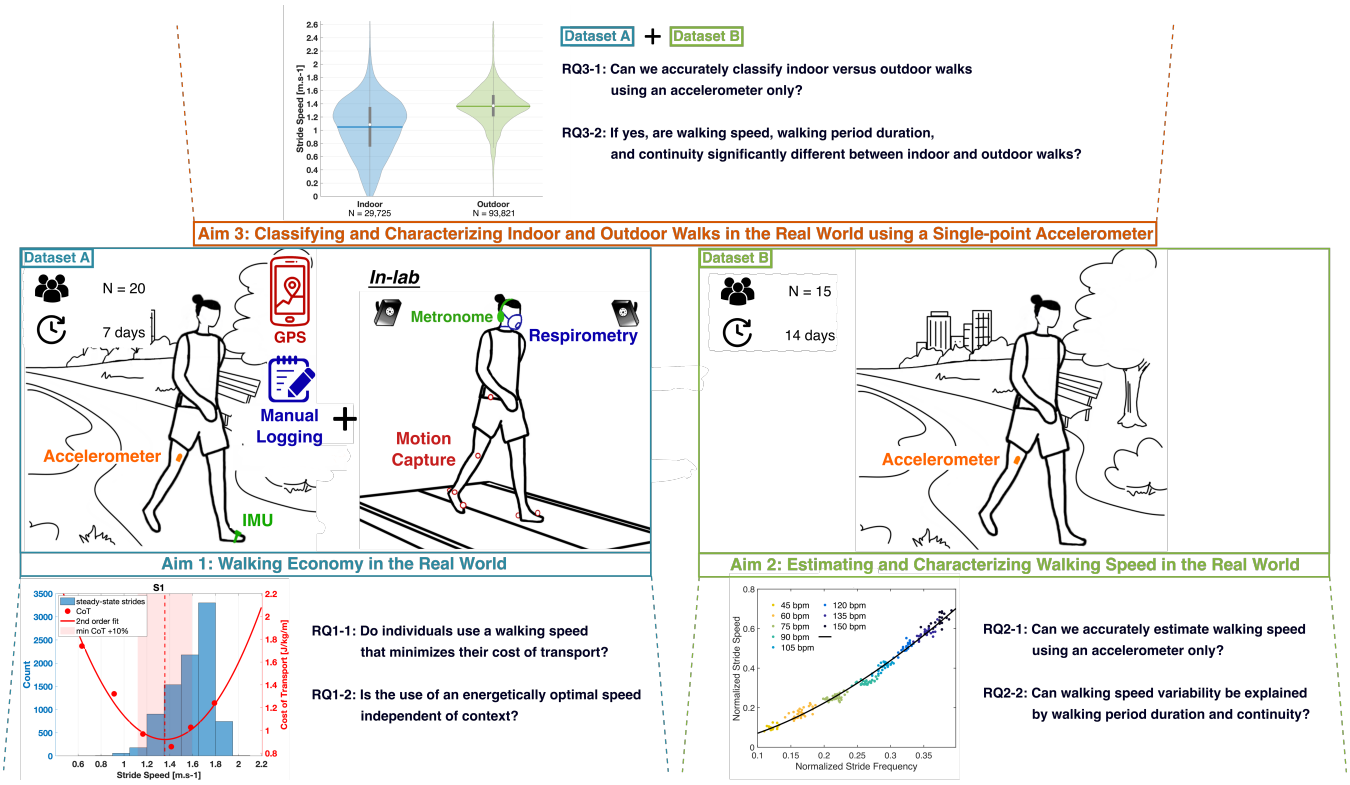

Figure 1.1: **Dissertation Overview** — This Figure presents the 3 aims in my dissertation with their associated dataset and research questions.

1.2 Dissertation Contributions

The objective of this dissertation is to create frameworks to quantify and explain the walking variability observed in the real world. These frameworks will allow us to investigate the different aspects that contribute to the variability an individual displays in their daily-life walking. We leveraged different types of wearable sensors and data collection methods to collect unique datasets and answer different research questions about real-world human walking. The contributions for this work are illustrated in Figure 1.1 and outlined below.

1.2.1 Aim 1: Walking economy in the real world

Since researchers have established that there are numerous differences between human walking behavior in the laboratory setting compared to the real world, it is unclear whether some of the

findings from the lab remain true outside of it. Here, we focus on the energetic principle of walking. The cost of transport represents the energetic cost required to travel a certain distance. As such, humans have a walking speed that allows them to travel the furthest while consuming the least energy. Researchers have found that individuals will tend to use a preferred walking speed that is similar to the speed that minimizes their cost of transport. Some recent work has investigated the relationship between the metabolic cost of walking and the environment in which an individual is walking in [54, 55]. However, these studies were focused on a particular contextual aspect (e.g., terrain type), and were carried out over short periods.

As such, in this first contribution, we investigated whether: 1) individuals use a walking speed that minimizes their cost of transport in the real world; and 2) the use of an energetically optimal speed was dependent on context. We collected motion data and contextual information on the location and purpose of a walk over a week for 17 individuals. In this work, we demonstrated:

1. The impact of contextual factors on walking strategy and its consequences on walking economy.

2. The importance of characterizing walking in the real world, as principles established in the lab are not necessarily ecologically relevant.

The findings have the potential to offer valuable perspectives not only for enhancing the understanding of human movement in relation to health, but also in the field of robotics, particularly in the development of assistive devices for the lower body. In fact, the reduction of energy when walking is often used as a metric to evaluate the efficacy of modern exoskeletons and prostheses. This work is presented in Chapter 2 and is under review for publication [56].

The dataset collected in this chapter leveraged additional measurement channels to obtain estimates of walking speed and contextual information. However, as we discussed earlier in the introduction, it is impractical to ask individuals to wear and maintain multiple sensors over extended periods. As such, we explored how we can explain the real-world variability of an essential health indicator, walking speed, using a single sensor.

1.2.2 Aim 2: Estimating and characterizing walking speed in the real world using a single-point accelerometer

A decline in walking speed can be associated with different health issues. However, the measurements of an individual's preferred walking speed in laboratory settings can be influenced and sometimes biased by different factors. For this reason, researchers are turning towards the monitoring and analysis of walking in real-life settings. Because walking behavior, and by extension, walking speed, is highly variable in the real world, motion data can be particularly challenging to interpret, especially when using a reduced set of sensors. There are few studies that have developed methods for the analysis of real-world walking speed over extended periods using a single-point accelerometer. There is a research group that has consistently demonstrated, over different studies, how the duration of a walking bout can be effectively leveraged to parse and interpret real-world walking data from clinical populations [42, 50].

Building on this work, we developed a framework for the characterization of walking speed variability in the real world, using a single thigh-worn accelerometer. For this contribution, we:

1. Developed a method for the accurate estimation of walking speed using a thigh-worn, low-resolution accelerometer (97% of estimation errors within $\pm 0.2 m \cdot s^{-1}$).

2. Created a classification algorithm to confidently isolate walking from running (99% of labelled run bouts removed).

3. Introduced the concept of walking period to better represent the start-and-stop nature of daily-life walks.

4. Identified two parameters that significantly influence walking speed in the real world: walking period duration and continuity.

5. Provided recommendations for the estimation of preferred walking speed in the real world for clinical applications.

Because of the use of a single sensor, this framework can be extended to clinical populations to further our understanding of real-world mobility and its association with health. This work is presented in Chapters 3 and 4 and published in [57, 58].

Although we were able to parse walking speed using walking period duration and continuity, we have seen in Chapter 2 the importance of having information on context to be able to better interpret and explain some of the variability observed in real-world walking. In the next aim, we explore the feasibility of obtaining contextual factors from our single accelerometer.

1.2.3 Aim 3: Classifying and characterizing indoor and outdoor walks in the real world using a single-point accelerometer

In Chapter 2, we used GPS data and self-report to learn about the context of each walk carried out by the different participants. This study highlighted the importance of context and how it can be used to further the understanding of human walking biomechanics in the real world. It is possible to gather contextual information using only motion sensors. Classification models have successfully leveraged IMU data to predict factors like terrain type, or indoor versus outdoor walking [51, 59]. However, these studies used synthetic datasets, created in a supervised environment, during steady-state walking. As such, these models may not be ecologically valid. In other words, they may not be representative of the real-world setting they aim to simulate.

Therefore, in this contribution, we address this gap by leveraging the real-world dataset we collected in the study conducted for Aim 1. In this contribution, we:

1. Demonstrated the feasibility of using a single-point accelerometer to build an accurate, feature-based classifier for real-world walking (94% accuracy).

2. Characterized the differences between indoor and outdoor walks to highlight how this classifier can be used in clinical applications.

This work provides a promising framework with the use of only one sensor to obtain critical information about context when walking in the real world. This framework has the potential to guide

and improve the interpretation of complex real-world data. This work is presented in Chapter 5.

1.3 Research Impact

The work in this dissertation demonstrates the possibilities to leverage the richness of real-world data and further the understanding of walking patterns, ultimately contributing to the improvement of health and well-being. Throughout this work, we highlighted different factors that can be used to obtain more sensitive and accurate representations of an individual's real-world movement profile. We also introduce methods and frameworks, utilizing various wearable sensor suites, which have the potential to be scaled and adapted across clinical populations. These methods can be leveraged to enhance the precision with which patients' mobility is characterized. As such, we provided evidence that can guide the healthcare ecosystem into improving the design of effective treatments and interventions that leverage technology. Overall, the work presented in this dissertation is a pivotal resource to help exploit and unlock the potential of real-world, long term monitoring of human movement.

1.4 Dissertation Outline

The structure of this dissertation is as follows. In Chapter 2, we present our analysis of walking energetics in the real world and its dependency on context. In Chapter 3, we detail our solution for the estimation of walking speed in the real world using an accelerometer only. Then, we deploy this accelerometer over an extended period on a population of healthy individuals to investigate the variability in walking speeds in the real world in Chapter 4. Chapter 5 proposes a classification framework to obtain contextual information from a single-point accelerometer. Finally, Chapter 6 presents a conclusion for this work and the potential for future research in the field.

CHAPTER 2

Understanding the Influence of Context on Real-World Walking Energetics

2.1 Motivation

Walking is an integral part of daily life, enabling movement in the environment and contributing to overall health and well-being. Studies investigating the relationship between walking kinematics and energetic cost conducted in the lab have demonstrated that humans tend to select movement patterns that minimize cost of transport [20]. Further, studies in controlled environments have demonstrated that key gait parameters (e.g. step width, step height, swing limb trajectory, arm motion) are self-selected to minimize energetic cost [21–25]. However, work has also demonstrated that gait observed in laboratory settings differs from unconstrained movement in the real world [27, 60–62].

Many of the advantages of in-lab gait analyses, such as increased control over participant behavior, also introduce biases and can make measurements unrealistic. First, although it is favorable for many experiments to study steady-state walking and reduce movement variability, human movement during daily life has been observed to consist of many short bouts or longer walks with punctuated stops from, for example, standing idle waiting to cross a street [58, 63]. Differences have also been observed in walking kinematics in different environments (inside vs outside walking), depending on behavioral context (purposeful vs recreational walks) [48, 49, 64]. Second, the direct observation of human walking offers greater control during an experiment. However,

researchers have shown that individuals alter their performance when observed compared to their natural behavior (a phenomenon known as the ”white-coat effect”) [26, 28].

Compact wearable sensing technologies can be used to measure kinematics and physiology during daily life to investigate walking biomechanics. Small low-power sensors, like accelerometers, have been embedded in shoe soles and belts, and are also commonly found in phones and watches [31, 65]. Sensing systems designed around accelerometers can make continuous measurements for weeks [58, 66]. Inertial measurement units (IMUs) combine accelerometers with gyroscopes and magnetometers to measure additional kinematics. IMUs require more power than an accelerometer alone, limiting recording duration to a day scale. But, these sensor data can be used to estimate parameters like foot orientation and speed, enabling position estimates of the foot during gait. The accuracy of the step-to-step position estimates has been shown to be comparable to measurements made using motion capture [39, 40, 67]. Using wearables to persistently monitor an individual enables the investigation of real-world movement patterns; however, behavioral and environmental contexts can also be used to explain the variability observed in real-world movement patterns.

Contextual information can have many forms, from the location of a walk to its purpose. Prior work has identified a dependency between terrain type and metabolic cost [54, 55]. Researchers have leveraged GPS data, as location is closely associated with someone’s activity [48, 49]. Gast, et al. demonstrated how humans might prefer a slower speed than the energetically optimal when walking on difficult terrains to increase stability. However, these experiments were focused on a specific contextual aspect over a short period. To gather contextual information over longer periods, technologies like cameras can offer a direct observation of the environment someone is moving in, but they are highly invasive and the analysis of the images can be burdensome. These issues impact the feasibility of using camera data for long-term monitoring. Alternatively, researchers have asked participants to keep a manual log of their daily activities to gain additional information on context [68, 69].

The objective of this work is to investigate the relationship between cost of transport, real-world walking speed, and context in young able-bodied adults. Specifically, we will quantify whether

the participants used self-selected walking speeds that minimize their cost of transport in the real world, where walking is highly variable and context-dependent. We hypothesize that in the real world: (1) Individuals will use on average a walking speed that minimizes their cost of transport, and (2) The use of a walking speed that minimizes cost of transport is independent of context. To test these hypotheses, we combined in-lab modeling to establish the subject-specific relationships between cost of transport and walking speed and long-term data collection to capture real-world walking speed and contextual factors. The results of this chapter provide insight into the energy expenses of walking in the real world and how contextual information can be effectively used to understand human locomotion. It also highlights the necessity to turn towards ecologically relevant experimental designs for the study of human movement, health, and overall behavior.

2.2 Methods

2.2.1 Experimental Protocol

2.2.1.1 Recruitment

Data and results from 17 subjects recruited from a healthy population are presented in this work (11 females, 6 males, $26yo \pm 6yo$, $168cm \pm 10cm$, $65kg \pm 9kg$). Participants were excluded if they had health issues that would limit their ability to walk or breath, such as severe cardiac disease or asthma. Participants signed an electronic consent form prior to the first visit, and the data collection was approved by the Institutional Review Board at the University of Michigan.

2.2.1.2 Real World Data Collection — First Visit

Movement and activity data were first collected over the course of a week from the subjects during their daily life. During an initial visit to the lab, participants were given an accelerometer (activPAL^{TM} [PAL Technologies Ltd., Glasgow, UK]) and an inertial measurement unit (IMU) (Opal, APDM, [Portland, OR, USA]) to wear during the 7 days of monitoring (see Table 2.1). The

activPAL was chosen for its small size and ability to log data continuously for the week-long trial. Additionally, activity classification algorithms developed by PAL Technologies were combined with custom algorithms to isolate walking [66, 70]. Wear time for each sensor can be found in Appendix A.1.

To facilitate labeling and classification, the participants kept an activity log detailing when they were walking, the purpose of the walk, and where they were (e.g., home, work, etc.). A log template and a detailed explanation about how to fill out the log were provided to the participants, along with a set of instructions that included information on how to charge and wear the sensors. Participants could also opt-in to receive daily text reminders to charge and wear the sensors, and to take their daily walk.

Table 2.1: **Sensor specifications** — We extracted walking using the activPAL and derived stride parameters using the IMU.

	activPAL	**Opal IMU**
Measurement	3-axis acceleration $\pm 4g$	3-axis acceleration $\pm 4g$ 3-axis angular velocity $\pm 200 deg \cdot s^{-1}$ 3-axis magnetometer $\pm 8 Gauss$
Placement	Thigh	Above shoe on foot dorsum
Attachment	Tape	Fabric pouch secured with laces
Battery life	14+ days	8+ hours
Sample rate	20Hz	100Hz
Size	(23.5 × 43 × 5 mm)	(55 × 40.2 × 12.5 mm)
Weight	9g	25g

2.2.1.3 In-Lab Data Collection — Second Visit

Exit Interview Following the week of real-world data collection, the participants returned the sensors and scheduled the in-lab visit. At the start of the second visit, an exit interview was conducted with the participant to clarify information from the log with the activPAL and GPS data. During the interview, participants were asked to provide supplemental information if the logs were incomplete (e.g. a walk was logged but the purpose is missing). The participants were also

asked to recall the context of recorded activities that were not logged (ex: a walk is classified from the sensor data but absent from the log). This interview ensured that the contextual information for the real-world walking data was complete and accurate.

Treadmill Walking and Energetics Measurements An experimental investigation of energetic cost during a range of walking speeds was then conducted with each participant. Sixteen reflective markers were first placed on the participants' lower-body to measure walking kinematics using a 26-camera Vicon Motion Capture system (Vicon, [Oxford, UK]) collecting data at 100 Hz. Markers were placed on the following locations on both right and left leg: Anterior superior iliac, posterior superior iliac, thigh, knee, tibia, toe, ankle, and heel. A COSMED K5 system (COSMED, [Rome, Italy]) was used to measure metabolic cost. This system uses a mask worn around the subject's mouth and nose and a small backpack that carries the portable measurement unit with the battery. Oxygen and carbon dioxide volumetric flow rate were measured breath-by-breath. To prevent measurement biases, participants were asked to refrain from eating, drinking caffeine, and exercising 5 hours prior to this second visit. Once the participants felt comfortable, they were instructed to perform a 5-min quiet standing to obtain resting metabolic rate. Walking trials were conducted on an instrumented split-belt treadmill (Bertec, [Columbus, OH, USA]) (Figure 2.1 - (A)). Ground reaction force data were sampled at 1,000Hz from both belts.

Participants were given time to familiarize themselves with the split-belt treadmill before the experiment was conducted. During the experiment, the participants were asked to walk on the treadmill at 6 different speeds for 6 minutes each. Data from the week-long data collection was used to determine the range of speeds used for this task. We separated equally in 6 speeds the interval between the maximum and minimum speed observed in the real world. Often, the fastest speed originally chosen had to be reduced to accommodate for the treadmill discomfort that participants felt. The order of the speeds was randomized and a 2-min seated resting period was allowed between each 6-min trial.

We wanted to ensure that participants maintained the walking strategy they used in their daily life

on the treadmill to obtain a cost of transport as ecologically valid as possible. However, walking on a treadmill can lead to a decrease in stride length for a given stride speed to increase stability compared to overground [71]. Thus, we enforced the relationship we found between stride length and stride speed from the real-world walking data for the treadmill trial, by leveraging the relationship between stride length and stride speed. The stride length l an individual chooses when walking at a stride speed v can be predicted for each individual using the following relationship:

$$l = a.v^b$$

where a and b are subject-specific model parameters [72, 73]. First, we identified the parameters a_{rw} and b_{rw} for the real-world model fit for each subject from the data collected prior. Then, we constrained both stride speed and stride length on the treadmill, using real-world subject-specific models. Stride speed was imposed by the treadmill, but stride length can be difficult to control. Instead, we leveraged the relationship between stride length, stride speed, and stride frequency f:

$$v = l \cdot f$$

to constrain stride frequency instead. As such, for a given treadmill speed, participants were given a frequency to follow that corresponded to:

$$f = \frac{1}{a_{rw}} v^{1-b_{rw}}.$$

A headset played the calculated metronome frequency and participants were instructed to synchronize their steps to each beat as best as they could. We ensured the person was able to comfortably match the given stride frequencies on the treadmill, specifically for the highest stride speed. Then, we built the subject-specific models of each participant on the treadmill and found a new set of parameters a_{tread} and b_{tread}. We compared the parameters a_{rw} and b_{rw} against a_{tread} and b_{tread} to evaluate whether participants successfully adapted their walking strategy (Appendix A.2).

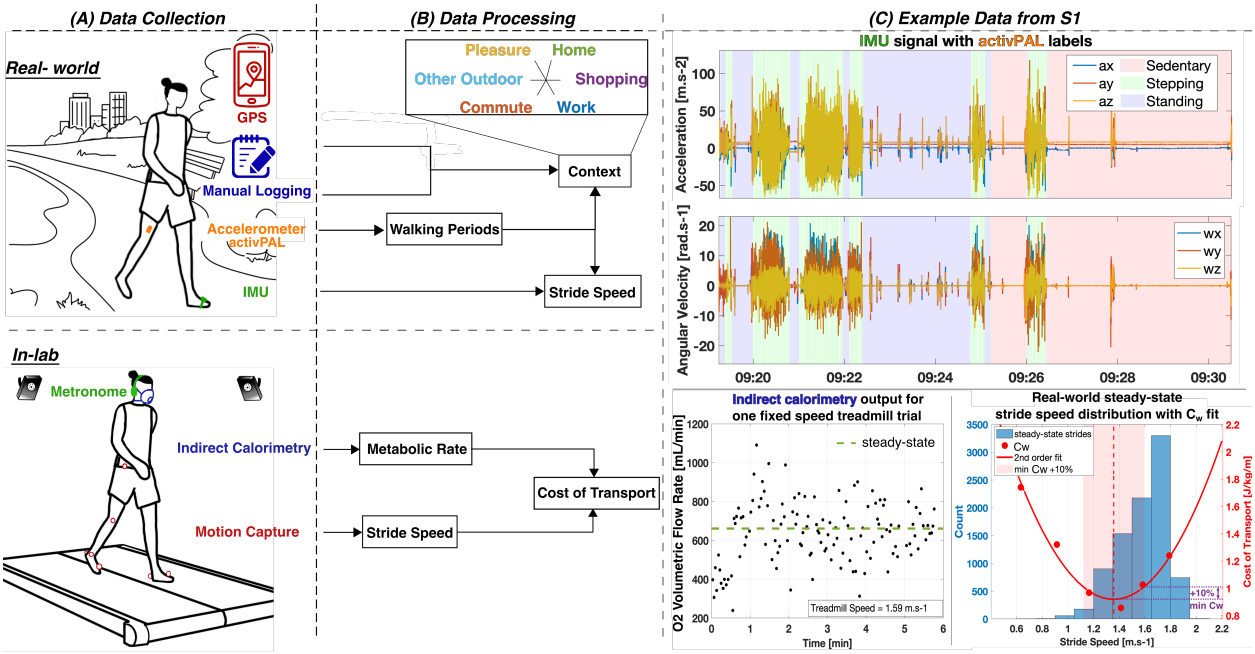

Figure 2.1: **Data Collection and Processing** — (A) Data collection combined a week of data collection in the real world and an in-lab treadmill walking task. (B) Data processing methods were used to combine the different sensor streams to obtain stride speed profiles in the real world with associated contexts, and a map of cost of transport vs. stride speed in the lab. (C) The activPAL labels were used to isolate walking periods in the IMU signal in the real world. From these walking periods, we obtained steady-state walking speed profiles. Subsequently, we collected indirect calorimetry data at a range of speeds on the treadmill. Then, we built subject-specific models of cost of transport vs. speed to identify the energetically optimal speed range for each individual. The energetically optimal speed range is defined as the minimum cost of transport, plus 10% of that minimum value (shaded region). Finally, we observed the overlap between that range and real-world speeds.

2.2.2 Data Processing

2.2.2.1 Grouping Real-world Movement Data into Walking Periods

We grouped the real-world walking data into walking periods following the method outlined in Baroudi et al. [58] (Figure 2.1 - (B)). Briefly, we used the proprietary algorithm from the activPAL, which identifies stepping [66, 70]. Then, we grouped consecutive stepping bouts into stepping periods if the individual was standing (based on the activPAL classification) for less than 1 minute in between two stepping bouts. The objective of this grouping is to capture the discontinuous nature of real-world walking. For instance, if an individual stops at a pedestrian light before crossing, the

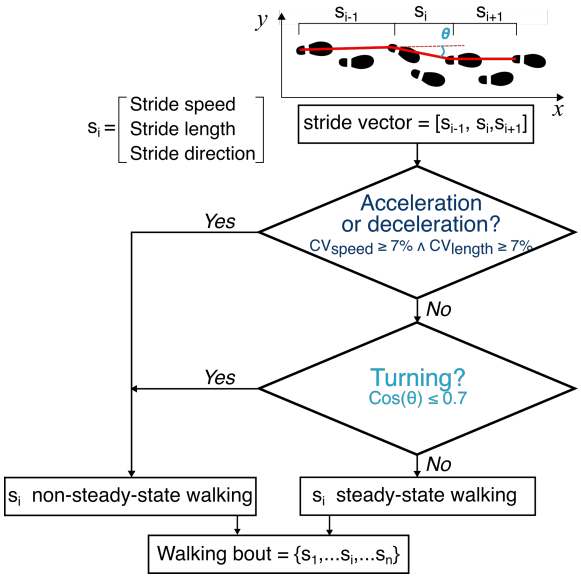

Figure 2.2: **Steady-state identification flowchart** — The algorithm and the cutoff choices are detailed in Appendix A.3 (CV: Coefficient of Variation)

walk before and after that stop were grouped together in a stepping period. Lastly, the activPAL algorithm does not distinguish between running and walking within stepping. Thus, we developed a classification algorithm to extract walking periods from all stepping periods.

2.2.2.2 Walking Speed Estimation for a Walking Period

Once we extracted walking periods for each participant, we used the foot-worn IMU data to estimate stride speed (Figure 2.1 - (B)). Heel strike events in a stride create high peaks in angular velocity that allow for stride detection. The x-axis signal, around which the foot flexes, was smoothed using a locally weighted scatterplot smoothing (LOWESS) method. A peak detection method was applied to isolate strides. Walking periods with less than 5 strides were discarded to reduce errors in gait parameter estimation. To estimate stride speed, we used the zero-velocity update (ZUPT) algorithm [39, 40, 67]. This algorithm leverages the assumption that the velocity of the foot on the ground is close to zero when a human is walking to integrate the acceleration while correcting for the IMU drift. The velocity and position of the foot are subsequently obtained. We followed the implementation formulated by Rebula et al. using the same hardware. From the foot position, we extracted stride length and we calculated stride speed by dividing stride length by stride time.

2.2.2.3 Identification of Real-world Steady-state Walking

A custom algorithm (detailed in Appendix A.3) was used to identify steady-state strides within a walking bout (Figure 2.2). Briefly, we considered a stride to be at steady-state when the individual was walking straight (e.g. not turning), with a constant velocity (e.g., not accelerating nor decelerating). We started by creating rolling windows of 3 strides in a walking bout with a 2-stride overlap. The second stride of each window was classified as steady-state or non-steady-state using the foot-worn IMU data. The first and last strides of a bout were discarded. Then, for each window, we created a vector with the three stride speeds and stride lengths calculated using the method outlined in the previous sub-section (Walking Speed Estimation for a Walking Period). From these vectors, we calculated the coefficients of variation (CV_{speed} and CV_{length}) to measure whether stride length and stride speed varied, indicating a possible acceleration or deceleration. If both of these coefficients were above 7%, we classified the stride as non-steady-state. In addition, we calculated cosine similarity between the direction of each pair of consecutive strides. Cosine similarity measures the similarity between two vectors and is bounded between 0 and 1. If the cosine similarity was under 0.7 (e.g., the stride directions are separated by a 45-deg angle), the stride was classified as non-steady-state. Otherwise, the stride was classified as steady-state. The thresholds for the different parameters were determined by conducting a sensitivity analysis as detailed in Appendix A.3. We evaluated this algorithm using a controlled experiment.

2.2.2.4 Real-world Walking Contexts

We manually labeled each walking period using a combination of the manual log given by the participant, the exit interview, and the GPS data (Figure 2.1 - (B)). For each walking period, we visualized the log entry with a satellite view of the GPS data to isolate the location and purpose of a walk. This process allowed us to isolate repeated locations for a participant, such as their home and workplace. Once all participants' data were labeled, we isolated six common contexts: *Work*, *Commute* (e.g., repeated trajectories between home and work), *Pleasure* (e.g., from the pleasure walk that was specifically asked from participants and labeled as such), *Shopping*, *Home*, and

Other Outdoor (e.g., any outdoor walk that was not classified as pleasure or commute). Other walks such as within a church, at the amusement park, or dog walks were labeled as *Other* as they were rare and often specific to a given participant. The few walking periods ($< 1\%$) that had missing labels were also labeled as *Other*.

2.2.2.5 In-lab Modelling of Cost of Transport against Stride Speed

We used the force plates from the instrumented treadmill to detect gait events. We discarded strides where the participants did not correctly place their feet on the corresponding belt. The heel marker was used to extract stride length since it moved the least throughout the trials (as opposed to the toe marker for instance that was scrunched during plantar flexion) and never got obstructed from our camera setup. To calculate stride length, we multiplied stride time by the speed of the treadmill belt (assumed constant), and we added the distance between two consecutive foot strikes from the same foot to account for back and forth movement of the participant on the treadmill. Stride speed was then calculated by dividing stride length by stride time.

To obtain metabolic rate at steady state, we used the last 2 minutes of each 6-min trial. The breath-by-breath measurements from the indirect calorimetry system were averaged; then, the Brockway equation was used to estimate whole-body metabolic rate [74]. Finally, we subtracted the resting metabolic rate measured during the quiet standing period. To ensure the validity of the derivation, we made sure the respiratory quotient never exceeded 1. We calculated cost of transport by dividing the metabolic rate by stride speed and normalizing by body mass. Lastly, we identified the coefficients of a 2nd order polynomial curve mapping cost of transport to stride speed using the MATLAB curve fitting toolbox. To identify the energetically optimal speed range, we looked at the minimum cost of transport value and added 10%. This resulted in two points on the cost of transport curve, one on the left and one on the right side of the minimum. The associated speeds with these two values of cost of transport were used to define the lower and higher boundary of the energetically optimal speed range. Specifically, the speed corresponding to the point on the left side of the minimum cost of transport represents the lower boundary, while the speed corre-

sponding to the point on the right side represents the higher boundary. By considering the range of speeds between these two points, we can identify an energetically optimal speed range where the cost of transport is minimal. To quantify whether humans used a walking speed within this energetically optimal range, we evaluated the proportion of steady-state strides for each context within the identified range.

For three participants, the measurements of metabolic rate failed for different reasons. One participant's respiratory quotient was consistently over one. The other did not place the mask properly and had only a limited number of breaths that were registered which did not allow for a sufficiently accurate estimate of metabolic rate. Finally, many participants reported that the mask irritated their eyes and caused nose congestion. One participant could not complete the trial for this reason. We suspect this particular discomfort came from the solution (cidex) used to disinfect the mask between participants.

2.2.3 Statistical Analysis

A t-test was used to evaluate if participants selected walking speeds that minimize their cost of transport. We tested if the difference between the observed distribution of steady-state stride speeds estimated during daily life and the energetically optimal speeds measured in the lab were significantly different than 0. To test if walking speeds that minimize cost of transport were independent of context, we calculated the percentage of real-world steady-state stride speeds within the energetically optimal speed range for each context and participant. We chose to use a linear mixed model to account for the random effect of participants within each context, given the hierarchical structure of our dataset (context was classified for identified walking periods for each participant) [75]. We compared different model complexities (with and without random effects) using the Akaike Information Criterion (AIC) [75, 76] and selected the model that explained the most variance in the data. The tests' significance was evaluated at the 0.05-level. All statistical analyses were conducted in R.

2.3 Results

2.3.1 Real-world Walking Behavior

We found 1,731 walking periods across all participants that met our criteria for steady-state (Figure 2.2 and Appendix C), with a total of 304,309 strides (Table 2.2). The majority (64%) of walking periods were under 5 minutes, with 15% under 1 minute (Figure 2.3). The context *Pleasure* contained the most strides (steady-state and non-steady-state) across participants and for almost all individual participants, although S4 and S9 did not take any pleasure walks. The context *Commute* also gathered around 7% of all strides even if only 8 participants had walks in this context (only 45 walking periods total). Gait observed during *Work* contained 25% of the total identified walking periods, but the average duration of these walks was the smallest (2.7min) and represented a little less than 5% of the total identified strides. It is important to note that the proportion of strides within each context was conditioned by the wear of the different sensors. As such, contexts like *Home* may be underrepresented because participants likely remove their shoes (and consequently the foot-worn IMU) when home.

Table 2.2: **Walking periods characterization** — There are variations between contexts in the number of strides and walking periods, as well as the proportion of steady-state within a walking period. Contexts with longer walking periods tend to have less walking periods, but more strides and steady-state strides.

	# Strides	**# Walking Periods**	**# Steady-state strides**	**Avg steady-state strides within walking period [%]**	**Avg Walking period duration [min]**
Other Outdoor	90,292	228	72,210	71.9	11.4
Pleasure	95,506	115	82,520	82.4	20.9
Commute	21,082	45	18,181	85.9	12.6
Work	14,173	431	7,524	48.4	2.7
Shopping	12,752	143	8,176	50.9	5.1
Home	15,338	344	5,681	30.7	4.3
All Walks	304,309	1,731	230,515	51.7	6.5

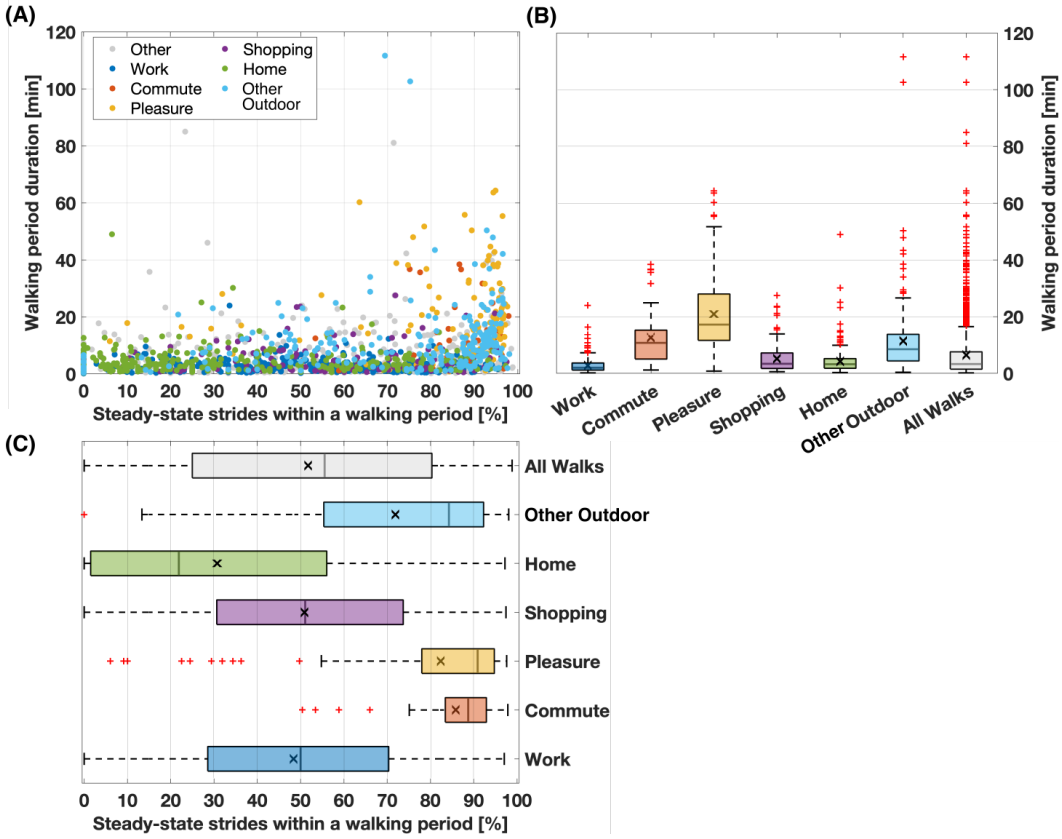

Figure 2.3: **Walking periods duration and their proportion of steady-state strides** — Relationship between walking period duration and percentage of steady-state strides within a walking period — (A) Each dot corresponds to a walking period. The different colors are for each context. (B) We binned all walking periods by their bout duration and looked at the percentages of steady-state strides within a walking period for each bin. (C) We binned all walking periods by their percentage of steady-state strides and looked at the walking period durations for each bin.

2.3.2 In-lab Cost of Transport Models

We mapped cost of transport to walking speed using data collected during the in-lab treadmill walking task (Figure 2.1 - C). The models had an average R^2 of 0.78 and RMSE of $0.20 J/kg/m$. Energetically optimal speeds that minimized cost of transport varied between individuals (Table 2.4 and Figure 2.5), ranging from $0.82 m \cdot s^{-1}$ for S8 to $1.37 m \cdot s^{-1}$ for S4 with an average minimum cost of $1.83 J/kg/m$.

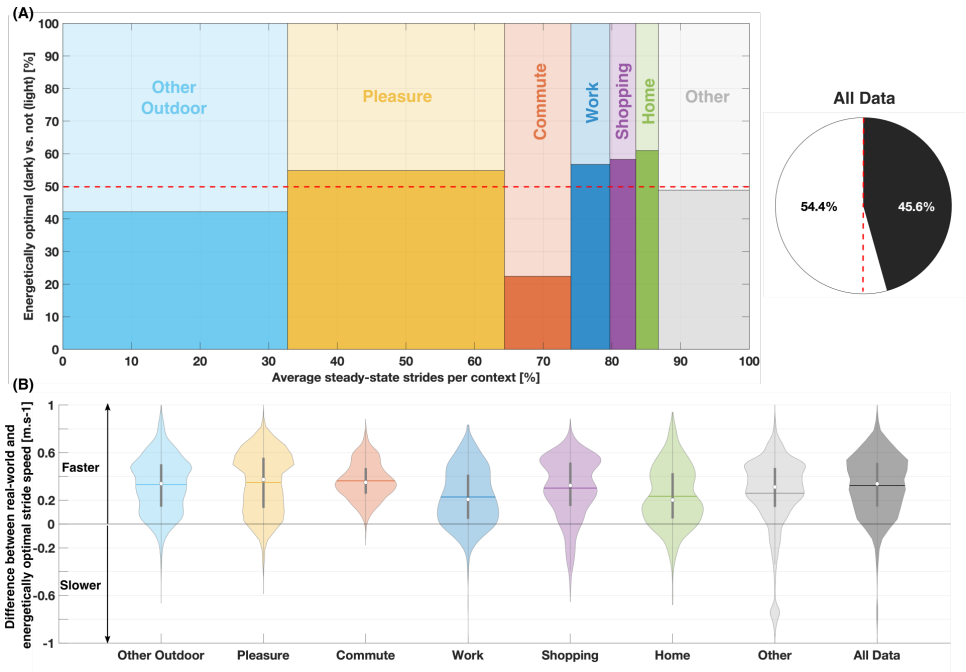

Figure 2.4: **Energetic optimality for steady-state strides in each context** — (A) Proportion of steady-state strides for each context for all participants with the associated proportion of strides within the energetically optimal speed range. The darker part of each bar represents the proportion of strides with speeds within the energetically optimal range. For instance, we read that the context Pleasure represents approximately 35% of the data and that a little more than half of the strides have a stride speed within the energetically optimal speed range. (B) Distribution of stride speed subtracted by the subject-specific speed at the minimum cost of transport for all subjects in each context. Each shaded area represents the shape of the distribution, and the horizontal lines mark the mean. For instance, we read that participants walked on average $0.35m \cdot s^{-1}$ faster than their energetically optimal when commuting.

2.3.3 Steady-state Walking and Context

Overall, an average of 51.7% of the identified strides were classified as steady state, but the percentage of steady-state strides varied by context. Around 30% of the strides identified during walking at home were steady state, while 86% of the strides during a commute were steady state (Figure 2.3). We observed high variability in the proportion of steady-state strides during walking in indoor contexts (e.g., *Home*, *Shopping*, and *Work*) (Figure 2.3). On the other hand, these particular contexts had a low variability in walking period duration with averages between 2.7 minutes for *Work* and 5.1 minutes for *Shopping*. Figure 2.4 presents a summary of the identified steady-state strides based on both context and energetically optimal stride speeds. We found that contexts containing

longer duration walking periods, such as *Commute* or *Pleasure*, also contained a higher percentage of steady-state strides (32.7% and 31.6% of all steady-state strides respectively).

Table 2.3: **Linear Mixed Model Coefficients**

	b	***SE b***	**p-value**
Commute	28.1	10.6	0.010
Home	34.0	9.7	0.001
Other Outdoor	13.1	9.6	0.098
Pleasure	29.3	9.9	0.004
Shopping	27.1	10.65	0.014
Work	31.3	10.0	0.003

2.3.4 Cost of Transport Minimization and Walking Speed Variability

Figure 2.4 — A) shows the proportion of energetically optimal speeds for each context and for all data. The distribution of the difference between real-world and energetically optimal stride speed for all participants combined is shown in Figure 2.4 — B). Figure 2.5 shows this same distribution but for each individual in each context. We tested whether our participants walked in the real world at speeds comparable to the energetically optimal speeds identified in the lab. We found that, across all participants and contexts, participants walked at a stride speed significantly higher than the energetically optimal ($p < 0.05$), with a mean difference of $0.32m \cdot s^{-1}$ (30% increase). However, a large percentage of the steady-state strides were still at energetically optimal speeds. Overall, participants walked within the energetically optimal range for $45.6\% \pm 33.0\%$ of their strides (Figure 2.4 and Figure 2.5). Next, we tested whether there was a dependence between the use of an energetically optimal walking speed and context. We found a significant relationship between the proportion of energetically optimal speeds (e.g., real-world stride speeds within the energetically optimal speed range) and contexts across participants, $SD = 0.29$ (95% CI: 0.19, 0.42). All contexts, apart from *Other Outdoor*, significantly predicted the proportion of strides at energetically optimal speeds. *Commute* was arbitrarily chosen as the baseline for the model. The coefficients indicate that participants were more likely to use energetically optimal speeds

in all contexts when compared to *Commute* (Figure 2.4). All of the coefficients are reported in Table 2.3. Individuals walked much faster when commuting relative to both the other contexts ($\sim +0.14m \cdot s^{-1}$) and to the energetically optimal speed range ($\sim +0.36m \cdot s^{-1}$).

The values and the variability of walking speed changed from one context to another for the same participant (Table 2.4 and Figure 2.5). For example, during commutes and pleasure walks, S1 exhibited low variability, but largely different walking speeds with a more energetically optimal walking speed used during pleasure walks ($\mu = 1.70 \pm 0.10m \cdot s^{-1}$ and $\mu = 1.34 \pm 0.06m \cdot s^{-1}$, respectively). On the other hand, when shopping or at work, the variability in the walking speeds was larger with greater overlap with the energetically optimal speed ranges ($\mu = 1.47 \pm 0.23m \cdot s^{-1}$ and $\mu = 1.46 \pm 0.16m \cdot s^{-1}$, respectively).

Table 2.4: **Subject-specific data** — Each participant had a different economical speed range, leading to varied proportions of economical walking speeds in the real world for the different contexts. For each context, participants displayed different walking strategies as well.

	Eco speed range	**Work**			**Commute**			**Pleasure**		
		# Walking Periods	# steady-state strides	Stride Speed (μ, σ)	# Walking Periods	# steady-state strides	Stride Speed (μ, σ)	# Walking Periods	# steady-state strides	Stride Speed (μ, σ)
S1	[1.12,1.36,1.59]	43	774	(1.46,0.16)	4	5027	(1.70,0.10)	1	532	(1.34,0.06)
S2	[0.63,0.86,1.10]	0	0	-	0	0	-	2	3329	(1.40,0.07)
S3	[0.74,1.00,1.26]	37	1104	(1.43,0.20)	11	977	(1.49,0.12)	1	787	(1.27,0.07)
S4	[1.11,1.37,1.62]	0	0	-	1	344	(1.57,0.06)	0	0	-
S5	[0.73,1.02,1.31]	16	531	(1.54,0.13)	1	257	(1.59,0.10)	18	13506	(1.67,0.08)
S6	[0.71,1.08,1.44]	118	1275	(1.09,0.12)	0	0	-	10	4653	(1.09,0.13)
S7	[0.97,1.27,1.27]	13	352	(1.27,0.15)	0	0	-	8	7784	(1.30,0.09)
S8	[0.37,0.82,1.28]	11	220	(1.24,0.12)	0	0	-	8	9661	(1.35,0.06)
S9	[0.43,0.94,1.46]	21	326	(1.36,0.10)	2	450	(1.60,0.10)	0	0	-
S10	[0.81,1.09,1.37]	11	173	(1.48,0.19)	4	2044	(1.54,0.10)	6	3863	(1.42,0.11)
S11	[0.84,1.05,1.26]	9	121	(1.23,0.09)	3	2532	(1.34,0.08)	9	11013	(1.30,0.10)
S12	[0.96,1.16,1.37]	0	0	-	0	0	-	9	2119	(1.14,0.09)
S13	[0.84,1.18,1.53]	44	981	(1.37,0.14)	0	0	-	5	927	(1.18,0.10)
S14	[0.66,0.96,1.26]	0	0	-	0	0	-	3	2837	(1.39,0.11)
S15	[0.78,1.07,1.37]	60	715	(1.27,0.15)	13	5103	(1.41,0.19)	4	2123	(1.28,0.12)
S16	[0.56,0.89,1.22]	0	0	-	0	0	-	8	3552	(1.35,0.31)
S17	[0.80,1.08,1.36]	2	1	(1.63,0)	0	0	-	1	550	(1.29,0.08)

	Eco speed range	**Shopping**			**Home**			**Other Outdoor**		
		# Walking Periods	# steady-state strides	Stride Speed (μ, σ)	# Walking Periods	# steady-state strides	Stride Speed (μ, σ)	# Walking Periods	# steady-state strides	Stride Speed (μ, σ)
S1	[1.12,1.36,1.59]	9	174	(1.47,0.23)	9	264	(1.48,0.08)	21	2254	(1.46,0.19)
S2	[0.63,0.86,1.10]	31	755	(1.29,0.17)	11	59	(1.11,0.33)	10	8240	(1.39,0.15)
S3	[0.74,1.00,1.26]	13	333	(1.29,0.21)	11	28	(1.24,1.16)	9	2740	(1.50,0.07)
S4	[1.11,1.37,1.62]	0	0	-	3	5	(1.16,0.03)	10	4286	(1.53,0.09)
S5	[0.73,1.02,1.31]	0	0	-	6	22	(1.55,0.20)	19	3811	(1.62,0.19)
S6	[0.71,1.08,1.44]	6	588	(1.23,0.18)	10	592	(1.18,0.12)	2	3215	(1.20,0.10)
S7	[0.97,1.27,1.27]	13	316	(1.14,0.15)	13	212	(1.28,0.09)	0	0	-
S8	[0.37,0.82,1.28]	10	1994	(1.38,0.08)	32	150	(1.36,0.12)	14	7443	(1.36,0.11)
S9	[0.43,0.94,1.46]	0	0	-	0	0	-	2	515	(1.49,0.08)
S10	[0.81,1.09,1.37]	5	237	(1.44,0.14)	7	124	(1.39,0.09)	27	6157	(1.52,0.13)
S11	[0.84,1.05,1.26]	0	0	-	8	22	(1.23,0.09)	19	10499	(1.36,0.12)
S12	[0.96,1.16,1.37]	11	360	(1.12,0.15)	1	9	(1.20,0.04)	47	10980	(1.19,0.11)
S13	[0.84,1.18,1.53]	8	497	(1.16,0.21)	5	32	(1.40,0.14)	6	1526	(1.44,0.12)
S14	[0.66,0.96,1.26]	0	0	-	82	753	(0.96,0.15)	0	0	-
S15	[0.78,1.07,1.37]	0	0	-	5	7	(0.65,0.14)	4	2444	(1.42,0.13)
S16	[0.56,0.89,1.22]	5	76	(1.01,0.16)	21	1333	(1.33,0.20)	7	1543	(1.51,0.41)
S17	[0.80,1.08,1.36]	15	1741	(1.35,0.10)	26	345	(1.28,0.16)	6	1456	(1.34,0.09)

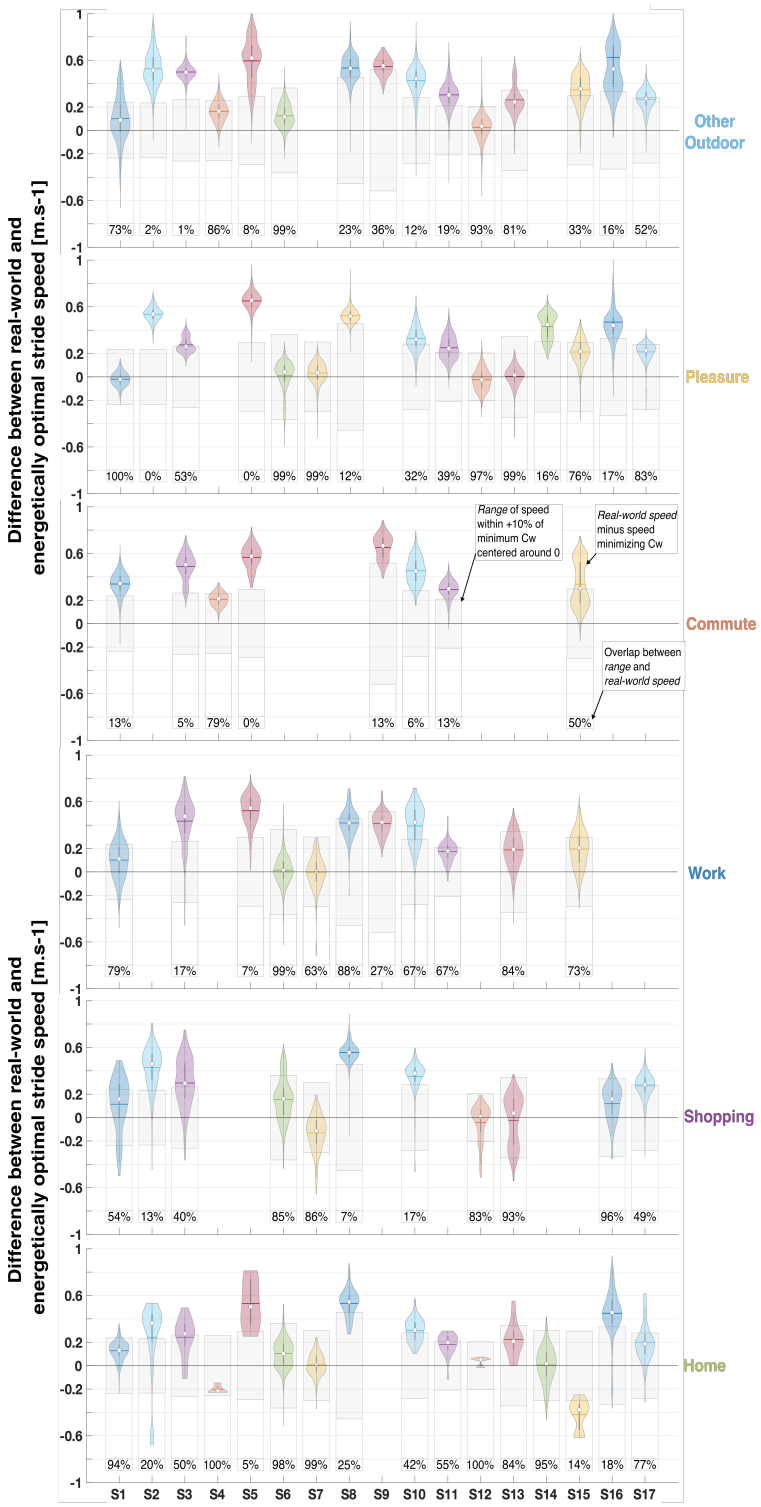

Figure 2.5: **Steady-state stride speed distributions and proportion of energetically optimal strides for each context** — Each shaded area represents the shape of the distribution of stride speed subtracted by the speed at the minimum cost of transport for the different contexts for a subject, with the horizontal line for the mean. The energetically optimal speed range is centered around 0 and represented by the grey boxes. The percentages are the proportion of speeds within the energetically optimal speed range. Some individuals had no data for a given context.

2.4 Discussion

Laboratory-based studies have found that individuals tend to use walking speeds that minimize cost of transport. Building on these results, the work presented here investigated walking economy in the real world by testing two hypotheses: (1) on average, individuals will self-select energetically optimal walking speeds and (2) the use of energetically optimal walking speeds is independent of context. We rejected both hypotheses as we found that: (1) participants most often used faster walking speeds than what is energetically optimal and (2) the proportion of walking speeds within the energetically optimal range varied based on context. This suggests that individuals have multiple competing objectives when walking in the real world, including minimizing cost, which influences walking strategy.

Real-world Walking Economy, Context, and its Applications Various in-lab studies have observed a convergence of different kinematics parameters towards an energetically optimal movement pattern [21, 24, 25]. Most of these studies were conducted in the lab, during steady-state walking, where participants walked for bouts shorter than 20 minutes. As such, we expected to see a similar relationship in the real world, particularly during long walks at steady state. First, we found that individuals walked approximately 30% faster in the real world compared to their energetically optimal speed across all contexts. Second, the amount of energetically optimal speeds that an individual used was found to be dependent on context.

We observed that the predominantly indoor contexts (*Shopping*, *Work*, *Home*) contained the most energetically optimal strides. In these contexts, physical constraints like halls, doors, rooms, and furniture may affect how individuals are able to move in the environment. While only around 12% of all steady-state strides were observed during these contexts, these constraints (e.g., with many starts/stops, and turns) might have led participants to slow down and walk at a stride speed closer to their energetically optimal (Figure 2.4 and Figure 2.3). These contexts also resulted in high variability in walking speeds, which might have led to a bigger overlap with the energetically optimal speed range (Figure 2.4 and Table 2.3). We expected participants to select energetically

optimal speeds in the contexts *Other Outdoor*, *Pleasure*, and *Commute*, as they contained longer walking periods with more steady-state behavior (Figure 2.3). These three contexts contained around 74% of all data. We found that 55% of the steady-state walking speeds during a *Pleasure* walk were energetically optimal, compared to 42% and 22% for *Other Outdoor* and *Commute* respectively. It is important to note that we specifically asked participants to take ”pleasure walks” to elicit a walk without any particular destination or objective other than walking. Therefore, the higher proportion of energetically optimal strides within this context may reflect the results from laboratory-based studies as there were no other competing objectives. In contrast, the other outdoor walks and commuting on foot often have fixed destinations and time constraints (e.g., getting to work on time), which could explain the use of faster walking speeds that have a higher energetic cost. This difference was particularly clear for commuting, where the highest walking speeds were measured (Table 2.3).

These findings can provide insight into research aiming to develop technological advancements based on human energetics, such as research in lower-body assistive devices. In fact, these fields of research often consider energy minimization as the main optimization objective. However, our results suggest that, depending on the context in which someone is walking, they may not prioritize walking at energetically optimal walking speeds. These walking speeds could still be optimal but for a different objective than energy minimization. It is possible that, given the many constraints of our real-world environment, individuals cannot necessarily use predominantly energetically optimal behavior. As such, experimental designs should evolve to take into account real-world scenarios in order to ensure the ecological relevance of technological innovations. In Slade et al., a subject-specific optimization of a lower-body exoskeleton was carried out in the real world [64]. The researchers recreated a realistic real-world scenario where participants walked short bouts in an uncontrolled environment, using ”ecologically relevant audio prompts” that elicited variability in the walking speed used by the participants. Such experimental design ensures that the technology (here an exoskeleton) can be used by individuals across different contexts and walking behaviors.

It is difficult to quantify the potential energetic consequences or penalties on the metabolism that someone experiences or perceives when deviating from their energetically optimal walking patterns. Across all individuals, we observe deviations in stride speed from the energetically optimum up to $0.65m \cdot s^{-1}$ (e.g., 57% more from min cost of transport for S5 in the context *Pleasure*). In Medrano et al., they estimated the "Just Noticeable Difference" in metabolic rate that individuals perceived with the assistance of a lower-body exoskeleton walking on a treadmill [77]. They found that participants (N = 10) were able to perceive changes of around $20\% \pm 5\%$ with an accuracy of 75%. Thus, individuals may be mostly unable to perceive the deviations we observed from the energetically optimal walking speed. Even if participants could perceive the deviation, the energetic penalty could potentially be negligible given that most walks were relatively short in distance and duration (Figure 2.3).

Steady-state Walking in the Real World In the animal kingdom, the best locomotion strategy depends on context and might not always involve steady-state. A prey evading a predator utilizes transient states with high acceleration that prioritize maneuverability over energetic consumption [78]. In this work, a large portion of the observed movement occurred during non-steady-state/transient behavior (48.3% of all strides were classified as non-steady-state), although participants did not have to evade predators (as far as we know). The proportion of steady-state strides was dependent on context. As expected, walks in more spatially constrained contexts (ex: at home) contained more non-steady-state behavior (Figure 2.3) [79]. Although fewer strides were identified in these contexts (compared to *Commute* or *Other Outdoor* for instance), they contained more walking periods. In other words, when an individual stood up to walk, they were more often inside, in contexts such as *Work* or *Home* (22.2% and 14.4% of walking periods, respectively). This prevalence of transient behavior highlights the importance of studying all types of human movement that can be observed in the real world, particularly for health and mobility. For example, LA King et al. leveraged the importance of turns and the potential risks associated with people with

Parkinson's Disease when turning [80].

Variability in Walking Strategy We observed large variability within the identified steady-state strides between, and within individuals. Between individuals, we noted a large variability in the overlap between the energetically optimal speed range and the real-world speed distribution within the same context (Figure 2.5). Overall, individuals used walking speeds that were faster than energetically optimal, but there did not seem to be a way to predict the overlap size for a given context for all participants. For instance, in the context *Pleasure*, the overlap ranged from 0% to 100%. This suggests that other variables could potentially explain the variability between individuals, such as fitness level. Second, within individuals, we observed a large variability in the walking speed used for different contexts (Figure 2.5 and Table 2.3). For instance, both *Commute* and *Other Outdoor* contained long walking periods with a large proportion of steady-state strides (Figure 2.3). However, we measured differences in walking speed up to $0.24m \cdot s^{-1}$. Preferred walking speed is a clinically important parameter used to quantify health and well-being [10, 81]. The variability observed in our data makes it challenging to estimate preferred walking speed in the real world. Speed estimated during a *Pleasure* walk is the least likely to be influenced by context, and may be the most comparable to data collected in the lab. However, future work should investigate whether leveraging the ensemble of the data and deriving a usable range of speeds to characterize preferred walking behavior could be a stronger health indicator. Taken together, these variabilities in walking strategy confirm that researchers should consider designing experiments that allow participants to display the range of behavior they naturally use in the real world. Additionally, the development of subject-specific models to capture an individual's natural movement profile could lead to more accurate representations of an individual's health and well-being.

Limitations and Potential Opportunities Our experimental design combined in-lab and real-world measurements. We built subject-specific energetically optimal speed ranges during in-lab measurements on the treadmill, and compared these ranges to real-world measurements. However, to mitigate the effect of the differences between the laboratory and the real world, we: 1) enforced

the relationship between stride speed and stride length found in the real world on the treadmill (Appendix A.2), and 2) used a large uncertainty interval of $+10\%$ around the minimum cost of transport (which creates a range of speeds that correspond to the minimum of the cost of transport curve) to capture possible differences between the lab and the real world. Additionally, future research should broaden the population diversity and increase the sample size. The methods and insights from this chapter could potentially be relevant for clinical populations. Finally, we defined context as a combination of location and purpose; however, there are many external contextual factors we did not include, such as terrain type or topography. Future studies should also consider internal contexts, such as an individual's mood or fatigue, as they may play a role in someone's movement in the real world.

2.5 Conclusion

Researchers now have the ability to measure human movement in the real world. Persistent monitoring is a powerful tool that can create rich datasets and provide a unique understanding of natural human behavior. In this chapter, we found that humans walk in a variety of contexts and exhibit a wide range of walking strategies and behavior. Consequently, individuals do not necessarily use a walking speed that minimizes their cost of transport in the real world. Overall, we recommend that researchers take into account the possible discrepancies between in-lab and real-world behavior when studying walking biomechanics. For instance, in-lab experiments can be designed to simulate real-world conditions to fully represent an individual's movement profile and capabilities. We believe the findings of this work can provide insight for improvements in the study of human mobility for health, but also in robotics for the design of lower-body assistive devices.

However, though providing a rich dataset, the data collection in this chapter can be burdensome for long-term monitoring. To ensure individual compliance in the real world, there is a need to develop methods that utilize a reduced sensor set, while providing meaningful information about an individual's movement and health. Therefore, in the next chapter, we present a method for the estimation of walking speed in the real world, using an accelerometer only.

CHAPTER 3

Estimating Walking Speed Using an Accelerometer Only

3.1 Motivation

Efforts to combat and prevent various health issues have shown physical activity to be vital in maintaining, improving, and even recovering cardiovascular health [82]. The ability to assess an individual's level of physical activity is a critical component of clinical evaluations. Questionnaires are often used to gather information about activity levels during daily life. However, among the large variety of existing questionnaires, it is uncertain whether these survey instruments are capable of representing reliable and valid quantification of a patient's activity level [83]. With recent technological progress in wearable sensing technology, fitness trackers offer a promising complementary tool for clinical assessments. Activity trackers are devices, usually in the form of a wristband, that are used to monitor physical activity in the free-living environment by deriving metrics such as estimated energy consumption, distance traveled, or step count. These activity budgets can be used by clinicians to prescribe tailored treatments, as well as to monitor adherence to these prescriptions [84–86]. Summary metrics from wearable sensors provide insight into the type and duration of physical activity. However, to provide information for clinical assessment of overall health, quantitative metrics from key activities such as walking speed should be accessible. Walking is a central activity of daily living; it is an easy, safe, and accessible aerobic exercise and does not require specialized skills or equipment. Given the cardiovascular benefits of walking,

this low-impact activity is often prescribed for patients as a way to meet their required amount of physical activity [7]. Walking speed can be used as a metric to capture the intensity of walking and serve as an effective surrogate to evaluate fitness [6, 87]. The correlation of walking speed with functional decline has also made it a widely used predictor for various health issues [81, 88]. In addition to the strong association with well-being, gait speed can be obtained in a clinical environment, is cost-effective, and is easy to interpret [10]. Clinical walking tests typically estimate walking speed by timing the subject as they walk a prescribed distance or by measuring the distance a subject can walk in a prescribed amount of time. However, the available space and time constraints imposed in clinical settings can lead to variations in the duration, distance traveled, and instructions provided to the patient when measuring speed [12, 13]. High day-to-day variabilities in the results of the same tests have also been observed [15]. In most cases, a manual stopwatch is used to measure time, which can lead to significant measurement errors when conducting short tests. Consequently, the different measurement approaches typically used in clinical settings do not provide consistent estimates of walking speed. Further, few studies have compared speed measured in the clinic to measurements during natural walking in a free-living environment [29, 30]. As there are fundamental contextual differences between supervised (e.g. laboratory or clinic) and unsupervised (e.g. free-living) environments [26], it is unclear whether the values of walking speed extracted in a clinical setting are representative of the true walking behavior of an individual. To further enhance clinical understanding of real-world gait performance, metrics from free-living observations must be provided.

The analysis of walking gait in the real world has benefited greatly from technological advancements in wearable technologies. In particular, with the development of micro-electromechanical systems (MEMS), inertial measurement units (IMUs) have become compact and low-cost, which make them instruments of choice for walking gait analysis [32]. High-resolution measurements are now possible outside laboratory settings [55, 89], with non-intrusive sensors, enabling the quantification of walking behaviors in a free-living environment over extended periods of time [48]. Among other walking parameters, stride speed can accurately be measured using a foot-worn IMU

[38–41]. However, IMUs present several challenges that limit their current use in real-world, long-term monitoring of clinical populations. Many sensors of this type need to be recharged after daily use and are usually secured to the body using elastic straps, which can lead to compliance issues (e.g. sensors lose power and stop collecting data, sensors are not donned at the beginning of the day). Additionally, research-grade IMUs often require the use of specific software packages to configure/reconfigure the devices to collect and download data. Alternative types of mobile accelerometry exist, which solve both compliance and battery life issues, though at the cost of a decrease in resolution (decreased sampling rate, no measure of angular velocity). These accelerometer-only devices are lighter in weight, smaller in size, and can be embedded in a belt or shoe sole [65, 90, 91], or worn on the leg for an extended period of time [92]. With these devices, there is no direct approach to measuring or calculating walking speed from the extracted signals. Some machine learning methods have been developed to estimate free-living walking speed from specific accelerometer-based sensors [93], or smartphones [94, 95]. However, the different models in [93–95] were mostly tested and validated in a supervised environment, using short distance walks in hallways, treadmills, or a measuring wheel rather than in the real world during unconstrained and unsupervised walking [26]. New validated models that derive speed using data from acceleration-only devices used in free-living environments remain an open research problem.

To help extend the wearable sensing paradigm to the clinical setting, we focus here on creating an efficient approach that combines fine-scale and low-resolution long-term measurements to estimate gait speed in the free-living environment. We use a low-power accelerometer secured on the thigh to address compliance and battery life issues; this sensor is used to make precise measures of stride frequency. Using a foot-worn IMU, high-resolution acceleration and angular rate measurements were used to calculate stride speed. Metrics from both systems were then leveraged in a custom-designed walking task to build a subject-specific data-driven walking model, mapping stride frequency to stride speed. To demonstrate the ecological validity of this model, walking data was collected in the free-living environment with both an IMU on the foot and the body-worn accelerometer. We define the accuracy of our model in estimating gait speed as the agreement be-

tween the model and IMU measurements, which have been used as a viable assessment of walking speed in an unsupervised real-world environment [38–41]. Once validated, this approach can then be used to perform monitoring on a week-long scale, with thorough quantification of the walking activity, to allow clinicians to gain a unique insight into the physical health of a subject in their natural environment.

3.2 Methods

3.2.1 Subjects

Ten subjects were recruited from a healthy population (Table 3.1). Leg length, defined as l_0, was measured from the anterior superior iliac spine to the floor, without shoes. The experiments were conducted in the free-living environment of each subject as no specific setting was required. Each participant provided written consent on a form where the purpose and detailed experimental protocol was explained. The data collection for this chapter was approved by the Institutional Review Board of the University of Michigan.

Table 3.1: **Subject Information**

	leg length l_0 [m]	**height [cm]**	**weight [kg]**	**age [yr]**	**gender**
Subject 1	0.94	169	71	23	F
Subject 2	0.91	160	54	36	F
Subject 3	0.88	160	53	22	F
Subject 4	1.01	179	70	23	M
Subject 5	0.94	165	64	22	F
Subject 6	1.06	178	70	38	M
Subject 7	0.99	173	68	25	M
Subject 8	1.03	183	70	27	M
Subject 9	1.00	180	71	30	M
Subject 10	1.00	175	75	27	F

3.2.2 Instruments

3.2.2.1 Free-living measurements

The activPAL^{TM} [PAL Technologies Ltd., Glasgow, UK] (AP) monitor is a low-power triaxial accelerometer-based bio-logging tag that can be placed on the thigh using an adhesive bandage tape. This lightweight (9g) waterproof sensor can be worn for seven consecutive days without being removed or recharged. AP's compact size (23.5 x 43 x 5mm) and shape make it an unobtrusive device; reducing the risk that a subject's behavior changes due to the consciousness of being studied (the Hawthorne effect) [26]. Proprietary algorithms enable the classification of the type and duration of different activity states (lying, sitting, standing, stepping, cycling, and driving). Summary metrics such as the number of steps, sit-to-stand transitions, or hours in each activity state are also calculated and summarized from the data. The reliability of this sensor and associated algorithms has been validated in the literature [92].

With a sampling rate of $20Hz$, the acceleration measurements from the AP monitor can be used to accurately detect strides. The sensor is instructed to be placed on the anterior surface of the thigh with the positive x-axis pointing inferiorly, the positive y-axis pointing medially, and the positive z-axis to be pointing anteriorly out of the thigh. Using the classification of the different activity states, bouts labeled as *"Walking"* were extracted from the long-term measurements; short bouts ($< 10s$) were discarded. To extract gait events, we isolated the accelerometer signal from the x-axis of the sensor. The raw accelerometer signal from this axis was smoothed using a locally weighted scatterplot smoothing (LOWESS) method. This technique removed noise while keeping the main peaks of the signal. We applied a peak detection method to identify stride frequency for each smoothed, steady-state walking bout longer than 10 seconds in duration (Figure 3.1). Sections used for analysis were required to contain at least 5 strides. A section started when the first peak above a fixed threshold was detected. Using labeled data, we heuristically determined a threshold of $-8m \cdot s^{-2}$ for all participants, illustrated by a red dashed line in Figure 3.1. We defined a minimum time interval between peaks assuming a minimum stride time

of 0.5 seconds, which corresponds to a very fast walking speed to make sure all strides were captured. We tracked the change in time between two consecutive peaks to identify incorrect peak detections or pauses in a walking bout. These identified outliers marked the end of a section. To account for the anthropometric differences between subjects, values of stride frequency were normalized by $\sqrt{g/l_0}$, where l_0 is the subject's leg length and g is the value of standard gravity [96].

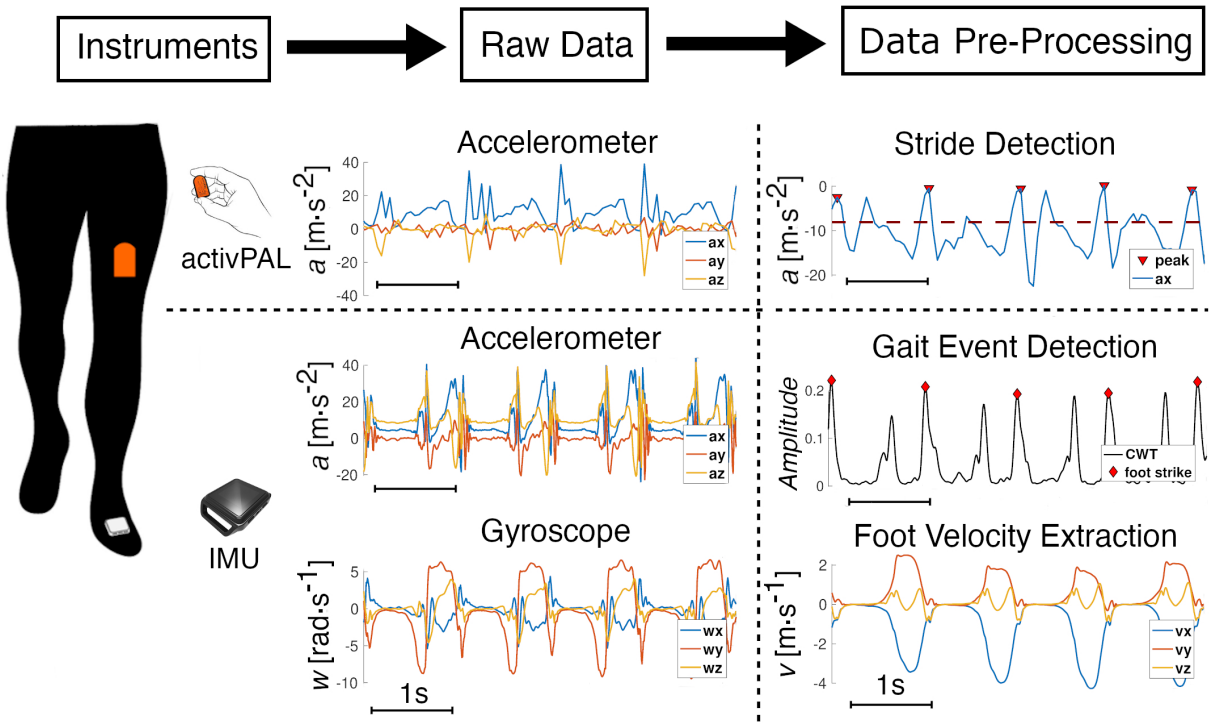

Figure 3.1: **Data Processing** —- Data extraction and pre-processing from the synchronized activPAL (AP) and the IMU. A representative window of 4 strides illustrates the pre-processing of the raw data from both sensors. The AP is worn on the thigh, and the accessible raw data is from the embedded 3-axis accelerometer. The x-axis signal, which is from the sensor-axis that is aligned with the thigh and is positive in the inferior direction, is smoothed and a peak detection (threshold in red-dotted line) method enables the detection of each stride. For the IMU, raw data from the embedded 3-axis accelerometer and gyroscope are processed using a continuous wavelet transform to detect gait events; foot velocity and position are then calculated using a ZUPT algorithm.

3.2.2.2 High-resolution short-term measurements

IMUs offer a reliable alternative to other methods such as optical or electromagnetic motion capture for capturing walking gait data [89]. In this work, we used the Opal sensor from APDM [Portland, OR, USA] which is a wearable IMU with a three-axis accelerometer (range $\pm 200g$), a three-axis gyroscope (range $\pm 200deg \cdot s^{-1}$), and a three-axis magnetometer (range $\pm 8Gauss$). The IMU was worn on the dorsum of the foot, on top of the shoe, using an elastic strap. The x-axis was positive in the distal direction and was aligned with the long axis of the foot, while the positive z-axis pointed superiorly out of the foot. The system was configured to record all signals at $128Hz$, resulting in battery life of at least 8 hours.

Continuous wavelet transform (CWT) was used for gait event detection using inertial sensor signals from real-world gait [97]. The continuous wavelet transforms were used to decompose the signal in the time-frequency domain to detect abrupt changes in a signal. In walking gait, foot strike events are one of the gait events that can be used to single out each gait cycle. They correspond to the impact of the foot on the ground, which creates a sudden variation in the foot acceleration. CWT can then be used on the raw acceleration signal to identify these events. Using custom code written in MATLAB (MathWorks, Inc., Natick, MA, USA), high-frequency content ($> 40Hz$) was kept from the CWT of the accelerations along the three axes, to ensure the analysis was insensitive to sensor orientation. The norm of each transform was summed, and using a peak detection method, we were able to identify foot strike events (Figure 3.1).

After identifying foot strikes, we utilized the zero-velocity update (ZUPT) algorithm to calculate stride lengths. ZUPT is a well-documented technique commonly used in pedestrian navigation systems [39, 41] and provides highly accurate estimates of foot position and stride parameters [40, 67]. IMU estimates of mean stride length and duration have been found to be within 1% of motion capture for walking The ZUPT algorithm [39–41, 67] uses the assumption that the velocity of the foot on the ground reaches zero or close to zero and uses these points of known zero velocity to correct the drift in the estimates of foot velocity. The implementation we used followed the formulation that is presented and evaluated the work in Rebula et al. 2013 and Potter et al. 2019

(which also uses the same hardware). With this method, stride speed and stride length, among other gait parameters, can be accurately calculated. Stride speed was normalized by $\sqrt{g \cdot l_0}$, and stride length by l_0 [96].

3.2.3 Subject-specific Model Derivation

Walking is a cyclic motion of the lower limbs, which can be described by parameters from the time and frequency domain. To minimize the energy consumption of the body, individuals naturally adapt some of these parameters to their walking speed. Particularly, data collected from individuals walking at different speeds have shown that, for each individual, there is a preferred stride length d for a chosen stride speed v [98]:

$$d = a \cdot v^b \tag{3.1}$$

where a and b are the parameters of the model, specific to each individual. Later, a simple walking model predicted the same relationship for a minimal metabolic rate in human walking [73]. Since stride frequency, f, can be expressed as the ratio v/d, Equation (1) can be used to calculate stride speed as a function of stride frequency:

$$v = \exp \frac{\ln (a \cdot f)}{1 - b} \tag{3.2}$$

In the current chapter, the parameters a and b were identified using data from a foot-worn IMU during a "metronome walk" conducted by each subject. In the metronome walk, subjects walked with a wide range of stride frequencies over a flat terrain. The location of the test was different for each participant. Overall, the flat terrains chosen were between 100m and 300m over the duration of the test. Step frequencies were imposed by a metronome set at 45, 60, 75, 90, 105, 120, 135, and 150 bpm. Participants traveled back and forth on the terrain at each step frequency, allowing the sensors to collect a minimum of 10 strides per metronome frequency. The overall time to execute the entire protocol was approximately 15min for every participant. Subjects were asked

to synchronize their steps as best as they could to the beats of the metronome. This protocol was designed to capture a full range of walking frequencies for each individual while walking in an unconstrained environment.

We define stride speed and stride length extracted from the IMU as v_{IMU} and d_{IMU} respectively. These two variables were extracted from each stride of the different walking bouts (defined by stride frequency) using the method described in 3.2.2.2. to identify a and b. Since subjects take a couple of steps to adapt to each stride frequency and tend to slow down towards the end of each walking bout, the transition steps from the beginning and the end of each walking bout were removed from the analysis. Through this designed protocol, we identified the parameters a and b unique to each subject using MATLAB's curve fitting toolbox. This toolbox uses least squares analysis, in our case non-linear least squares, to fit the data with the power model. We used the default fit options for our analysis. (Figure 3.2 - A).

3.2.4 Model Evaluation

The model parameters a and b were determined using measures of stride frequency and stride speed from a prescribed and supervised walk in an unconstrained environment. Thus, there was no certainty that the identified parameters remain the same if walking data was collected in the free-living (unsupervised) environment. Therefore, we designed a protocol to verify that our model can be used in the real-world (unsupervised and unconstrained environment).

Each subject performed a long unsupervised walk at their self-selected pace, with no specific time or environment (inside or outside) constraints, while wearing both an IMU on the foot and the AP on the thigh. Each participant was shown how to place the sensors on themselves through a demonstration. Sensor locations were then verified on each user by examining the raw data. Note that orientation of the sensors did not influence the analysis. The participants were advised to complete a minimum of 30 minutes of walking in total but were free to use the time as they saw fit. To analyze the same walking bouts using both sensors, the IMU data

were downsampled and synchronized with the data from the AP. Then, we identified steady-state walking bouts from which we extracted stride frequency f_{AP} from the thigh-worn accelerometer signal using the methodology introduced in 3.2.2.1. We used the subject-specific models (created as described in 3.2.3) to map each value of stride frequency to its corresponding stride speed v_{AP}. To quantify the error associated with these estimates of stride speed, a ground truth measure of speed was established by leveraging the accuracy of the IMU using the method described in 3.2.2.2. Therefore, with this protocol, we evaluated the performance of our model in an uncontrolled environment over an extended period of time during which natural walking behaviors can be observed (Figure 3.2 - B).

3.2.5 Statistical Analysis

3.2.5.1 Goodness of fit of the subject-specific model

We evaluated the subject-specific models that were built for each subject to quantify the confidence in the identified parameters a and b. The parameters used to evaluate the goodness of fit of the power regression are R-squared (coefficient of determination), the confidence intervals around the identified parameters, and the root mean square error (RMSE). R-squared is a statistic that quantifies how well our models explain the variation of the data. The confidence intervals of a and b quantify the confidence in the fitted coefficients and provide significant insight into whether or not more data are needed to build the model. The RMSE, also known as the standard error of regression, is an assessment of how spread out the data are around the regression line.

3.2.5.2 Analysis of the residuals

Data from the unsupervised long walk were used to evaluate the accuracy of the subject-specific models for predicting walking speed. We utilized multiple statistical methods to allow for direct

comparison with previous and future related work. We used the Bland-Altman analysis to assess the concurrence between the estimated speed from our model and the ground truth walking speed calculated from the foot-worn IMU data. The Bland-Altman analysis is a data visualization tool based on the study of the mean difference and the definition of limits of agreements within which $\sim 95\%$ of the data falls [99]. The distribution of the points around the mean difference and their distance to this value are visual and numerical indicators of the agreement between the estimated (from AP) and the true values (from the foot-mounted IMU) of walking speed. Besides the visualization of the error, the randomness of the points can reveal whether the model chosen (e.g. the power model) is appropriate. By visualizing the Q-Q plot for the estimated and true speed, we confirmed normality of the distributions was a reasonably good approximation.

To complement this analysis, we calculated two other statistical metrics to assess the validity of the created model. The coverage probability (CP_κ) represents the probability Pr that the residuals will be within a defined boundary κ [100]. In this work, it can be translated by the following equation:

$$CP_\kappa = Pr(|v_{IMU} - v_{AP}| < \kappa) \tag{3.3}$$

Three different boundaries were evaluated at 0.1, 0.2, and $0.3m \cdot s^{-1}$. To be able to confidently use the model created in a clinical setting, the error observed between the true and estimated stride speed should be within the minimal clinically important difference. For gait speed, it has been established that the minimal clinically important difference is between 0.1 and $0.2m \cdot s^{-1}$ [101]. Thus, we considered a subject's model valid if $\sim 95\%$ of the residuals were within the $\pm 0.2m \cdot s^{-1}$. We also calculated the concordance correlation coefficient (CCC). This metric has been created to measure the variation of measures (X, Y) from the $X = Y$ line [102]. It represents a more appropriate way to evaluate the correlation between two measurements than the traditional Pearson correlation coefficient, as it captures any location or scale shift in measurements. It can take any value between $0 - 1$, with 1 being a perfect concordance between the measurements.

3.2.6 Model Correction

If the analysis of the residuals revealed a clinically significant difference for a subject, with less than 95% of the residuals within $\pm 0.2m \cdot s^{-1}$, corresponding to $CP_{0.2} > 0.95$, we did an exploratory analysis of the metronome walk data to determine the source of discrepancies between true and estimated speed. We started with an observation of the statistical analyses to localize if a specific range of stride speed was being estimated poorly. This enabled us to find which data in the metronome walk was not representative of the natural behavior of the subject. By combining these observations with the knowledge of the effects in the variation of the parameters of the power model, we designed an iterative algorithm to obtain better estimates of the true parameters a and b. This algorithm started with an initial guess of the parameters based on the observation made on the primary data collected and terminated when the analysis of the residuals led to a valid model as defined in section 3.2.5.2. (Figure 3.2 - A).

Then, we investigated the effects of variations in the parameters a and b to visualize the underlying biomechanics behind the power model. By fixing one parameter and changing the other, we can isolate the influence of each parameter on the shape of the power curve.

3.2.7 Week-Long quantification of the Walking Activity

Once the models were validated, we collected data for one week from the AP worn by one participant from this chapter (Figure 3.2 - C). We identified steady-state walking bouts from the raw accelerometer signal as explained in section 3.2.2.1. Then, we used the model that we built and validated to estimate stride speed from each walking bout. We investigated walking speed across different time scales within a week to explore how the data could be used in future work.

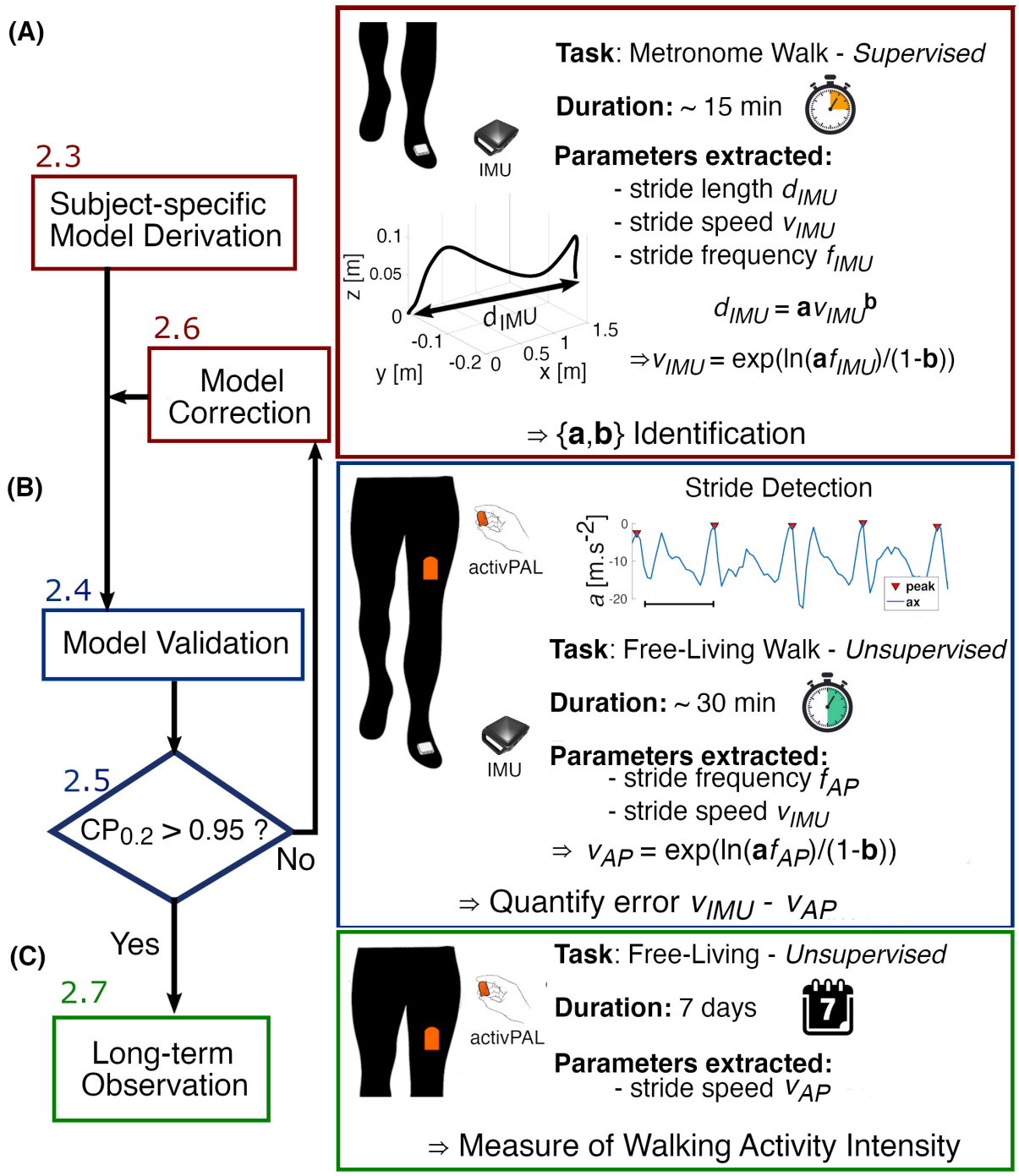

Figure 3.2: **Experimental flow chart** — **(A)** We start by deriving the parameters a and b of the power model using data collected from the IMU worn on the foot during the designed Metronome Walk. **(B)** To verify the accuracy of the model and validate the identified parameters, each subject performs a long unsupervised walk in the real world wearing both the activPAL (AP) on the thigh and the IMU on the foot. The error between the estimated speed from the AP and the speed extracted from the IMU is then analyzed. If the error is not clinically acceptable (Coverage probability with boundaries $\pm 0.2 m \cdot s^{-1}$ $CP_{0.2} > 0.95$), the model is adjusted by finding new parameters a' and b'. **(C)** Once the model is validated, we can proceed to a longer observation with the AP only.

3.3 Results

3.3.1 Mapping from Stride Frequency to Stride Speed

Data from the subject's metronome walk data were used to identify parameters for the power regression model (a and b). The subject-specific models account for at least $\sim 97.8\%$ of the variance, and the maximum RMSE is $0.013 m.s^{-1}$, which indicates a good fit for all models (Table 3.2). We observed maximum confidence interval widths of 0.081 and 0.034 for a and b, respectively (Table 3.2). The parameters a and b vary from 1.961 to 2.295 and 0.292 to 0.397 respectively (Table 3.2). The fitted line for a representative subject illustrates the utility of the designed walking task (Figure 3.3A), which resulted in a wide range of walking frequencies and speeds for model identification, where distinct clouds of points corresponding to each prescribed stride frequency and the corresponding range of stride speeds.

Table 3.2: **Goodness of fit** - Analysis of the goodness of fit of the power model built during the Metronome Walk for each subject. (CI: Confidence interval; RMSE: Root mean square error)

	a	**b**	**R-squared**	**CI a**	**CI b**	**RMSE**
Subject 1	2.009	0.292	0.992	(1.991, 2.027)	(0.283, 0.300)	0.008
Subject 2	2.050	0.335	0.987	(2.017, 2.084)	(0.319, 0.352)	0.009
Subject 3	1.997	0.314	0.981	(1.948, 2.006)	(0.301, 0.328)	0.011
Subject 4	2.028	0.397	0.986	(2.005, 2.051)	(0.386, 0.408)	0.009
Subject 5	2.109	0.372	0.984	(2.068, 2.149)	(0.356, 0.389)	0.011
Subject 6	2.014	0.375	0.991	(1.998, 2.03)	(0.367, 0.382)	0.009
Subject 7	2.002	0.305	0.992	(1.98, 2.025)	(0.295, 0.316)	0.008
Subject 8	1.961	0.324	0.991	(1.938, 1.985)	(0.313, 0.335)	0.009
Subject 9	2.295	0.392	0.978	(2.259, 2.331)	(0.376, 0.407)	0.013
Subject 10	2.173	0.384	0.986	(2.137, 2.208)	(0.368, 0.400)	0.010

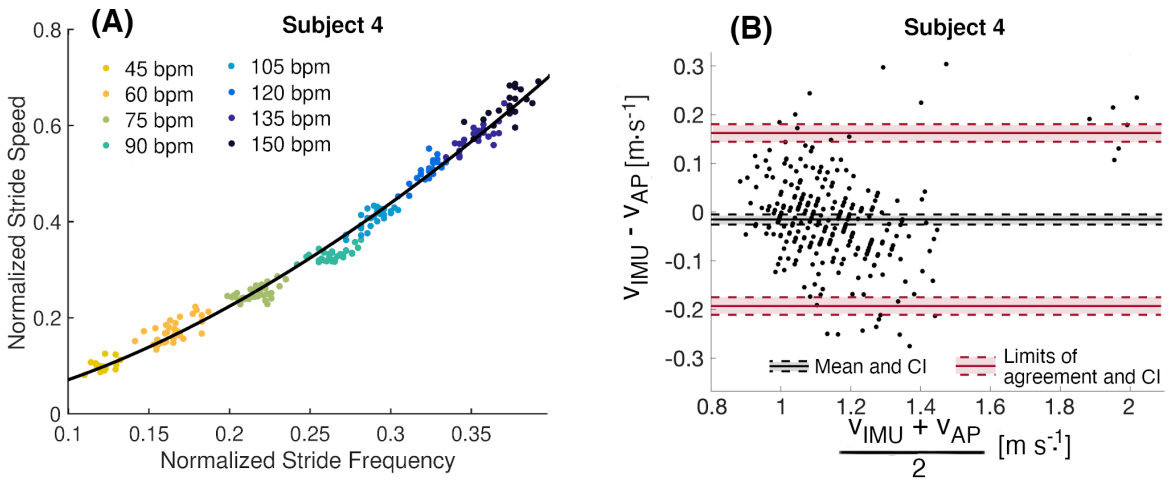

Figure 3.3: **Subject 4 analysis — (A)** Subject-specific data-driven map from stride frequency to stride speed built from the metronome walk. Each cloud of points corresponds to an imposed stride frequency. **(B)** Bland Altman analysis of the residuals with mean difference, limits of agreement, and their confidence intervals (CI).

3.3.2 Quantification of the Walking Speed Estimate Error

The Bland-Altman analysis indicates that all subjects, except Subject 2 and Subject 9, have limits of agreement within $\pm 0.2 m \cdot s^{-1}$ (Table 3.3). Subject 2 also presents the highest mean difference between estimated and true walking speed, followed by Subject 7 and Subject 9 (Table 3.2 and Figure 3.4). The violin plot (Figure 3.4) shows that the majority of residuals fall into the $\pm 0.1 m \cdot s^{-1}$ range, except for Subject 2, where we observe that the true speed is clearly underestimated by the model. The other subjects have a small mean difference between -0.058 and $0.008 m \cdot s^{-1}$. The Bland-Altman plot for a representative subject of this chapter, Subject 4, shows a concentration of the points between 0.8 and $1.4 m \cdot s^{-1}$ (Figure 3.3B).

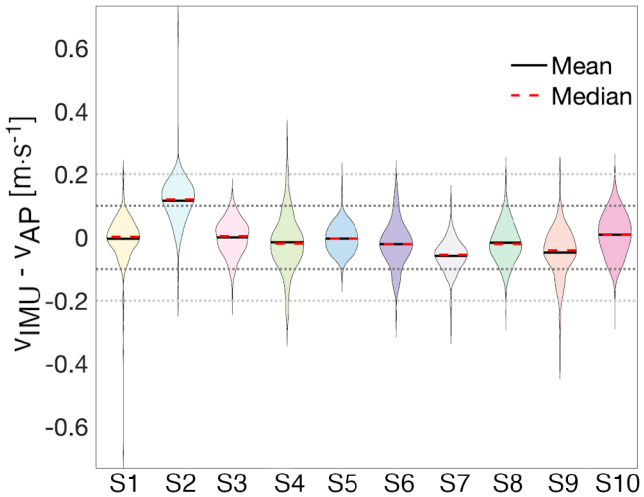

Figure 3.4: **Distribution of residuals** — The violin plot enables the visualization of the distribution of the error for each subject with $\pm 0.1 m \cdot s^{-1}$ (black-dotted line) and $\pm 0.2 m \cdot s^{-1}$ (grey-dotted line) bands. Each shaded area represents the shape of the distribution of residuals for a particular subject.

Table 3.3: **Bland-Altman Analysis** — Bland & Altman plot statistics for all subjects. μ and σ correspond to the mean and standard deviation respectively.

	Sample size	$\mu(v_{IMU} - v_{AP})$	$\sigma(v_{IMU} - v_{AP})$	**Limits of agreement**	
				Inferior	**Superior**
Subject 1	245	-0.013	0.078	-0.157	0.148
Subject 2	248	0.116	0.084	-0.048	0.280
Subject 3	465	0.000	0.054	-0.107	0.107
Subject 4	294	-0.015	0.091	-0.193	0.162
Subject 5	449	-0.004	0.044	-0.091	0.083
Subject 6	144	-0.021	0.071	-0.159	0.117
Subject 7	530	-0.058	0.053	-0.162	0.045
Subject 8	482	-0.017	0.061	-0.137	0.104
Subject 9	534	-0.048	0.079	-0.203	0.108
Subject 10	478	0.009	0.067	-0.123	0.140

To quantify the agreement of the estimated speed from the AP and the speed extracted from the IMU, we calculate CPs for each subject for three different clinically meaningful boundaries and computed the CCC (Table 3.4). All subjects data, except Subject 2's, contain at least 70% of the error within $\pm 0.1 m \cdot s^{-1}$ and at least 97% within $\pm 0.2 m \cdot s^{-1}$. An analysis of all subjects suggests

that 97% of the residuals are within $\pm 0.2m \cdot s^{-1}$. The CCC values range from 0.65 for Subject 2 to 0.96 for Subject 6, with an average of 0.80.

Table 3.4: **Measures of Agreement** — Coverage probabilities (CP) for the boundaries 0.1, 0.2, and $0.3m \cdot s^{-1}$ and concordance correlation coefficient (CCC) with its confidence interval (CI)

	$CP_{0.1}$	$CP_{0.2}$	$CP_{0.3}$	CCC	CCC CI inf	CCC CI sup
Subject 1	0.80	0.99	1.00	0.82	0.78	0.86
Subject 2	0.33	0.78	0.98	0.65	0.60	0.70
Subject 3	0.93	1.00	1.00	0.90	0.88	0.92
Subject 4	0.72	0.97	1.00	0.86	0.83	0.89
Subject 5	0.97	1.00	1.00	0.91	0.89	0.92
Subject 6	0.82	0.99	1.00	0.96	0.95	0.97
Subject 7	0.78	1.00	1.00	0.62	0.58	0.66
Subject 8	0.88	1.00	1.00	0.78	0.74	0.81
Subject 9	0.71	0.97	1.00	0.66	0.61	0.70
Subject 10	0.86	1.00	1.00	0.84	0.82	0.86
Average	0.78	0.97	1.00	0.80	0.77	0.83

Results from Subject 2 show a large difference ($CP_{0.2} > 0.95$) between estimated and true walking speeds. Indeed, only 78%, instead of 95%, of the residuals were within the $\pm 0.2m \cdot s^{-1}$ boundary. The Bland-Altman plot for this individual (Figure 3.5B) illustrates a small cloud of points, corresponding to low values of stride speeds, around zero. From this observation, we identified different parameters $a' = 2.266$ and $b' = 0.399$ with respective confidence intervals $(2.161, 2.370)$ and $(0.369, 0.431)$ by fitting a power model only to the 4 slowest stride frequencies (Figure 3.5A). The R-squared for this fit is 0.961 and the RMSE is 0.008. A new analysis of the residuals revealed better performance of the updated model, with a mean error of only $0.039m \cdot s^{-1}$ and limits of agreements of $0.214m \cdot s^{-1}$ and $-0.136m \cdot s^{-1}$ (Figure 3.5C). The new CP values indicate 69% of the error within $\pm 0.1m \cdot s^{-1}$ and 96% within $\pm 0.2m \cdot s^{-1}$. The CCC of the corrected model is 0.85 compared to 0.65 for the fitted model.

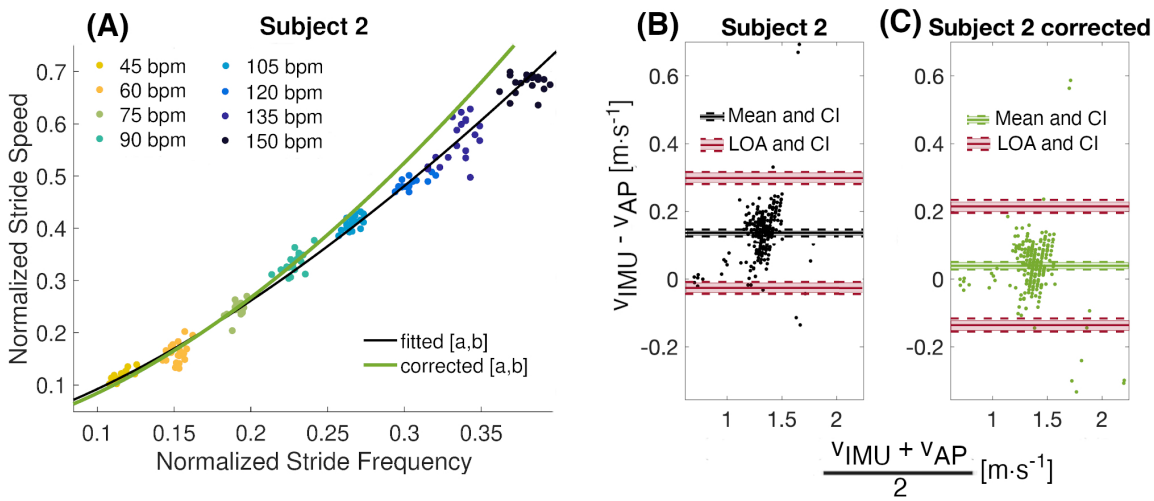

Figure 3.5: **Model Correction — (A)** Observation of the metronome walk fitted curve ($a = 2.050$ and $b = 0.335$) against the corrected power model ($a' = 2.266$ and $b' = 0.399$) for Subject 2. **(B)** Bland Altman analyses for the original and **(C)** corrected models with mean differences, limits of agreements, and their confidence intervals (CI).

3.3.3 A Week in the Life of Subject 1

During the week-long experiment, 168 hours of data were collected from subject 1. The histogram of the average steady-state speed indicates a strong preference to walk at 1.47 and $1.58m \cdot s^{-1}$ (Figure 3.6A). During that time, 167 bouts of walking (as defined in Methods) were identified with an average of 16 strides per bout. Overall, the subject had an average steady-state speed of $1.53m \cdot s^{-1}$. There were not large daily differences in the data, with the slowest average day of $1.36m \cdot s^{-1}$ and the fastest of $1.50m \cdot s^{-1}$ (Figure 3.6B). Figure 3.6C illustrates the variability in stride speed over the course of a day; 85% of the data is contained within $1.00m \cdot s^{-1}$ and $1.80m \cdot s^{-1}$, with a maximum speed recorded around 5 pm at $2.85m \cdot s^{-1}$ and a minimum speed recorded around 7:20 pm at $0.22m \cdot s^{-1}$.

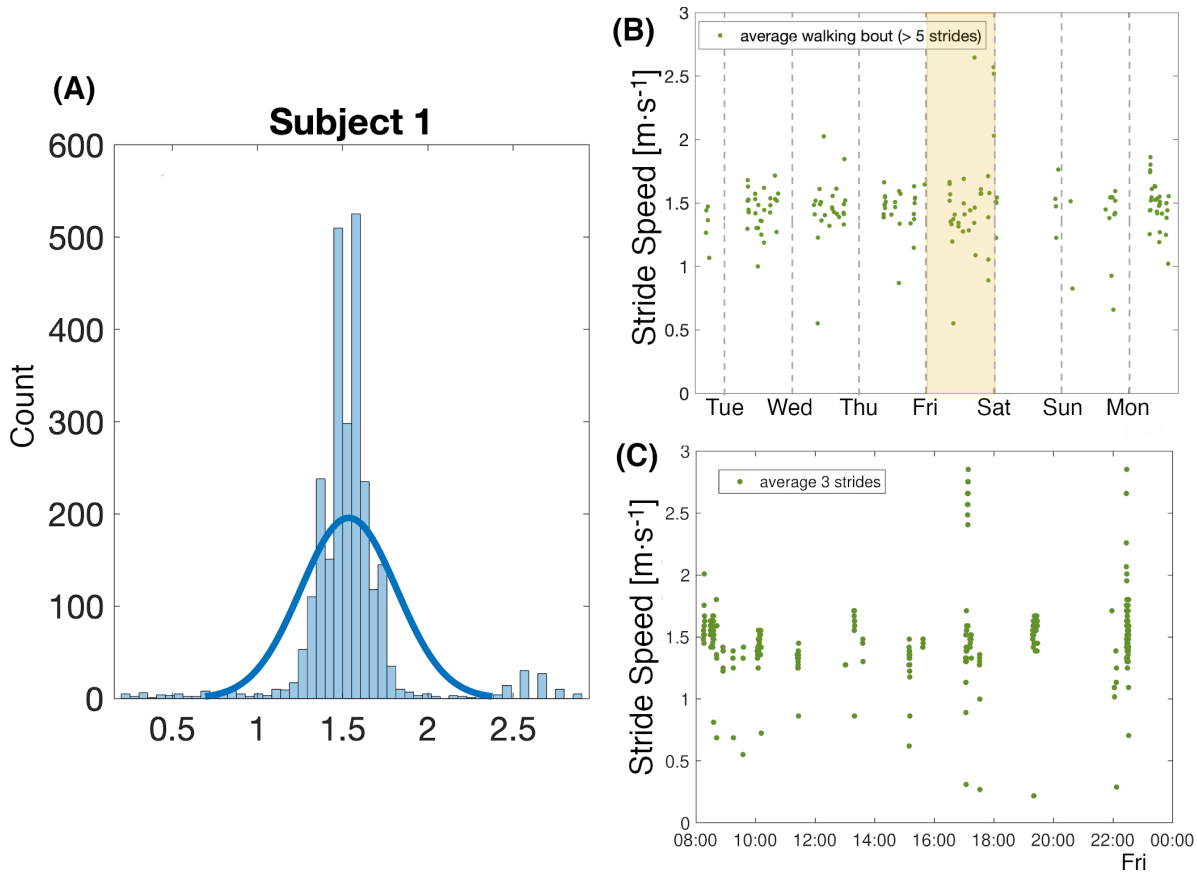

Figure 3.6: **Week Analysis** — **(A)** Analysis of the distribution of all stride speed values collected over a week for one subject. **(B)** Observation of the evolution of walking speed in a week. Each point corresponds to the average of the values of stride speed in a quasi-steady-state walking bout as defined in Methods. **(C)** A closer look at the values of stride speed on a particular day, shaded in yellow in the figure above. Each point corresponds to the average of three strides.

3.4 Discussion

Walking is an important activity of daily life for many individuals, and the ability to monitor and assess gait in a free-living environment is key to an improved understanding of an individual's physical health. Here, we utilized fine-scale measurements from a prescribed walking task to build subject-specific walking models that accurately estimate gait speed from low-resolution long-term accelerometers, in an unconstrained environment. Finally, a representative subject wore the bio-logging tag for a week to demonstrate the viability of this approach for the extraction of

clinically relevant parameters in the real world.

Data to generate the subject-specific model parameters were collected using a metronome to create a large range of stride speeds and frequencies without the constraints that result from walking over a range of fixed speeds on a treadmill [103]. The identified parameters (a and b) for the power model are similar in magnitude to the first study (to our knowledge) which used this model [72]. The goodness of fit measures presented in Table 3.2 further demonstrate that the power model captures the relationship between stride speed and frequency well. Figure 3.3B illustrates a random and equal distribution of points around a zero mean difference in the Bland Altman plots, which can be used to verify the modeled relationship between stride frequency and speed.

Analysis of the subject-specific models indicates that individuals with similar anthropometric parameters do not always have the same relationship between stride speed and frequency. Subjects 4 and 9 have almost equal leg lengths and heights, but their identified parameters a differ by 0.267. Subject 9's fit resulted in the largest a value, while Subject 4's fit has a fairly small a but the second largest b value (Figure 3.7 - A). To achieve a given speed, Subject 9 used longer strides at a lower frequency, while Subject 4 employed shorter steps at a higher frequency (Figure 3.7 - B). Environmental or contextual differences, like the type of footwear [48], might also influence the parameters of the model and warrant further investigation. For example, Wang and Adamczyk have shown that gait parameters can change between walking with sandals and athletic shoes. All participants wore athletic shoes for this study. Additionally, the analysis of Subject 2's statistics indicated that the walking speeds at the higher step frequencies were slower than during free walking. All subjects were given limited time just before the task to familiarize themselves with the metronome walk before data was recorded. In the future, more time to learn and practice the metronome walk could improve the data utilized for the model identification.

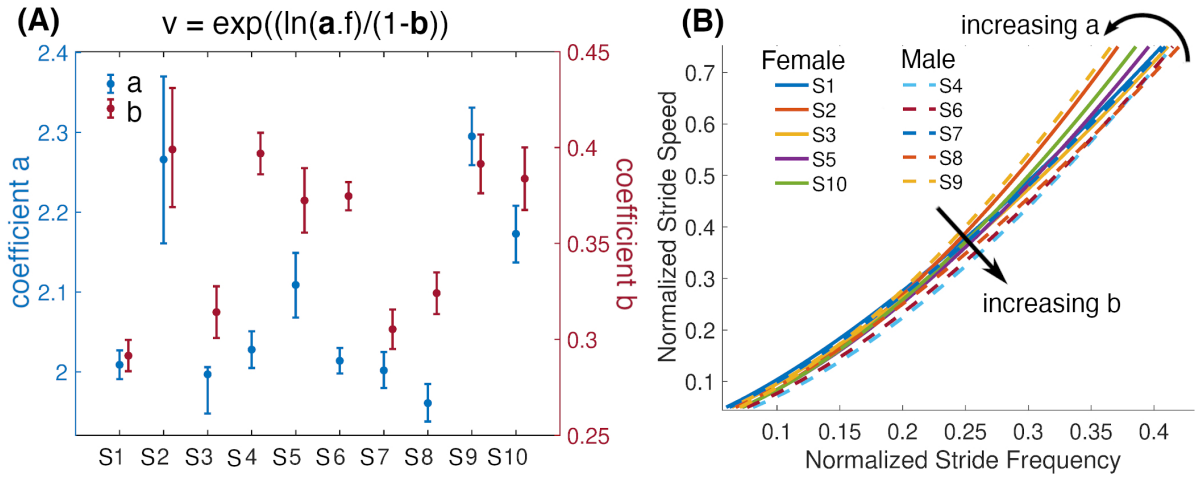

Figure 3.7: **Subjects' models and their parameters** — **(A)** Parameters a and b from each subjects power model and their 95% confidence intervals. **(B)** Fitted lines for all subjects and visualization of the effects of variations of the parameters a and b. Females are represented with solid lines and males with dashed lines.

To evaluate our approach, estimates of stride speed calculated from the foot-worn IMU were compared to the model-based estimates during an unsupervised long walk in the real world for each subject (Figure 3.8); for Subject 2 the corrected model was used. Qualitatively, the speed distribution for the two estimates is in good agreement for all subjects. Quantitatively, more than 95% of the error between the estimated speed from our model and the speed extracted from the foot-worn IMU were within $\pm 0.2 m \cdot s^{-1}$, with the estimated mean walking speed comparing well to the true value for the majority of subjects. The CCC values can be visualized by looking at the overlapping regions of the distributions of v_{IMU} and v_{AP}. Subject 6 presents almost a perfect overlap with a corresponding CCC value of 0.95 whereas there is a slight shift in Subject 7's distributions which presents a CCC value of 0.58. The study from Schimpl et al. [93] compared different methods to extract stride speed from a single waist-worn accelerometer in the free-living environment. The method that gave the best results when tested during outdoor walking with self-selected speed used a support vector regression algorithm. The values of CP and CCC reported by this study when using this method are comparable with the value obtained in our study. The Bland Altman analysis of the results from the thigh-worn accelerometer also has

smaller bias and limits of agreements for estimated walking speed than results in the literature that used smartphone data collected at different locations (e.g. body, bag, belt, hand, and pocket) to estimate speed [94]. This points to the benefit of data collection from a fixed point on the lower body.

Extending this work to the clinical environment will require data collection over multiple days in the real-world environment. The wearable sensor used in this work is capable of capturing 7 days of continuous motion data, and the attachment on the thigh enables unobtrusive data acquisition in the free-living environment. Using this sensor platform we were able to collect data for a week from a single representative subject for this study. The week-long assessment demonstrates the potential of this approach to gain a unique insight into movement and activity at different temporal resolutions; we expect similar results when we extend our approach to assess a larger subject population. The capacity to extract average stride speeds from 167 bouts of walking (duration > 10 seconds and strides > 5) enables estimation of an individual's preferred walking speed in their daily environment. In the future, we expect that the extraction of walking speed, in combination with other parameters, over an extended time period could allow clinicians to get a more objective and complete picture of the walking activity of individuals in their free-living environment, compared to a traditional in-laboratory walking test. Fine-grain observations of daily trends could be used to build more tailored prescriptions related to physical activity.

A potential shortcoming in this chapter is the use of an IMU-based estimate of stride speed to derive and verify the speed estimates presented in this work. IMU-based estimates are known to contain small measurement errors on the order of $1 - 5\%$ depending on gait speed [39–41, 67]. Multi-camera motion capture and force plates are tools that have been proven to be highly accurate to estimate gait parameters [104, 105]. However, these measuring instruments cannot be used outside the laboratory and constrain data collection to a limited capture volume. Therefore, the ZUPT approach is one of the most viable methods to accurately and unobtrusively assess the ecological validity of walking gait measures in the real world. To our knowledge, the potential errors of the ZUPT algorithm have not been assessed in the free-living environment, since most

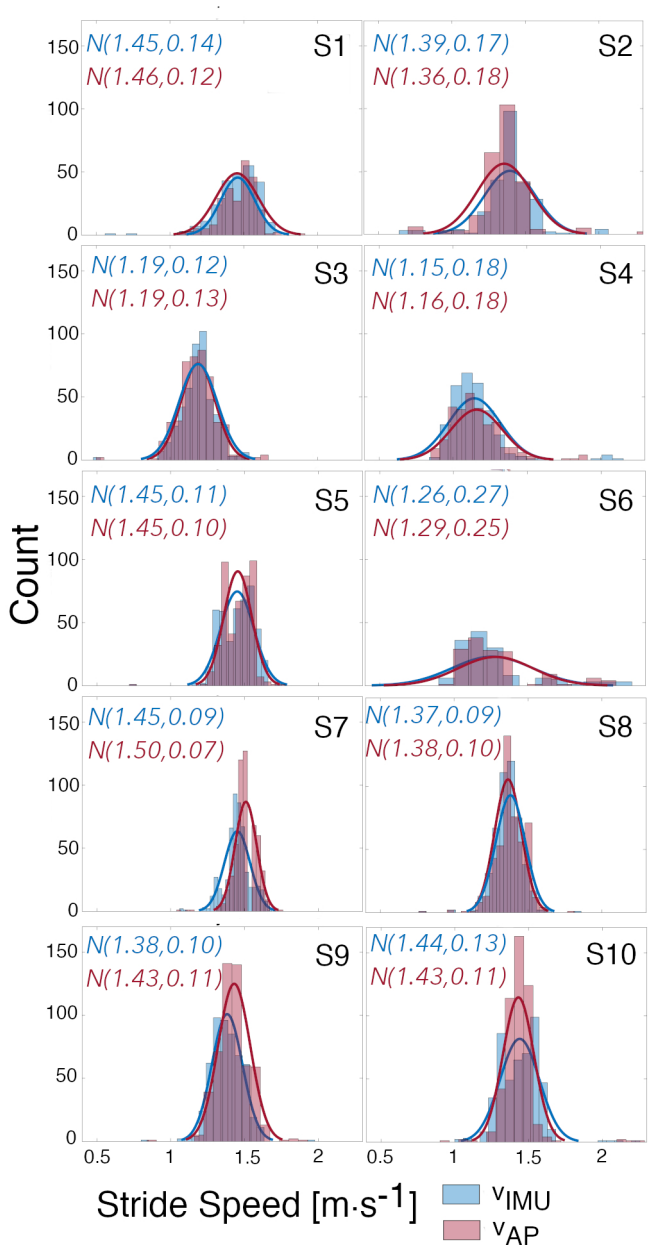

Figure 3.8: **Distributions of estimated and true speed** — Distributions of the estimated speeds from the AP using the built models, and of the true speeds calculated from the IMU. Gaussian curves were fitted to each distribution and the mean and standard deviation for each curve are given.

validation methods are bound to the laboratory setting. However, the method has been validated during uncontrolled hallway walking with a large number of strides collected (Rebula et al., 2013). The conditions of this study are close to the walking conditions in which subjects performed the

model validation. This makes us confident regarding our choice to use the ZUPT algorithm to obtain ground truth stride speed in this study. Another limitation to consider is the sample size and the population recruited in this work. Our experiment involved young healthy subjects. However, different studies have shown the impact of weight [106, 107] or age [108, 109] on gait parameters. Additional work is needed to evaluate whether the power model can still be used with different study populations. In addition, the frequencies used during the metronome walk might also need to be adapted to participant or patient's ability. This approach could also be enhanced by including parameters to inform how behavior of an individual extracted from a bio-logging sensor is interpreted. For example, being able to add a layer of physiological and contextual data to the current analysis would allow a more objective evaluation of a patient's level of physical activity [110]. These types of additions will further enable clinicians to design and monitor the compliance to tailored treatments to improve patient care and outcomes.

3.5 Conclusion

Objective assessments of the level of physical activity of an individual can significantly improve clinical decision-making for numerous health issues. In particular, walking speed is a powerful metric for clinicians as it captures the performance of a common physical activity, can easily be obtained in the clinical setting, and most importantly, is highly correlated with various health issues and outcomes. Wearable sensing technologies offer new opportunities to complement clinical assessments of walking. However, the continuous and unobtrusive monitoring of individuals in their daily life requires low-power and compact sensors, which often do not enable direct measurement or calculation of walking speed. We propose an innovative approach to accurately estimate walking speed in the free-living environment using a low-power, lightweight wearable sensor secured on the thigh. During a designed short walking task, high-resolution measurements of stride speed enable the derivation of subject-specific models to map stride frequencies extracted from the thigh-worn sensor to stride speeds. The performance of the subject-specific models in the real world was eval-

uated using a long unsupervised walk in the free-living environment with stride speed calculated from a foot-worn inertial measurement unit used as the gold standard. Our results demonstrate that stride speeds can be accurately estimated using low-power and low-resolution sensors. We believe that our approach enables new exciting opportunities for objectively measuring physical activity in the real world, which will ultimately provide clinicians with a more complete picture of patient health.

However, given the large variability in real-world behavior, it can be difficult to interpret long-term measurements of stride speed in an unsupervised environment. In fact, while using an accelerometer only enhances overall compliance, it reduces the availability of contextual information. As such, in the following chapter, we will leverage the stride speed estimation method we developed in this chapter to create a framework for the characterization of walking speed variability in the real world using the single-point accelerometer previously used.

CHAPTER 4

Characterizing Walking Speed Variability Using an Accelerometer Only

4.1 Motivation

Walking is the principal mode of human locomotion, and gait characterization is important for both clinical evaluation and treatment. Walking speed correlates strongly with overall health [10, 81] and researchers are increasingly using real-world data collection to quantify this parameter. Walking speed is influenced by contextual factors, such as environment (inside vs outside), or walking type (recreation vs destination) that vary throughout the day [48, 49, 111]. Position data, measured using GPS or estimated from wearable sensors, have been used to further parse movement based on repeated trajectories [48] or on location (inside vs outside) [49]. While additional sensor measurements result in richer datasets, compliance suffers when participants are asked to carry multiple rechargeable sensors. As a result, long-duration studies often utilize accelerometers [112]. A single, low-powered accelerometer may improve compliance, but also reduces concurrent contextual information. Walking bout length estimated from accelerometry has been used to parse real-world walking data [42, 50]. Real-world walking is rarely continuous and the number of pauses within a walk (continuity) can also be measured with an accelerometer [63].

Building on prior research, we propose a framework that uses two weeks of accelerometer and heart rate data from young healthy individuals to: 1) classify walking from running and other stepping instances; 2) group walking bouts based on duration and continuity; 3) estimate an indi-

vidual's preferred walking speeds; and 4) examine the range of speeds individuals use in the real world. This novel framework provides an approach for the processing of real-world accelerometer data that will allow researchers to extract meaningful information from persistent monitoring.

4.2 Methods

4.2.1 Subjects

We recruited 15 subjects from a healthy population (7 females, 8 males, 25 ± 5 years, leg length l_0 1.0 ± 0.1m), with 5 subjects specifically recruited from a population of recreational runners who perform a minimum of three runs of at least 20 minutes per week to obtain running data for classification. We measured leg length l_0, from the anterior superior iliac spine to the floor, with shoes, to normalize our results [96]. All participants electronically signed a consent form approved by the Institutional Review Board of the University of Michigan.

4.2.2 Long-term Free-living Measurements

4.2.2.1 Sensors, Experiment, and Compliance

Following the completion of the initial visit, participants were sent home with an accelerometer (activPAL^{TM} [PAL Technologies Ltd., Glasgow, UK]) and a heart rate monitor ([Polar, Electro Oy, Kempele, Finland]) (Table 4.1). We selected the accelerometer for its compact size (23.5 x 43 x 5mm), lightweight (9g), and unobtrusive placement on the body to facilitate user compliance. The five recreational runners were asked to log the run start times and durations during the study period. The activPAL software was initially used to classify stepping activity from the accelerometry [70]. Heart rate data were used to develop an algorithm to classify running and walking from data in the stepping state (detailed in Walking Periods Classification). Wear time for each sensor can be found in appendix B.1.

Table 4.1: **Sensor specifications**

	activPAL	**Polar OH1**
Measurement	3-axis acceleration $\pm 4g$	Heart rate
Placement	Thigh	Forearm or upper arm
Attachment	Tape	Elastic adjustable band
Battery life	14+ days	12 hours
Sample rate	20Hz	1Hz

4.2.2.2 Characterization of a Walking Period

Walking data was then further analyzed to capture the stop-and-go nature of unconstrained walking. For instance, if a pedestrian pauses briefly at a light during a walk, the corresponding walking period should include gait before and after the pause, as well as the pause itself.

Stepping Periods Identification Activity recognition from the activPAL was used to identify stepping periods. A stepping period starts when a stepping event is detected and ends when extended standing ($> 1min$) or a state transition (e.g., sitting) occurs (Figure 4.1-A). The threshold of one minute was adapted from the definition of maximum resting period from Barry et al, and the average cycle time of traffic lights (National Association of City Transportation) [113].

Walking Periods Classification A custom algorithm was used to identify and discard running within stepping periods. Stepping periods were divided into a series of 5-stride windows to reduce the impact of potential abnormal strides or errors from the stride detection algorithm [114] (Figure 4.1-B). A supervised classification algorithm (detailed in Appendix B.2 and B.3) was used to classify each window into ”Running”, ”Walking”, or ”Other” (Figure 4.1-B). To determine whether a stepping period, which contains several 5-stride windows of stepping, corresponded to walking, we set a threshold λ, between 0% and 100% such that, if the percentage of 5-stride

windows labeled walking within a stepping event was greater than λ, the event was identified as walking, otherwise the entire event was discarded (Figure 4.1 - C). This algorithm was validated using the running logs and heart rate data.

Duration and Continuity of a Walking Period Duration, p_d, and continuity, p_c (from 0% to 100%), were used to parameterize each walking period:

$$p_c = \frac{p_d - p_r}{p_d} \times 100, \tag{4.1}$$

with p_r corresponding to the total standing time within a period. This metric is expressed as a percentage and quantifies the continuity of a walking period, with 100% corresponding to a walk without pauses. A walking period also contained values of stride speed, v, that were calculated from the 5-stride windows using the method described in [57]; the number of stride speed values per walking period varied depending on the duration and continuity of the period. Researchers reported that a change of $0.1 - 0.2m \cdot s^{-1}$ in walking speed can be clinically relevant [101]. With our method, 78% of the error in stride speed estimates (evaluated in the real world [57]) are under $0.1m \cdot s^{-1}$. This percentage increases to 82% when the data from one outlying subject is removed. For all subjects, 97% of the error in stride speed estimates is under $0.2m \cdot s^{-1}$. The resulting framework outputs can be used to capture relative speed ranges that individuals present in the real world.

To further understand how stride speed varies with period duration and continuity, we parsed walking periods into 5 different modes (defined below) that vary in both continuity and duration. The definition of the modes was arbitrary for period continuity, as there is no literature (to our knowledge) to support a specific cutoff. For period duration, we used a cut-off of 10 minutes as it is the minimum recommended duration for an aerobic activity to benefit health [115]. These cut-offs can be adjusted based on the studied population's level of physical activity.

Mode 1 - Short and Discontinuous

$$p_d \leq 10min \ \wedge \ p_c < 100\%$$

Mode 2 - Short and Continuous

$$p_d \leq 10min \ \wedge \ p_c = 100\%$$

Mode 3 - Long and Discontinuous

$$p_d > 10min \ \wedge \ p_c \leq 60\%$$

Mode 4 - Long and moderately Continuous

$$p_d > 10min \ \wedge \ 60\% < p_c \leq 80\%$$

Mode 5 - Long and highly Continuous

$$p_d > 10min \ \wedge \ p_c > 80\%$$

4.2.3 Statistical Analysis

4.2.3.1 Multi-level Modeling

A multi-level modeling (MLM) [116] approach was used to investigate the effect of period duration, period continuity, and the interaction between the two on walking speed while controlling for the effect of subjects and walking periods. A nested structure with 3 levels was used (from high to low): subjects, walking periods, and the parameters (period duration p_d, period continuity, p_c, and walking speed, v). We also analyzed the difference in stride speed between Modes using a similar

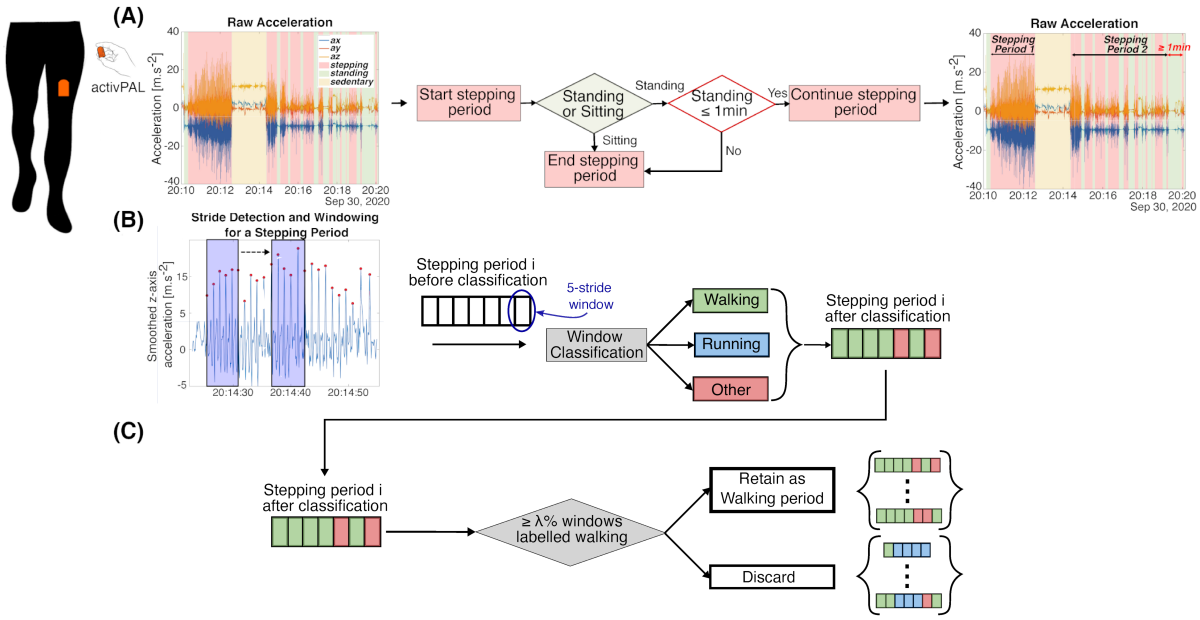

Figure 4.1: **Characterization of a Walking Period** — **(A)** Raw acceleration data and activity state were used to parameterize stepping periods. **(B)** To identify a stepping period 5 strides windows were first defined. A decision tree classified each window as either walking, running, or other. **(C)** Finally, we evaluate the percentage of 5-stride windows labeled as walking within each stepping period to determine walking period.

structure.

The models were built gradually, using R, starting with fixed coefficients then adding random effects one by one and comparing model performance. The Akaike Information Criterion (AIC) was used to identify the model that explained the most variance in our data and chose the autoregressive (Lag 1) covariance structure to model our data. The significance of the different model coefficients was evaluated at the 0.05-level.

4.2.3.2 Power Analysis

A power analysis was conducted to determine the minimum sample size for this work. Using pilot data, we modeled the distribution and dependencies of each variable. Data from the literature were used to determine ranges of walking speeds and activity levels that correspond to healthy young

adults [63, 117]. We found that 3 subjects were sufficient to obtain 90% power in our analysis. This low number can be explained by the very high number of 5-stride windows present within each individual. For instance, in our dataset, the lowest number of 5-stride windows for an individual subject was 1435.

4.3 Results

4.3.1 Real-world data pre-processing

The compact low-power accelerometer we used collected data continuously during a wide range of activities and facilitated compliance. Pre-processing was essential to filter the gait events identified initially using an unsupervised classification approach. Around 869,470 strides were originally registered by the activPAL for all subjects. We filtered the data to retain walks (e.g., remove runs and outliers) with at least 5 strides, resulting in the removal of approximately 69% of strides (Table 4.2). Filtering eliminated many activities that involve stepping but are not walking, reducing the error in the estimates of walking kinematics.

4.3.2 Walking Periods Classification

The classification algorithm removed 99% of the logged running data. Stepping periods were discarded if the percentage of 5-stride windows labeled walking was lower than 77% (λ). The average heart rate for walking periods was 103 bpm, compared to 140 bpm for discarded events. An average of 12% of the data from 3 non-runners was removed using this method (appendix B.2).

4.3.3 Walking Period Characteristics

An average of 290 walking periods per person were identified (Table 4.2). Stride numbers for analysis ranged from 7,175 (S14) to 30,770 (S13), but some participants wore the sensor for less time (Appendix B.1). Period duration (Figure 4.2 – A) is skewed towards low values (skewness

= 4.32, kurtosis = 28.04), with an average of 3.59 minutes. Mean percentage of continuity for a walking period was 64.08%. On average, around one-third of the per-person periods had a continuity of 100%. Within these continuous periods, 99% were under 5 minutes. On average a walking period contained 14 5-stride windows (1 to 494 windows per period), resulting in an average of 70 strides ($14 \cdot 5$ strides) per walking period for analysis. Average stride speed for all walking periods across participants was $1.34m \cdot s^{-1}$ ($SD = 0.31m \cdot s^{-1}$).

4.3.4 Influence of Period Continuity and Duration on Walking Speed

A multilevel model was used to determine the influence of period duration and continuity on estimates of stride speed. A significant effect was found for both period duration and continuity, $b = -0.008$, $t(50702) = -4.18$, $p < 0.001$, and $b = 0.004$, $t(50702) = 21.14$, $p < 0.001$. The interaction between variables was also significant, $b = 0.0002$, $t(50702) = 6.26$, $p < 0.001$. These coefficients indicate that a 1-minute increase in period duration decreases estimated stride speed by $0.008m \cdot s^{-1}$. Similarly, an increase of 10% in continuity would lead to an increase of $0.04m \cdot s^{-1}$ in the estimated stride speed.

Finally, we examined the differences in stride speed estimates across 5 distinct walking modes (Figure 4.2 – A, B, and C, Figure 4.3, and Table 4.3). Average stride speed varied between modes, with the largest differences generally observed between Mode 3 and Mode 5 within participants (Figure 4.2 – C) and in all subjects (Figure 4.3 - B). Mode 3 largely presented the lowest average stride speed, between $0.70m \cdot s^{-1}$ and $1.26m \cdot s^{-1}$ and the largest variability, between $0.23m \cdot s^{-1}$ and $0.44m \cdot s^{-1}$ (Table 4.3). The highest values of stride speed, from $1.19m \cdot s^{-1}$ to $1.68m \cdot s^{-1}$ and lowest standard deviations, from $0.07m \cdot s^{-1}$ to $0.23m \cdot s^{-1}$ were found within Mode 5. For each subject, the average stride speed value for each mode was different from the average of all stride speed values (Table 4.2 and 4.3). In particular, we found a statistically significant difference between the average stride speed of long continuous walks (Mode 4 and 5) and the average stride speed of the ensemble of the data, $b = 0.19$, $t(50704) = 15.16$, $p < 0.001$, (Figure 4.3).

Table 4.2: **Walking periods and associated parameters** — Number of walking period N for each participant and all participants with number of strides analyzed n, average μ and standard deviation σ of period duration, period continuity, and stride speed.

	Walking Period	**Strides Analyzed**	**Period Duration [min]**		**Period Continuity [%]**		**Stride Speed [m.s-1]**	
	N	**n**	μ	σ	μ	σ	μ	σ
S1	241	14,110	2.95	4.46	65.38	26.79	1.30	0.23
S2	309	19,405	3.40	5.54	65.28	26.49	1.26	0.30
S3	406	30,350	3.86	7.60	62.14	24.62	1.29	0.32
S4	153	19,330	5.04	7.15	65.34	26.57	1.62	0.23
S5	256	26,495	4.57	6.93	58.45	26.58	1.53	0.24
S6	290	8,060	1.98	4.11	62.81	24.46	1.29	0.33
S7	315	19,985	3.38	5.35	60.87	24.41	1.34	0.26
S8	183	16,510	5.06	8.26	64.76	24.18	1.33	0.27
S9	188	13,090	3.83	7.70	69.14	24.46	1.35	0.23
S10	439	28,885	4.22	6.52	64.25	23.33	1.30	0.27
S11	252	16,320	3.00	4.85	64.97	25.13	1.57	0.34
S12	158	11,115	3.48	5.27	71.09	22.85	1.30	0.25
S13	579	30,770	2.99	4.35	61.63	26.62	1.05	0.30
S14	149	7,175	4.08	7.57	72.97	24.55	1.27	0.26
S15	102	11,085	3.84	6.09	67.54	24.13	1.35	0.16
All	4020	272,685	4.16	6.63	55.80	20.59	1.34	0.31

Table 4.3: **Stride speed for each mode** — Number of stride speed values N, average μ, and standard deviation σ of stride speed within each mode for each participant and all participants. The '-' notation means the subject did not present any walking period in this mode.

	Mode 1			**Mode 2**			**Mode 3**			**Mode 4**			**Mode 5**		
	N	$\boldsymbol{\mu}$	$\boldsymbol{\sigma}$	**N**	$\boldsymbol{\mu}$	σ	**N**	$\boldsymbol{\mu}$	$\boldsymbol{\sigma}$	**N**	$\boldsymbol{\mu}$	$\boldsymbol{\sigma}$	**N**	$\boldsymbol{\mu}$	$\boldsymbol{\sigma}$
S1	880	1.20	0.30	224	1.30	0.23	139	1.07	0.23	542	1.38	0.15	1037	1.38	0.09
S2	1382	1.24	0.33	145	1.17	0.27	233	1.10	0.38	723	1.19	0.29	1398	1.36	0.21
S3	2069	1.29	0.35	169	1.30	0.32	46	1.14	0.44	2631	1.23	0.33	1155	1.44	0.15
S4	850	1.52	0.31	279	1.58	0.19	0	-	-	655	1.71	0.15	2082	1.64	0.21
S5	1166	1.37	0.40	57	1.22	0.38	80	1.22	0.44	731	1.56	0.13	3365	1.60	0.09
S6	678	1.12	0.35	183	1.33	0.21	26	0.93	0.34	0	-	-	725	1.46	0.21
S7	1412	1.26	0.34	116	1.32	0.22	83	1.10	0.36	546	1.46	0.16	1840	1.39	0.17
S8	1029	1.32	0.26	139	1.38	0.20	597	1.16	0.41	664	1.38	0.24	873	1.41	0.07
S9	955	1.37	0.26	88	1.38	0.27	0	-	-	188	1.47	0.19	1386	1.32	0.20
S10	1628	1.25	0.29	143	1.25	0.24	155	1.26	0.30	1164	1.24	0.33	2687	1.37	0.20
S11	1025	1.38	0.40	86	1.30	0.30	0	-	-	632	1.64	0.32	1521	1.68	0.23
S12	1005	1.26	0.27	112	1.25	0.31	62	1.10	0.28	477	1.28	0.23	567	1.42	0.13
S13	2658	0.95	0.35	504	1.10	0.23	232	0.70	0.40	929	1.13	0.23	1831	1.19	0.15
S14	442	1.12	0.27	92	1.20	0.23	0	-	-	158	1.21	0.17	743	1.37	0.23
S15	685	1.31	0.22	51	1.30	0.24	0	-	-	283	1.35	0.07	1198	1.38	0.12
All	17864	1.24	0.36	2388	1.28	0.28	1654	1.08	0.41	10323	1.34	0.31	22408	1.44	0.22

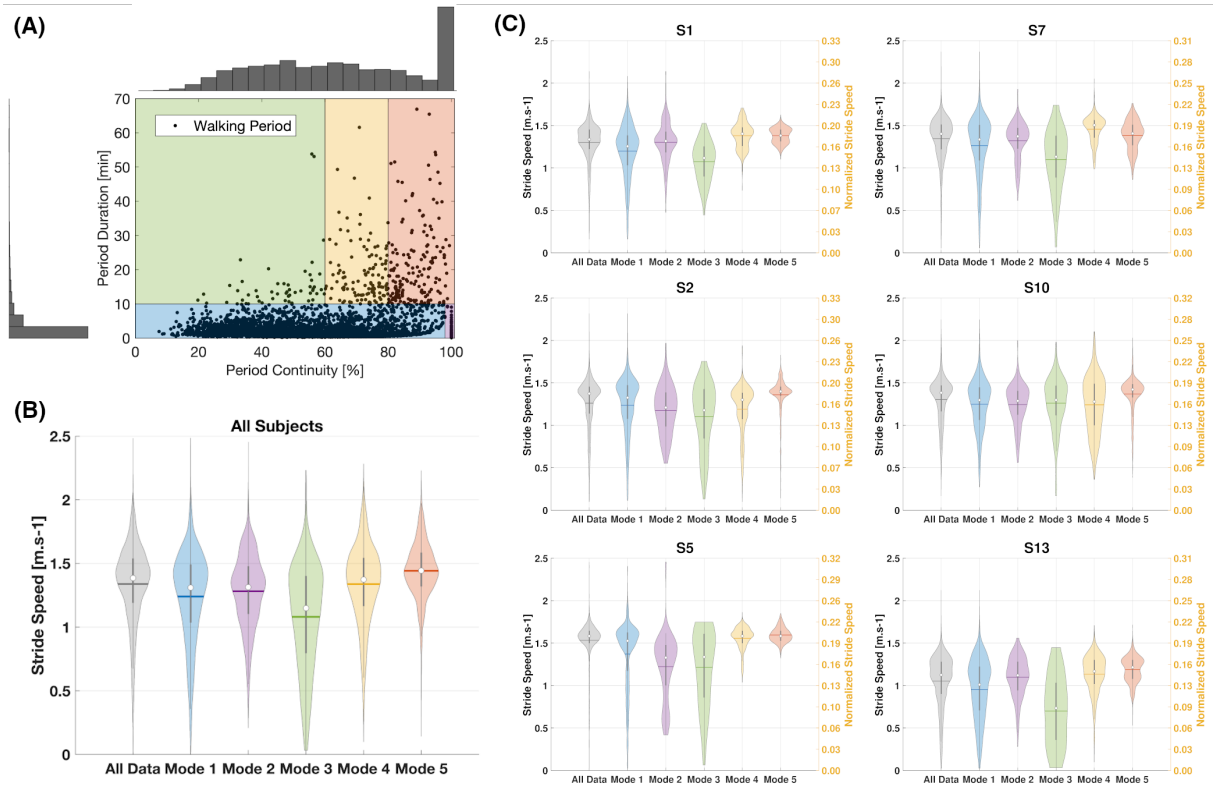

Figure 4.2: **Stride speed distribution across walking modes — (A)** Map of the different walking modes based on their duration and continuity. Each point represents a walking period, containing at least 5 strides. The distribution of duration and continuity are on the left and top of the figure respectively. **(B)** Distribution of stride speed over the different walking modes for all subjects. Each shaded area represents the shape of the distribution for a mode, with the horizontal line representing the mean. **(C)** Distribution of stride speed over the different walking modes for 6 representative subjects. Each shaded area represents the shape of the distribution for a mode, with the horizontal line representing the mean. Stride speed normalized by leg length can be found on the right y-axis.

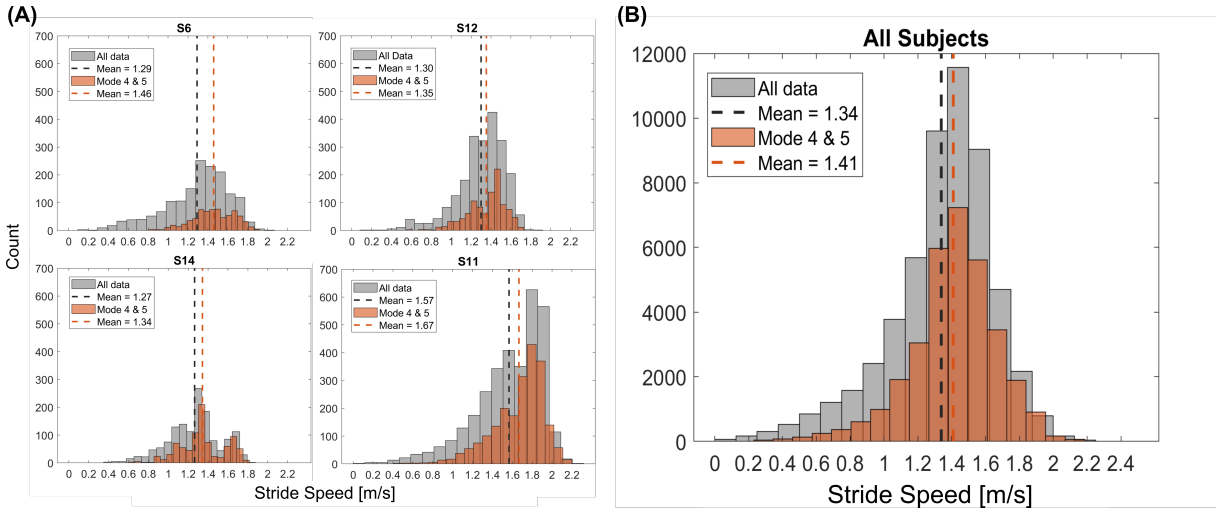

Figure 4.3: **Stride speed distribution for all data and for data from Mode 4 and Mode 5** — Histograms for four representative subjects **(A)** and for all subjects **(B)** representing the distribution of stride speed values for all data and for data from Mode 4 and Mode 5. The dashed lines illustrate the mean of each distribution.

4.4 Discussion

Walking speed estimated in the real world using wearable sensors can provide new insights for clinical assessment and diagnosis of clinical populations (ex: elderly). Here, we formulated a novel framework that uses features present in accelerometer measurements of real-world walking (duration and continuity) to cluster walking speed estimates. We tested this framework on an accessible population, young healthy individuals. We found that both continuity and duration of a walking bout are significantly related to estimated walking speed, suggesting that these features should be considered when analyzing real-world walking data. This framework enables a better understanding of walking behavior, variability of self-selected speeds, and preferred walking speed.

Explaining walking speed variability Walking speed is a critical parameter for clinical assessment of health and well-being [10]. Persistent monitoring methods capture the range of walking speed an individual chooses in their daily life. We found distributions with variabilities larger

than 0.16m/s for the ensemble of the walking speed values (Table 4.2). Given that increments of $0.10m \cdot s^{-1}$ in stride speed have been used to classify an individual's health status [118], it is important to reduce variability in walking speed estimates. Grouping stride speed within walking periods by duration and continuity explained some of the observed variability. Previous work has recognized the importance of labeling real-world data to enhance analyses. Direct measures of contextual factors, like location in the environment (GPS), have successfully been used to label walking data [48, 49]. Bout duration has also been used to explain the variability observed in gait biomechanics but not continuity [42, 50]. Our analysis also revealed a significant interaction between duration and continuity, which increased the capability of our model to explain walking speed variability. In other words, the effect of duration on walking speed varied based on continuity. This highlights the importance of using continuity to complement duration to improve our understanding of the changes in an individual's movement patterns. Because this framework uses data from a minimal set of sensors, the likelihood of subject compliance can be improved, which is key to the data collection necessary for an improved understanding of real-world walking behaviors.

Preferred walking speed Preferred/self-selected walking speed tends to be measured in the lab and clinic on a level ground during a continuous walk at a self-selected pace. Because real-world walking speed varies greatly, it is important to identify comparable periods when estimating preferred walking speed from these data. In this work, data from the long continuous walks grouped in Modes 4 and 5 may provide the best estimate of preferred walking speed for comparison with lab-based measurements. We observed that long continuous walking periods (Mode 4 and 5), although rare (0.01% of all walking periods were above 27 minutes), contain most of the strides ($\sim 60\%$ of all strides). We also observed a dependency between continuity and duration, such that there were no walking periods longer than 30 minutes with a period continuity under 50%. This could indicate that these long continuous walks are more directed, resulting in fewer pauses. An

individual is also more inclined to walk at a comfortable speed and reach steady state if walking for longer. In our population, the preferred walking speed, calculated from Mode 4 and 5, ranged from $1.17m \cdot s^{-1}$ (S13) to $1.67m \cdot s^{-1}$ (S11), with an average of $1.41m \cdot s^{-1}$ (SD = $0.26m \cdot s^{-1}$).

Walking "modes" The relationship between duration/continuity and stride speed was investigated heuristically by separating data into 5 modes (Figure 4.2 – A, B, and C). In this data set, most walking periods were short duration with variable stride speed (Mode 1, Table 4.3 and Figure 4.2). In contrast, there were fewer (between 0% and 17% of all walking periods) long discontinuous walking periods characterized by low estimates of stride speed and high variability (Mode 3, Table 4.3 and Figure 4.2). Values of stride speed from this mode ($1.08 \pm 0.16m \cdot s^{-1}$) were below the range of preferred stride speed (e.g., $1.2m \cdot s^{-1} - 1.6m \cdot s^{-1}$) observed in [117] and outside the lab [119], suggesting that the gait during these walks may not be the most efficient for the subjects [120]. This grouping demonstrates that individuals tend to select different walking speeds and can be used to create individual walking speed profiles.

This parsing can also be used to better understand someone's level of physical activity. Step count alone is often used as an indicator of physical activity level [121]. With the grouping of walking by mode, the average daily step count of an individual can further be categorized to understand the type of physical activity a step is associated with. For instance, S13 has more walking periods and strides analyzed than S10 (Table 4.2). However, S10 spent 14 hours in Mode 4 and 5 versus 7 hours for S13 over the two-week study indicating a difference in intensity of the activity. A better characterization of someone's physical activity profile could be used to tailor interventions to increase fitness and overall health.

Transient gait The distribution of period duration for all individuals (Figure 4.2 - A) indicates walking lasted less than 5 minutes, consistent with previous findings on human walking behavior in the real world [63]. In contrast, very few walking periods were long, ranging from 27 minutes (S1) to 67 minutes (S3). Most walking bouts contained pauses ($\sim 67\%$) (Figure 4.2 – A). The transient nature of the daily walking observed here indicates that participants may not be primarily

walking for transportation, and that the proportion of steady-state gait during a walking period may be limited. This observation has important implications for the use of real-world data to inform clinical decisions since in lab gait analysis tends to be conducted at steady-state. Constraints (e.g. fixed speed treadmill walking) are imposed to limit variability in the observed gait parameters, and the transient gait periods (starting and stopping) are often discarded. The results presented here suggest that investigating the relationship between parameters extracted from transient gait and health/welfare would be an important complement to traditional steady-state analysis.

Limitations This study offers new insights as to how duration and continuity can be used as elements of context, but future work should integrate multiple contextual factors to enrich the understanding of human movement in the real world (e.g., location, purpose of a walk, weather). Further, we only collected 2 weeks of data from the subjects during portions of the COVID-19 pandemic. As such, follow-up studies should conduct sensitivity analyses to determine the optimal duration of data collection when movement and behavior may be less affected by public health requirements. Lastly, expanding population diversity should be pursued, as walking speed is mainly a health indicator for clinical populations and the elderly. We also recognize that the error in our walking speed estimation method may be critical for clinical purposes, particularly for populations requiring the detection of changes in stride speed smaller than $0.1m \cdot s^{-1}$. The integration of an IMU on the foot could be a solution for more direct and accurate measurements of kinematics data.

4.5 Conclusion

Humans use a range of walking speeds to move in the real world. Therefore, it is important to capture this variability and understand how contextual factors influence the behavior. We found that some of the variability in real-world walking speed could be explained by the inherent duration and continuity of a walk. The proposed analysis framework used the wealth of information contained in real-world data to group observed walking into five modes as a way to further the understanding

of walking behavior. In light of this grouping, we recommend the use of continuous walks longer than 10 minutes to estimate preferred walking speed, and that overall walking performance may better be captured by a range of self-selected walking speeds.

Although the framework introduced in this chapter improved our ability to interpret the movement data collected in the real world, having additional contextual information can be essential for a more comprehensive assessment of an individual's movement profile.

CHAPTER 5

Classifying Context Using an Accelerometer Only

5.1 Motivation

Walking is a fundamental human movement that has many benefits for mental and physical health [6–9]. With the advancements of micro-electromechanical systems (MEMS), researchers are now able to measure human motion outside the lab for extended periods. Real-world measurements are often conducted over long periods where there is little to no control over or explicit knowledge of a participant's behavior. Generally, people engage in numerous activities across different contexts in their daily life. Various methods have been developed to gather information about what an individual is doing. Human activity recognition (HAR) serves as the initial step in understanding real-world data as it allows for the classification of an individual's activities and the identification of walking instances. HAR research has successfully utilized different combinations of wearable sensors (such as mobile phones and inertial measurement units) and methods (including classic machine learning models and deep learning) to achieve accurate classification performance [122–126]. However, even within the walking activity itself, there exists a range of contexts that give rise to different behaviors.

There are countless factors that can cause changes in gait. Firstly, the location where an individual is walking has a significant impact on their kinematics. Different terrains have been shown to influence how people negotiate their walk [55, 59]. The location where someone walks can provide insight into their habits, such as whether they explore beyond their home and engage with the com-

munity [49]. Additionally, certain features of the built environment that individuals navigate can impact their mobility [127, 128]. These various factors are directly related to health and well-being and therefore important to monitor. Secondly, the purpose of a walk can result in different walking strategies, even when individuals are walking in the same location [56]. For example, people tend to walk faster when commuting compared to a leisurely walk, despite both taking place outdoors in similar locations. Thirdly, there are internal factors that can affect human movement, such as mood. Contrasting moods, like happiness versus sadness, can lead individuals to exhibit different walking behavior [52, 53, 129]. Overall, acquiring information about these factors is crucial for understanding any observed variability in real-world walking.

The utilization of GPS data has proven to be successful in answering various research questions related to real-world human movement and mobility [130–132]. Kim et al. found that both lower-limb amputees and non-amputees tend to walk faster when they are away from their homes [49]. Similarly, Baroudi et al. recently quantified differences in walking speed for individuals walking in different real-world contexts, such as work, home, or commuting [56]. These studies used either dedicated GPS receivers or leveraged the GPS capabilities of mobile phones. However, GPS receivers can be cumbersome to use over extended periods as they require frequent recharging, cause privacy concerns, and add an extra device for individuals to carry; mobile phones do not offer the same level of resolution and can result in sparse data that is challenging to utilize effectively. Another tool researchers have employed for gaining insights into an individual's real-world context is self-reporting [68, 69]. Self-reporting enables the collection of more detailed data, but it heavily relies on the participant's compliance and often leads to incomplete datasets. Furthermore, self-reporting is burdensome and not practical for extended periods of data collection. Cameras offer arguably the most direct means of gathering information about a person's whereabouts. Doherty et al. used both a camera and an accelerometer to objectively quantify real-world activity [44]. Researchers have also developed accurate frameworks for the classification of camera data to obtain information on terrain types and surface inclines [45]. However, the use of camera data can raise privacy concerns, especially when used over extended periods. Practicality is another considera-

tion as individuals need to carry the camera, keep it charged, and ensure there are no obstructions. Overall, although these methods are advantageous in many aspects, factors such as practicality, participant burden, and privacy need to be taken into account for real-world data collection.

Accelerometer-based methods have emerged as an alternative for analyzing real-world data with regard to context. Hu et al. used a single inertial measurement unit (IMU) on the lower back to differentiate between flat and uneven terrain, as well as distinguishing between older and younger participants [51]. Hashmi et al. used IMUs embedded in a smartphone, placed on the lower back and chest, to classify various terrain features [59]. While both studies demonstrated the feasibility of using IMUs to accurately classify terrain, the datasets used were created in a controlled environment, with participants walking at steady state on selected surfaces. This synthetic aspect of data collection may limit the ecological validity of the classifiers in real-world scenarios. Additionally, the sensor placements used in these studies may restrict the practical implementation of these solutions over extended periods.

In this study, we propose a solution for the identification of walking context in the real world utilizing a single thigh-worn accelerometer. We developed a classification algorithm that leverages the natural grouping of real-world walking into bouts to identify walks indoor versus outdoor. To train and validate the model, we used a dataset generated from a data collection on 20 participants in the real world over a week, where GPS and self-reporting information were collected to label the different walks. Once validated, we used our model to label indoor and outdoor walks from a different dataset, where 15 participants were equipped with the accelerometer over two consecutive weeks. Finally, we characterized the influence of walking indoor versus outdoor on walking kinematics. This novel approach has the potential to facilitate the parsing and analysis of real-world walking data while utilizing only an accelerometer.

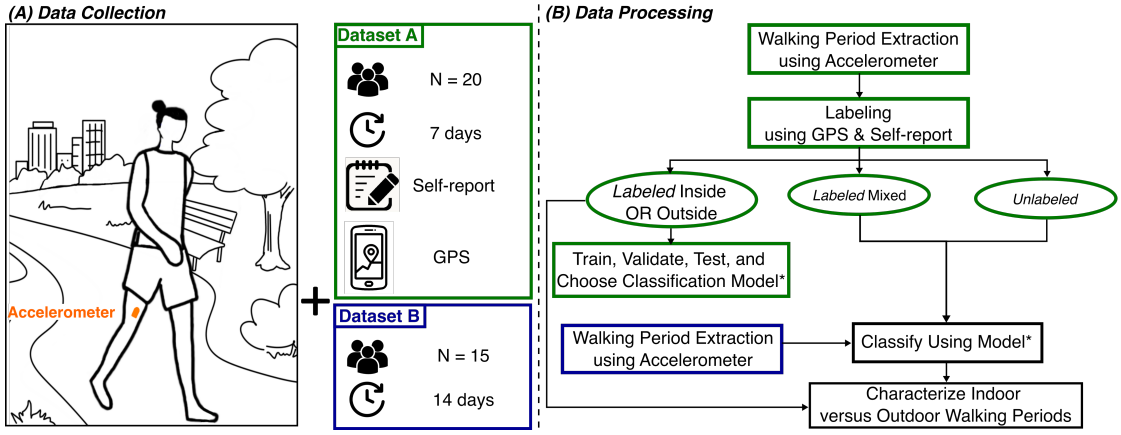

Figure 5.1: **Data Collection and Processing Overview** — **(A)** Dataset A was collected over 7 days on 20 participants, using an accelerometer, self-report, and GPS data from the participants' phones. Dataset B was collected over 14 days on 15 participants using an accelerometer. **(B)** The walking periods from dataset A were labeled using the GPS and self-report data. Walking periods labeled exclusively indoor or outdoor were used to train, validate, and test a classification model. The walking periods labeled mixed (e.g., inside and outside), as well as all the unlabeled walking periods from dataset A and B were classified using the model to characterize indoor versus outdoor walks.

5.2 Methods

5.2.1 Overview

Figure 5.1 shows an overview of the data collection and processing framework. We leveraged two datasets in this study: datasets A and B. Dataset A was collected using a thigh-worn accelerometer, self-report, and GPS data over 7 days with 20 participants. Participants were asked to report the purpose and location of the walks carried out throughout their day. Dataset B was collected using only the thigh-worn accelerometer over 14 days with 15 participants. We used the self-report and GPS data to label the walking periods from Dataset A. The walking periods labeled exclusively inside or outside were used to train, validate, and test a classification model. Then, we used the classification model to label the walking periods labeled as mixed (e.g., inside and outside), as well as the unlabeled walking periods from Dataset A, and all the walking periods from Dataset B. Finally, all the labeled walking periods from both Dataset A and B were used to characterize the

differences between indoor and outdoor walking periods.

5.2.2 Datasets

Table 5.1: **Datasets details**

	Dataset A	**Dataset B**
Sample Size	20	15
Age	$\mu = 26.1$ $\sigma = 6.1$	$\mu = 25.3$ $\sigma = 2.1$
Male:Female	6:11	7:8
Measurements	activPAL Self-report GPS	activPAL
Duration	7 days	14 days

The details for the data collection of Dataset A and B can be found here [56, 58]. Briefly, for Dataset A, we collected data on 20 participants over a week in the real world (Table 5.1). Contextual information was collected using self-reporting and GPS data from their phones using an app called Ethica app (Ethica Data [Toronto, Canada]). For the self-reporting, participants were asked to maintain an activity log describing where they walked (ex: home, work, etc.) and the purpose of their walk (ex: going to work). We also conducted an exit interview after the real-world data collection to ensure that the self-reporting was complete and accurate. Motion data was collected using the activPAL (activPAL™ [PAL Technologies Ltd., Glasgow, UK]), a thigh-worn accelerometer. This device can be placed on the thigh using tape and offers 2-week continuous monitoring. It samples at 20Hz and possesses a 3-axis accelerometer ($range = \pm 4g$). The sensor's size and battery life allow for an unobtrusive placement and high compliance. Additionally, the proprietary algorithm of the sensor offers an accurate classification of activities that we used to isolate walking [66, 70]. Dataset B was collected on 15 participants over 2 weeks in the real world, using only the activPAL (Table 5.1). It is important to note that 4 subjects are in both datasets. Additionally, although dataset B was over a longer period, the data collection period was amidst the COVID-19 pandemic, which might lead to a decrease in measured activity.

5.2.3 Classification Algorithm Development

Figure 5.2 shows the data processing framework we used to create the algorithm to classify walking periods into outdoor or indoor.

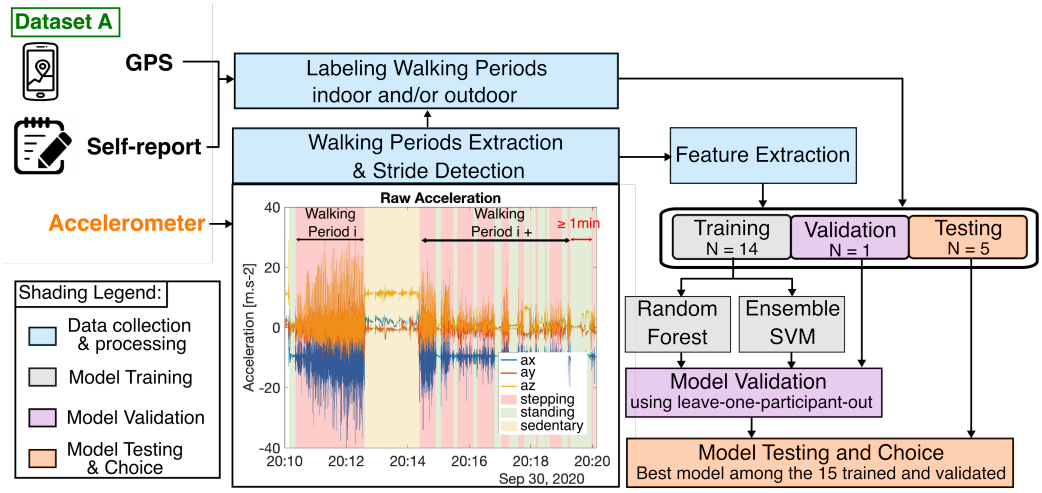

Figure 5.2: **Classification Model** — We extracted walking periods from the accelerometer that we then labeled using self-report and GPS data. We extracted features from the accelerometer data and the stride detection. Labeled walking periods were then split into training, validation, and testing set. We trained and validated two different learning algorithms, Random Forest and Ensemble SVM, using a leave-one-participant-out scheme. This led to 15 trained models that were then tested on the 5 remaining untouched participants' data. The best-performing model was chosen for the rest of the analyses.

5.2.3.1 Walking Period Extraction

Walking in the real world can be understood as an ensemble of walking bouts. However, there are bouts of walking that are likely to belong to a same walking activity. For instance, if an individual stops at a pedestrian light, the walks before and after that stop could be grouped together. We introduced the notion of walking period to capture this start-and-stop dynamic of real-world walking. This method was created and outlined in earlier work [58]. Briefly, we used the activPAL to identify stepping bouts. Then, bouts that were separated by a standing period of less than 1 minute were grouped together into a stepping period. Lastly, we developed a classification algorithm to extract walking periods from these stepping periods, since the activPAL does not distinguish between walking and running [58].

5.2.3.2 Data Labeling

We manually labeled the walking periods from Dataset A using the self-report and GPS data. We combined a visualization of the GPS data with a satellite map and the information given in the participants' self-report to assign either an inside or outside label, or a mixed label when it appeared participants were walking both inside and outside (Figure 5.3). There are walking periods that were not labeled, either because there was no associated GPS data, because the self-report was missing, or both.

Figure 5.3: **Data Labeling using GPS and self-report data** — We show here 3 examples for walking periods labeled indoor, outdoor, and both indoor and outdoor. The GPS sampling was variable and dependent to the type of phone used. The text in quotations corresponds to the participant's self-report.

5.2.3.3 Feature Extraction

We used a custom algorithm to extract strides from the thigh-worn accelerometer. Using the distance between strides, we computed stride time and stride frequency for each stride in a walking period. Then, we first extracted a set of biomechanics features, based on our domain knowledge. This set includes walking period duration, walking period continuity (e.g., proportion of total standing time within a period, with 100 being no standing time), mean and standard deviation of stride frequency. Stride frequency was normalized by $\sqrt{g \cdot l_0}$, with l_0 being leg length [96]. Leg length was measured from the anterior superior iliac spine to the floor. Walking period continuity

was defined as:

$$period\ continuity = \frac{period\ duration - standing\ time}{period\ duration} \times 100, \tag{5.1}$$

Additionally, we computed 20 other features from both stride frequency and the raw accelerometer signal (Appendix C).

5.2.3.4 Classification Model

Learning Algorithms We compared the performances of two supervised ensemble learning algorithms that use different classification principles to separate indoor versus outdoor walking periods: Ensemble Support Vector Machine (SVM) [133] and Random Forest [134]. We used ensemble methods to solve the issue of imbalanced classes but also improve the generalizability of our model [135]. Ensemble methods combine multiple base models to improve classification performances. Both SVM and Random Forest algorithms have successfully been used for terrain classification tasks with both humans and robots [59]. We used grid search to optimize the hyperparameters of both algorithms. The ensemble SVM we used is a bagging (e.g., bootstrap aggregation) classifier with SVM as a base model, 60 estimators, and a radial basis function kernel. The Random Forest algorithm used 40 estimators and used bootstrapping to build the trees. We trained both algorithms on the set of biomechanics features and all features. In summary, we evaluated 4 different cases: Ensemble SVM with biomechanics features, Ensemble SVM with all features, Random Forest with biomechanics features, and Random Forest with all features. We used the Scikit-learn library (version 1.0.2) from Python to train and evaluate the different learning algorithms [136].

Model Training, Validation, and Testing To build our model, we only used walking periods labeled exclusively indoor or outdoor (Figure 5.1). We divided our dataset into training, validation, and testing sets. The training and validation set contained walking periods from 15 participants and followed a leave-one-participant-out method to tune the hyperparameters of our models and

evaluate the generalizability to new participants. In other words, we trained a model on data from 14 participants and validated it on the remaining participant. This process was iteratively performed 15 times, with each participant serving as the validation set once, and for each of the four cases described in the previous paragraph (2 algorithms $\times$ 2 features sets). This provided 15 models that we evaluated and we chose the best-performing case to use on the 5-participant testing set. For instance, if the average performance of the models that were trained and validated using Ensemble SVM on all features is the highest, we will use the 15 models from this case on the testing set. The model that performed the best on the testing set among the 15 trained models for the best case was chosen for the classification of the walking periods labeled as mixed and the unlabeled walking periods of dataset A, as well as all the walking periods in dataset B (Figure 5.1).

Model Evaluation We used different metrics to evaluate our model and represent its performances both during training and testing in the different cases and for the different models. First, we used accuracy to determine the overall proportion of correctly classified walking periods. We complemented accuracy with F1-score since accuracy can be misleading when dealing with imbalanced datasets. F1-score takes into account both false positives and false negatives to ensure that the performance is not biased towards the more frequent class. Finally, we also used Area Under the ROC Curve (AUC) to measure the model's ability to separate between indoor and outdoor classes. AUC is also useful for imbalanced datasets as it takes into account false positives and false negatives. The combination of these different performance metrics provides a more comprehensive picture of the model's performance.

Feature Importance We used feature permutation to estimate the importance of each feature in the performances of our model. This method consists of randomly shuffling the values of a given feature in the validation set and calculating the change in performance of the model with the shuffled data. We used the test set to evaluate feature importance.

Analysis of Walking Periods labeled indoor and outdoor We did not use walking periods that happened both inside and outside to train our model to avoid decreasing the model's performance. However, we investigated how the chosen model classified these mixed walking periods. We labeled as best as possible the mixed walking periods based on whether they were mostly indoor or mostly outdoor, to investigate whether the model would classify a mostly indoor walk as indoor and vice versa. It is important to note that the GPS data can be noisy and interpretation can be difficult, even with the support of the self-report data (Figure 5.3).

5.2.4 Outdoor versus Indoor Walking Analysis

Once we chose the best performing model, we classified the walking periods labeled indoor and outdoor and the unlabeled walking periods of dataset A, as well as all the walking periods in dataset B (Figure 5.1). Then, we characterized the differences between indoor and outdoor walking periods. We looked at the differences in walking period duration and continuity, as well as in an essential health indicator: walking speed.

5.2.4.1 Walking Speed Estimation

We used the method described in Baroudi et al. [57] to estimate stride speed from the accelerometer. Briefly, this method leveraged the relationship between stride speed v and stride frequency f [72, 73]:

$$v = \exp \frac{\ln (a \cdot f)}{1 - b} \tag{5.2}$$

where a and b are model parameters. Stride frequency f can be accurately estimated from stride detection using the accelerometer and we identified in previous studies the parameters a and b for each subject in both datasets using a foot-worn inertial measurement unit [56, 58]. Researchers reported that 97% of the stride speed error was under $0.2m \cdot s^{-1}$ using this method. This framework can be used to estimate the relative speed differences for individuals walking in the real world using only an accelerometer.

5.2.4.2 Statistical Analysis

Our goal was to understand the difference in walking speed, walking period duration, and continuity between indoor and outdoor settings, whilst taking into account the nested nature of our data: walking speeds are nested within walking periods, and walking periods are nested within participants. To tackle these inherent dependencies and repeated measures from each participant, we used linear mixed-effects models. This strategy facilitated the management of our multilevel data structure, properly adjusting for the correlations among multiple walking speeds, walking period duration, and continuity measures taken from the same walking period and participant. We built three models, using walking speed, walking period duration, and walking period continuity as the dependent variables, while the indoor/outdoor condition was the fixed effect, and the walking period (for the walking speed model only) and participant identifiers were the random effects. We tested the assumption of normally distributed and homogeneous residuals by visualizing QQ-plots and residuals versus fitted values plots. We normalized walking speed by $\sqrt{g \cdot l_0}$, with l_0 being the participant's leg length [96]. This design effectively captured the variability in walking period parameters both within and across periods and participants. The models were implemented in R using the 'lme' function from the 'nlme' package [137]. We explored different correlation structures for the random effects and selected the most appropriate model based on the Akaike Information Criterion (AIC) [75, 76]. The model with the lowest AIC was deemed the best fit for our data. The estimated fixed effect for the condition serves as an indication of the expected change in parameters when transitioning from indoor to outdoor environments, while accounting for the nested structure of the data.

5.3 Results

5.3.1 Classification Algorithm Evaluation

5.3.1.1 Model validation

Table 5.2 and table 5.3 summarize the validation results for the different cases. The data from subjects 1, 4, 7, 17, and 19 were randomly selected to be kept for the test set. The training set contained between 957 and 1040 walking periods, with $67.9 \pm 4.4\%$ (range) of indoor labels. The validation set contained between 29 and 112 walking periods, with $66.0 \pm 51.4\%$ of indoor labels. The test set contained 339 walking periods with 78.8% of indoor labels. The models perform better when using the biomechanics feature set. The average accuracy, F1-score, and AUC increase of approximately 0.2 for both Ensemble SVM and Random Forest models from using all features to the biomechanics features only. Random Forest and Ensemble SVM perform comparably with both sets of features. Because Random Forest algorithms are easier to interpret and use, we chose the Random Forest algorithm with the biomechanics feature set to use with our test set. The model trained and validated using Random Forest and the biomechancs features with S8 held out performed the worst ($accuracy = 0.828$, $F1 - score = 0.857$, $AUC = 0.815$) while the one with S9 held out performed the best ($accuracy = 1.000$, $F1 - score = 1.000$, $AUC = 1.000$).

5.3.1.2 Model Testing and Choice

We evaluated the 15 models validated using Random Forest and the biomechanics feature set on the 5-participant test set. We found that Model 13 (e.g., the model that was trained and validated with S16 held out) outperforms the other models, with an accuracy of 0.941, an F1-score of 0.963, and an AUC of 0.881. As such, we chose this model to label the rest of the data and characterize the differences between indoor and outdoor walking periods.

Table 5.2: **Model Validation with All Features**

	Accuracy		F1-score		AUC	
Held out Subject	**Ensemble SVM**	**Random Forest**	**Ensemble SVM**	**Random Forest**	**Ensemble SVM**	**Random Forest**
S2	**0.958**	0.938	**0.974**	**0.960**	**0.909**	**0.896**
S3	**0.911**	**0.911**	**0.949**	0.948	0.737	**0.758**
S5	0.789	**0.853**	0.853	**0.892**	0.726	**0.812**
S6	0.862	**0.879**	0.833	**0.851**	0.895	**0.908**
S8	**0.862**	**0.862**	**0.889**	**0.889**	**0.846**	**0.846**
S9	**1.000**	**1.000**	**1.000**	**1.000**	**1.000**	**1.000**
S10	0.897	**0.936**	0.927	**0.953**	0.852	**0.907**
S11	0.788	**0.859**	0.862	**0.913**	0.842	**0.848**
S12	**0.990**	**0.990**	**0.994**	**0.994**	**0.972**	**0.972**
S13	**0.863**	0.843	**0.851**	0.833	**0.876**	0.860
S14	**0.900**	0.867	**0.906**	0.875	**0.907**	0.873
S15	0.709	**0.722**	0.693	**0.711**	0.758	**0.776**
S16	0.907	**0.926**	0.944	**0.955**	0.792	**0.833**
S18	0.978	**0.989**	0.986	**0.993**	0.960	**0.980**
S20	**0.781**	**0.781**	**0.840**	**0.840**	**0.798**	**0.798**
Average	0.880	**0.890**	0.900	**0.907**	0.858	**0.871**

5.3.1.3 Feature Importance

We found that walking period duration was the most important feature in the model we chose (Figure 5.4). Its shuffling led to a decrease in accuracy of 0.19. Walking period continuity, mean stride frequency, and standard deviation of stride frequency led to decreases in accuracy of 0.04, 0.06, and 0.02 respectively.

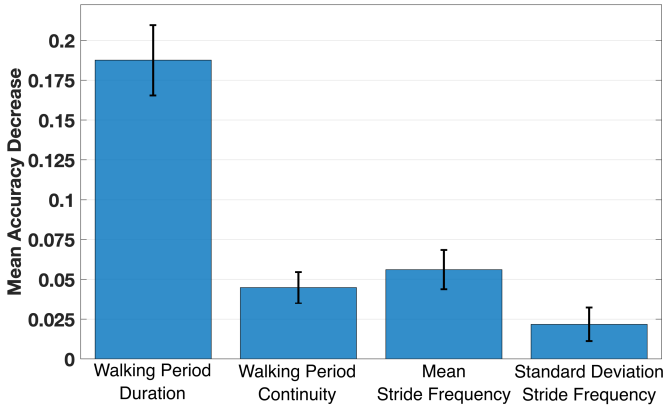

Figure 5.4: **Feature Importance using Feature Permutation** — Decrease in model accuracy for each shuffled feature. The error bars represent standard deviation.

Table 5.3: **Model Validation with Biomechanics Features**

	Accuracy		F1-score		AUC	
Held out Subject	**Ensemble SVM**	**Random Forest**	**Ensemble SVM**	**Random Forest**	**Ensemble SVM**	**Random Forest**
S2	0.917	**0.938**	0.947	**0.960**	0.850	**0.896**
S3	**0.893**	0.884	**0.939**	0.933	0.684	**0.721**
S5	**0.874**	0.863	**0.909**	0.901	**0.829**	0.820
S6	0.862	**0.879**	0.833	**0.851**	0.895	**0.908**
S8	**0.862**	0.828	**0.889**	0.857	**0.846**	0.815
S9	**1.000**	**1.000**	**1.000**	**1.000**	**1.000**	**1.000**
S10	0.885	**0.923**	0.919	**0.944**	0.833	**0.889**
S11	**0.941**	0.882	**0.966**	0.929	0.896	0.862
S12	**0.990**	0.962	**0.994**	0.976	**0.972**	0.955
S13	**0.863**	**0.863**	**0.851**	**0.851**	**0.876**	**0.876**
S14	0.950	**0.967**	0.958	**0.971**	0.942	**0.962**
S15	0.810	**0.848**	0.776	**0.806**	0.837	**0.858**
S16	**0.926**	0.889	**0.955**	0.930	**0.833**	0.810
S18	0.978	**0.989**	0.985	**0.993**	0.973	**0.993**
S20	**0.822**	**0.822**	**0.876**	0.874	0.807	**0.826**
Average	**0.905**	0.902	**0.920**	0.918	0.872	**0.879**

Table 5.4: **Model Choice** — Results of the 15 models with the 5-participant test set. Each model corresponds to the models trained and validated with the leave-one-participant-out scheme using the Random Forest algorithm with the biomechanics features set as shown in Table 5.3. Model 13 performs the best.

	Accuracy	**F1-score**	**AUC**
Model 1	0.917	0.948	0.861
Model 2	0.917	0.948	0.861
Model 3	0.909	0.942	0.851
Model 4	0.920	0.950	0.853
Model 5	0.917	0.948	0.861
Model 6	0.929	0.956	0.874
Model 7	0.920	0.951	0.848
Model 8	0.917	0.948	0.866
Model 9	0.920	0.950	0.863
Model 10	0.926	0.954	0.872
Model 11	0.914	0.946	0.865
Model 12	0.932	0.958	0.861
Model 13	**0.941**	**0.963**	**0.881**
Model 14	0.923	0.952	0.860
Model 15	0.923	0.952	0.875
Best Model	0.941	0.963	0.881

5.3.2 Model Classifications on Mixed Walking Periods

Figure 5.5 shows a visualization of walking periods labeled mixed (e.g., indoor and outdoor) using principal component analysis with the walking periods labeled only indoor or outdoor. We observed that the majority of walks labeled mostly indoor clusters with the walks labeled only indoor and vice versa for outdoor walking periods. The model we chose classified 71% of mostly outdoor walks as outdoor and 88% of mostly indoor walks as indoor. Figure 5.5 also shows the self-report and GPS data from two walking periods that were likely mislabeled by the researcher as mostly indoor and outdoor.

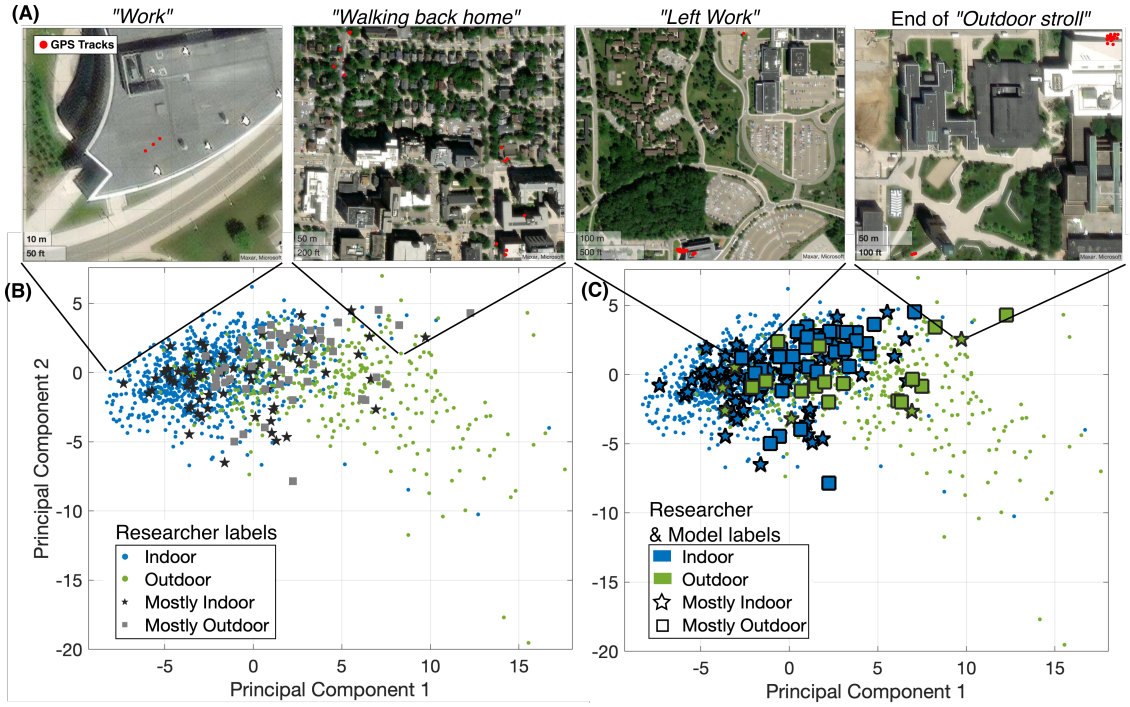

Figure 5.5: **Analysis of Walks labeled both Indoor and Outdoor** — (A) GPS and self-report data is shown for a sample of walks labeled indoor only, outdoor only, mostly indoor, and mostly outdoor by the researcher (from left to right). The mixed walking periods highlighted here are likely to be mislabeled. The sampling rate of the GPS data is variable and depends on the participant's phone type. (B) Principal component analysis for walking periods labeled indoor, outdoor, mostly indoor, and mostly outdoor by the researcher. (C) Principal component analysis with the mixed walking periods labeled by the model. We can see that the majority of mostly indoor walks are labeled indoor and vice versa, and that the walking periods that were likely mislabeled by the researcher are likely correctly labeled by the model.

5.3.3 Characterization of Indoor versus Outdoor Walking Periods

After all walking periods were labeled, we had 69,616 stride speed values and 3,766 walking periods from dataset A, compared to 53,930 stride speed values and 3,701 walking periods from dataset B. The ratio of indoor versus outdoor was approximately 80:20 for both datasets. Different linear mixed models were built to evaluate the effect of context (e.g., walking environment) on walking speeds, walking period duration, and continuity. First, we found a large significant effect of context on walking speed $b = 0.095$, $t(117678) = 79.5$, $p < 0.001$. This indicates that normalized walking speed increases by 0.095 from indoor to outdoor walks (0.095 corresponds to approximately $0.29m \cdot s^{-1}$ depending on the participant's leg length). We also found a large significant effect of context on walking period duration and continuity, $b = 9.25$, $t(7446) = 48.9$, $p < 0.001$ and $b = 20.14$, $t(7446) = 26.2$, $p < 0.001$. These results suggest that duration increases by 9.25 minutes and continuity by 20.14% from indoor to outdoor walks.

These results are illustrated in Figure 5.6 and Figure 5.7. We observe that outdoor walking periods have overall higher duration ($\mu_{outdoor} = 11.4min$ versus $\mu_{indoor} = 2.2min$) and continuity ($\mu_{outdoor} = 81.7\%$ versus $\mu_{indoor} = 61.6\%$). Participants walked on average $0.28m \cdot s^{-1}$ faster when walking outdoor compared to indoor. We also observe a larger variability in the distribution of stride speed indoor compared to outdoor ($\sigma_{indoor} = 0.43m \cdot s^{-1}$ versus $\sigma_{outdoor} = 0.31m \cdot s^{-1}$).

5.4 Discussion

In the real world, individuals exhibit great variability in walking patterns and are able to adapt to diverse environmental contexts. Understanding these contexts is essential for extracting meaningful information about a person's mobility. Determining whether an individual is walking indoors or outdoors is a critical element of context, given the stark differences in environment and conditions that these two settings present. Here, we developed a novel framework that utilizes only an accelerometer to accurately classify indoor versus outdoor walks. We used a unique dataset collected in the real world to ensure the ecological validity of our model. Then, we used this approach

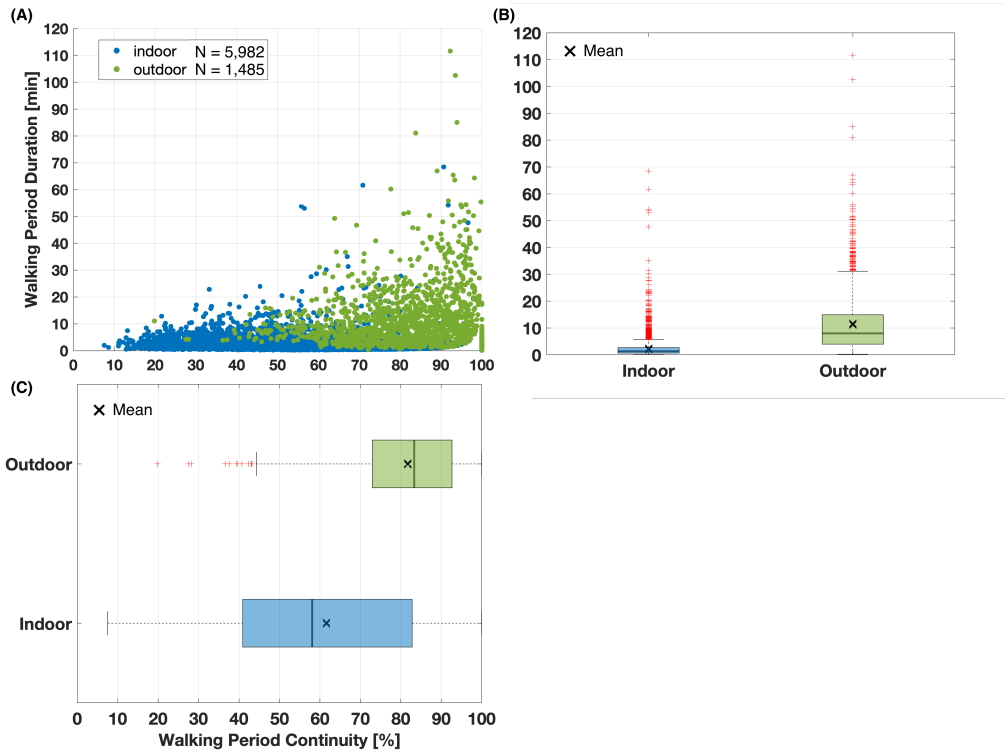

Figure 5.6: **Indoor and Outdoor Walking Periods Duration and Continuity** — Relationship between walking period duration and continuity — (A) Each dot corresponds to a walking period. (B) and (C) We binned all walking periods by their context and looked at their durations and continuity.

to quantify the differences between indoor and outdoor walking patterns. This framework not only demonstrates the potential to use a minimal sensor suite to successfully gain important contextual information but also enables a more comprehensive understanding of real-world walking behavior.

Both Ensemble SVM and Random Forest trained with different feature sets were able to learn the characteristics of indoor and outdoor walks. The performances across models were very high, as reflected by average accuracies, F1-scores, and AUC exceeding 0.88, 0.90, and 0.86 respectively for all training scenarios (Table 5.2 and Table 5.3). Trained models performed better with the biomechanics feature set, suggesting that these features are sufficient to capture the inherent differences between indoor and outdoor walking periods (Table 5.3). Notably, walking period duration was the most important feature (Figure 5.4) with outdoor walks being longer on average than indoor walks ($\sim +9min$) (Figure 5.6). Average stride frequency was also an important feature,

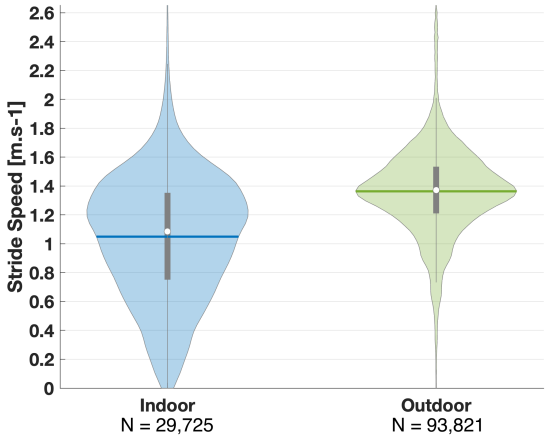

Figure 5.7: **Stride Speed for Walking Periods Indoor vs. Outdoor** — Distribution of stride speeds for all participants grouped by context. Each shaded area represents the shape of the distribution, and the horizontal lines mark the mean.

as outdoor walks tend to have a higher intensity than indoor walks. The high performance of the classifier also suggests that the grouping of walking bouts into walking periods is an effective representation of real-world walking [58]. We chose the best performing model that used the Random Forest algorithm trained with the biomechanics feature set (Table 5.4). Using the biomechanics feature set as opposed to the raw data enables the model to be reused with different sensor types and placements. In fact, stride frequency was chosen because it can easily be derived directly from various sensors, even from smartwatches [138–140]. The choice of Random Forest also increases the interpretability and generalizability of our model for other populations. As such, the model we developed could be extended to other studies of mobility and help improve the understanding of human data from wearable sensors.

We used the developed model to characterize the differences between walking indoor compared to outdoor using a large dataset. We found that outdoor walking periods were significantly longer, more continuous (e.g., less standing time), and had higher stride speed (Figure 5.6 and Figure 5.7). Researchers have been increasingly interested in the measurement of walking speed in the real world, as it is a critical health indicator for various health issues [6, 10, 81, 87]. Our observations show that individuals greatly vary their walking speed indoor (Figure 5.7). On the other hand,

individuals took more strides outdoor, with less variability in walking speed. This suggests that isolating outdoor walks could potentially improve estimates of preferred walking speed in the real world. This substantiates the findings that longer walks show greater discriminative power for clinical populations [42]. Understanding the proportion of activity spent indoor versus outdoor can also be useful for the improvement of physical activity. Although any increase in physical activity matters, there are proven benefits to walking outdoors [141–143]. As such, our models could be used in the different stages of intervention design, from the baseline physical activity assessment to the monitoring of intervention efficacy. The reduced sensor set also enables higher compliance (e.g., the degree to which users correctly and consistently wear the device as intended), which is essential for the reliability and validity of data collected in the real world.

While this study integrates fundamental elements of context for real-world walking, there are numerous other contextual factors that can have an impact on walking behavior and biomechanics. There are also nuances within indoor and outdoor walks, such as terrain type, that also induce changes in walking patterns [55, 59]. Future work should investigate those factors and their relationships with motion to potentially integrate additional classes or sub-classes into the model we developed. Further, we developed our model with 20 young adults. Thus, the accuracy and generalizability of our model can be improved by collecting a larger dataset with a more diverse population. Lastly, our method was mainly developed for offline classifications, in the scenario where data is retrieved and post-processed to gain information on an individual's behavior. Expanding this framework for online classification should be pursued, for potential use in fields like rehabilitation or assistive robotics.

5.5 Conclusion

One of the main challenges in interpreting real-world walking data from wearable sensors is the unsupervised nature of the data collection. There is a need for the development of methods that leverage motion data to predict contextual information. To address this, we proposed an accurate

and ecologically valid classification algorithm that distinguishes between walking in indoor and outdoor environments. This algorithm can be used with data collected from other wearable devices measuring motion. We also provided a detailed characterization of the differences between these two environments. Indoor versus outdoor represents arguably one of the primary layers of real-world context. The stark contrasts in constraints, terrain types, weather, etc., between these two environments significantly influence individuals' walking biomechanics. This information can ultimately help researchers or healthcare professionals better interpret the walking data, understand individuals' mobility patterns and needs, and design more effective interventions or treatments.

CHAPTER 6

Conclusions and Future Directions

The dynamics of human walking contain a wealth of information that can be leveraged toward the understanding of someone's health condition. Traditionally, a patient's walk is evaluated during clinical assessments, which are punctual and offer merely a snapshot of someone's capabilities (also called episodic care). As such, the healthcare industry is turning towards the promise of digital health, particularly wearable sensors, to integrate technology that can improve patient care. Initially popular among consumers wanting to self-quantify their health, clinicians are starting to see the potential and the new opportunities for patient care that wearable sensors can offer. In particular, these technologies enable continuous monitoring of patients over extended periods, allowing clinicians to gain a unique insight into their daily habits. The datasets collected greatly enhance the current resolution of mobility assessments and can improve the detection of changes in health. However, the adoption of these technologies in the clinical world is still in its early stages. Major challenges include analyzing and making sense of real-world data. In fact, researchers have found that different factors can affect an individual's walking biomechanics in the real world. Since real-world data is most often collected without supervision, it can be difficult to parse the data and extract meaningful information. There are gaps in the existing literature regarding the processing methods of wearable sensor datasets collected in the real world over extended periods. This dissertation addresses these gaps by proposing methods that leverage different time scales and sensor suites to quantify walking in the real world.

6.1 Contributions

In this section, we summarize the major contributions made in this dissertation.

Aim 1: Understanding walking economy in the real world

When humans walk, their metabolism consumes energy. Researchers have found that individuals can modulate certain aspects of their walking gait, such as their walking speed, to minimize their energy consumption when walking. In this dissertation, we investigated whether this finding remains true in the real world, where individuals walk in a variety of contexts. We tested whether individuals use on average a walking speed that minimized their cost of transport, and whether this use was independent of context. To test these hypotheses, we collected a unique dataset and developed methods to fuse different measurement streams - capturing motion, physiological, and contextual data - to characterize walking economy across a range of real-world contexts. We found that individuals tend to walk faster than what is energetically optimal, and that they adapt their gait based on context, making their walk more or less efficient. This work highlighted the importance of taking measurements outside of the lab to be able to obtain a representation of an individual's natural behavior. The findings have the potential to inspire changes in the design of experiments in the field of biomechanics for health, but also for roboticists developing lower-body assistive devices.

Aim 2: Estimating and characterizing walking speed in the real world using a single-point accelerometer

We presented a framework to estimate and characterize a key health indicator: walking speed. The method we proposed leverages a single accelerometer placed on the thigh, reducing the burden of data collection. First, we developed a model to obtain accurate measurements of walking speed using this single sensor, that we validated in the real world to ensure ecological validity. Then, we created a framework to explain the variability of real-world walking speed. We introduced the notion of walking periods, to represent the start-and-stop nature of real-world walks. We found that the duration and continuity (e.g., the proportion of stops) of a walking period can be used to

parse walking speed and isolate walks with reduced variability. Long continuous walks contain many strides with a low variability and can potentially be used to provide estimates of preferred walking speed. Because of the simplicity of this framework and the use of a single low-resolution accelerometer, it can be leveraged toward evaluations of clinical populations' mobility and overall health.

Aim 3: Classifying and characterizing indoor and outdoor walks in the real world using a single-point accelerometer

In Aim 1, we demonstrated the impact of context on various aspects of human walking biomechanics. Despite successfully explaining some of the variability in walking speed using the characteristics of a walking period in Aim 2, it remains essential to understand the specific context in which individuals are walking. As such, in this aim, we focused on developing a method to distinguish between indoor and outdoor walks, as these two settings represent fundamental elements of real-world context. We proposed a machine learning approach, using the dataset collected in Aim 1, to classify context using a single-point accelerometer. We used a random forest architecture with a straightforward and intuitive set of features to increase the interpretability, explainability, and usability of our model across different experimental setups and sensing systems. We then used the validated model to characterize the differences between walking indoor versus outdoor, using the datasets collected for Aim 1 and Aim 2. We found a significant impact of the contextual environment on the duration and continuity of a walk, and, more importantly, on walking speed. This framework has the potential to be extended for clinical populations, offering a more comprehensive picture of an individual's walking capabilities and overall physical activity level. It represents a step towards improving the use of digital health technologies to gain insight into patients' functional mobility in the real world.

6.2 Opportunities for Future Work

In this dissertation, we have created different frameworks for the analysis of real-world data using wearable sensing technologies. We quantified many aspects of human walking and the different factors that can influence it. However, there are still endless opportunities to improve our understanding of human walking in the real world, and create methods to extract meaningful information from real-world data. The limitations of this work represent potential opportunities for future research. We describe three promising areas of research that can build on this dissertation.

Improving the assessment of patient's mobility with long-term monitoring

The different datasets from this work have been collected from healthy young adults. Although this data allowed the identification of important factors that influence mobility in daily life, additional data needs to be collected from clinical populations to generalize these methods. The frameworks developed can enhance our understanding of the environments in which patients move, paving the way for more informed and effective treatment designs and interventions. For example, a traditional intervention for patients with cardiovascular issues involves promoting walking [6, 115]. Wearable sensors have been successfully utilized to measure baseline physical activity levels and monitor tailored interventions. However, there is often little to no knowledge about the nature of the walking activity. Adapting and expanding the frameworks presented in this dissertation, could facilitate the creation of more customized interventions and enable more accurate monitoring of their efficacy.

Investigating additional contextual factors that significantly impact walking

Throughout this dissertation, we isolated different factors that influence walking biomechanics. In Aim 1, we measured participants' locations and purposes during walking and identified specific sub-contexts that had a significant impact on walking kinematics. In Aim 2, we found that the duration and continuity of a walking bout can be used to explain the variability in real-world walking speed. Finally, in Aim 3, we characterized the differences between walking indoor

versus outdoor. However, it is important to note that the contextual factors explored in this work represent only a small subset of the multitude of factors that can influence an individual's walking pattern. For example, researchers have found correlations between an individual's mood and their gait [52, 53, 129]. With the advancement of machine learning, accurate modeling of these relationships between motion and contextual factors holds the potential for predicting context using only wearables. This has implications for advancing the understanding of human movement in the real world and ultimately, for the improvement of patient health.

Developing methods for an advance use of consumer-grade wearable sensors

In this dissertation, we utilized different measurement tools and sensors to collect data. The motion sensors used are research-grade devices, which are relatively expensive and require expertise to operate. To facilitate the adoption of wearable devices in healthcare, researchers need to develop tools that leverage consumer-grade wearables. Fitness trackers and smartwatches have become ubiquitous in our daily lives and continue to gain interest. These devices are not only cost-effective and user-friendly, but also provide the important feature of feedback to the user. In fact, the popularity of these devices stems from their capability to provide different health metrics to the user, from step count to heart rate. The devices often already integrate suggestions to help the user improve their health. However, these devices typically provide summary metrics that do not capture the nuances and variability of real-world movement. Future research can build on this dissertation to develop methods adapted for consumer-grade wearables, to obtain more detailed movement profiles that could be leveraged in clinical settings. Breakthroughs in this area (in collaboration with wearable manufacturers) would significantly advance the potential for the integration of wearable sensors in healthcare analytics, offering more accessible and data-driven approaches to patient care.

Contributing to improvements in assistive robotics

Drawing inspiration from nature is crucial for innovation in lower-body assistive devices. Gaining

a deeper understanding of an individual's everyday movements can help establish design requirements that truly reflect the demands of daily life. In this dissertation, we investigated different aspects of normative walking in the real world. In particular, we highlighted some of the differences between laboratory-based and real-world walking behavior as well as the changes in walking gait due to context. These findings suggest the need for experimental designs that are ecologically valid and that take into account the natural variability of human movements. Future research can leverage the findings in this work to adapt the functional requirements for the design and control of exoskeletons and prostheses, but also other assistive devices like angle-foot orthoses. The deployment of wearable sensing solutions or the use of sensing modalities within those devices can help understand the needs of clinical populations like lower-limb amputees as well as evaluate the efficacy of the different designs [49, 64].

6.3 Broader Impact

I imagine a future where wearable sensors are an integral part of clinical assessments. At the end of a typical physical exam, your doctor hands you a sensor and asks you to put it on and come back in a month. Upon return, the doctor extracts the data from the wearable sensor to give you medical information and advice that is personalized with contextual information, high-resolution, and objectively quantitative, to complement their original assessment. There is a long way to go before this vision can become reality, and the work in this dissertation represents a step toward it. The research presented in this dissertation demonstrates the potential of wearable sensors to gain insight into the different dimensions contributing to someone's health and well-being. The frameworks we developed can be extended for clinical populations to improve the sensitivity and precision of mobility assessments. Additionally, this work advances our understanding of the factors that influence walking in daily life. Overall, by fusing expert knowledge and data-driven approaches, we demonstrated how we can further the interpretation of data collected in the real world.

Looking ahead, as wearable technologies continue to evolve, richer datasets will require the development of more advanced and complex data processing methods. This dissertation lays the groundwork to leverage the potential of extended real-world movement monitoring. Ultimately, this type of data collection offers new avenues for the improvement of personalized healthcare. Persistent monitoring using wearable sensors can be leveraged to turn towards preventative and predictive healthcare paradigms, which could ultimately improve human health and well-being.

APPENDIX A

Chapter 2 - Supplementary Material

A.1 Sensor Wear Time

Participants were instructed to wear the activPAL during the whole week but were allowed to remove it overnight if they wished. As such, the compliance for this sensor was high. We had an average of 6h of non-wear time for the week across all participants. S1 accumulated the most non-wear time over the week (36.4h). They removed the sensor for an entire day and one night for personal reasons. 13 participants had less than 5h of non-wear time over the weak.

The IMU was attached to the participant's shoe using a pouch secured with their laces. As such, participants were instructed to wear the IMU whenever they went out and were wearing their shoes. On average, participants wore the sensor for 9.2h per day. The average daily wear time ranged from 6.9h for S3, to 13.2h for S12. Many participants were able to recharge the sensor during the day, which explains high daily wear time. Sundays were the days with the least wear time (8.4h). Some participants did not wear the sensor for an entire day, either because they forgot to place the sensor in their shoe, or because they did not wear that specific pair of shoes, or because they did not leave their home on that day.

A.2 Enforcing Real-world Walking Strategy on the Treadmill

As explained in the materials and methods (Experimental Protocol - In-Lab Data Collection — Second Visit - Treadmill Walking and Energetics Measurements), we constrained participants'

stride frequency for a given treadmill speed to enforce the parameters a and b of the power model:

$$l = a.v^b$$

Here, we show the results of the difference in the parameters we found in the real world and those the participants displayed on the treadmill.

We found less than 10% change in parameter a apart for S12 and S15. There was more change in parameter b, with an average difference of 23%. For 10 participants, the change in parameter b was an increase. For 15 participants, the change in parameter a was a decrease. This reflects the tendency of participants to lower their stride length for a given stride speed, and particularly for faster speeds. In fact, when b increases, stride length decreases for a higher stride speed, and when a decreases, stride length decreases for all given stride speeds. Figure A.1 shows an example with 2 different participants' real-world vs. treadmill power models. S7 adopted a consistently lower stride length for a given stride speed when walking on the treadmill, whereas S12 matched successfully their in-lab walking to the real world.

A.3 Steady-state Walking in the Real World

The notion of steady state can be used to describe any type of dynamic process that reaches an unvarying condition. For human movement, steady-state walking is the convergence of specific parameters to a point of stability. The most common characterizations of steady-state walking use either physiological parameters (e.g., heart rate, oxygen consumption) [144], mechanical parameters (e.g., stride speed, stride frequency) [145–147], or a combination of both. In the real world, the large variability of contexts can lead to a range of walking behavior involving a combination of steady-state and non-steady-state. Slowing down, stopping, starting, or turning are all motions that can lead to non-steady-state gait. In our study, we wanted to extract steady-state walking from real-world data using our set of sensors. We used mechanical parameters to characterize and differentiate steady-state and non-steady-state walking.

A.3.1 The Algorithm

The algorithm (detailed below) was applied to all walking bouts (within walking periods) for a specific subject. We iterated through all strides (N) within a bout and discarded the first and last strides. We started by creating vectors of stride speeds and stride lengths using three consecutive strides (s_{i-1}, s_i, and s_{i+1}). The coefficient of variation CV was calculated for each of these vectors (CV_{length} and CV_{speed}). A high coefficient of variation is indicative of large variations from the mean in a given vector. In our case, it would indicate a change in stride speed or stride length within the three selected strides. Then, we calculated the direction of the strides s_{i-1} and s_i using the foot position derived from the integration of the IMU data as explained in the sub-section (Walking Speed Estimation for a Walking Period). Cosine similarity $cos\theta$ was calculated, with θ being the angle between the direction of s_{i-1} and s_i. Cosine similarity was chosen to evaluate the alignment in the direction of the two consecutive strides. If $cos(\theta)$ is close to 1, it means the vectors are almost aligned. Finally, we compared CV_{length}, CV_{speed}, and $cos\theta$ against thresholds to classify the stride s_i. The choice of thresholds is explained in the next section.

Algorithm 1 Steady-state classification of strides

```
for walking bouts in subject_s do
    for i = 2, ..., N − 1 do
        vector_speed = [speed_s_{i−1}, speed_s_i, speed_s_{i+1}]
        vector_length = [length_s_{i−1}, length_s_i, length_s_{i+1}]
        CV_speed = σ_{vector_speed} / μ_{vector_speed}
        CV_length = σ_{vector_length} / μ_{vector_length}
        cosθ = (s_{i−1} · s_i) / (‖s_{i−1}‖‖s_i‖)
        if CV_speed ≥ 0.07 & CV_length ≥ 0.07 then
            steady_state_i = 0
        else if cosθ ≤ 0.7 then
            steady_state_i = 0
        else
            steady_state_i = 1
        end if
    end for
end for
```

A.3.2 Sensitivity Analysis for Threshold Selection

To determine the thresholds for the three parameters we selected, we conducted a sensitivity analysis following the leave-one-out method. We varied one parameter while fixing the two others to explore how sensitive our outputs were to each variable. The outputs we monitored were: (1) the distribution of steady-state stride speed for each participant, and (2) the percentage of strides identified as steady state across all participants. We fixed CV_{speed} and CV_{length} to 0.07 and 0.07 respectively. Those fixed values were derived from Macfarlane et al. [145]. We fixed $cos(\theta)$ to 0.7, which translates to a maximum of 45 degrees between the direction of two consecutive strides.

We did not observe a large sensitivity of the average and standard deviation of steady-state stride speed when varying the different parameters. Thus, we did not use this output to select the thresholds for each parameter.

In Figure A.2 - (A) and (B), we observe that the variation of both CV_{speed} and CV_{length} influences the percentage of identified steady-state strides following a first-order response trend, with convergence to a value close to 80% for a representative subject. On the other hand, the variation $cos(\theta)$ did not influence the percentage of identified steady-state strides apart for very large values (e.g., $cos(\theta) > 0.97$) (Figure A.2 - (C)). Humans generally vary their stride speed and stride length when they are about to turn. Thus, this result indicates that most turns in the real world are likely captured by a change of CV_{speed} and/or CV_{length}. We used the results from the sensitivity analysis on this output to determine thresholds for each parameter. Since $cos(\theta)$ did not influence either output in a meaningful way, we kept a threshold of 0.7. For CV_{speed} and CV_{length}, we picked the value at which the percentage of identified steady-state strides crossed the $\pm 2\%$ boundary around the value this output converged to (Figure A.2 - (A) and (B)). This resulted in a choice of 0.07 for both CV_{speed} and CV_{length}.

A.3.3 Validity of Thresholds

To confirm the validity of the thresholds we chose, we used a controlled in-lab experiment in which participants walked back and forth in a hallway. We reconstructed the track of each participant and observed the identified steady-state strides using our selected thresholds. Figure A.3 shows a representative subject's track with the associated changes in parameters CV_{length}, CV_{speed}, and $cos(\theta)$. Steps around a turn to walk back in the hallway were identified as non-steady-state. We also notice that the second stride and the second to last stride were classified as non-steady-state. This corresponds to the transition between walking and stopping. As a reminder, the first and last strides were discarded to be able to run the designed algorithm. Each parameter shows how the accelerations and decelerations as well as the turns are captured by the different chosen thresholds (Figure A.3 - (B)).

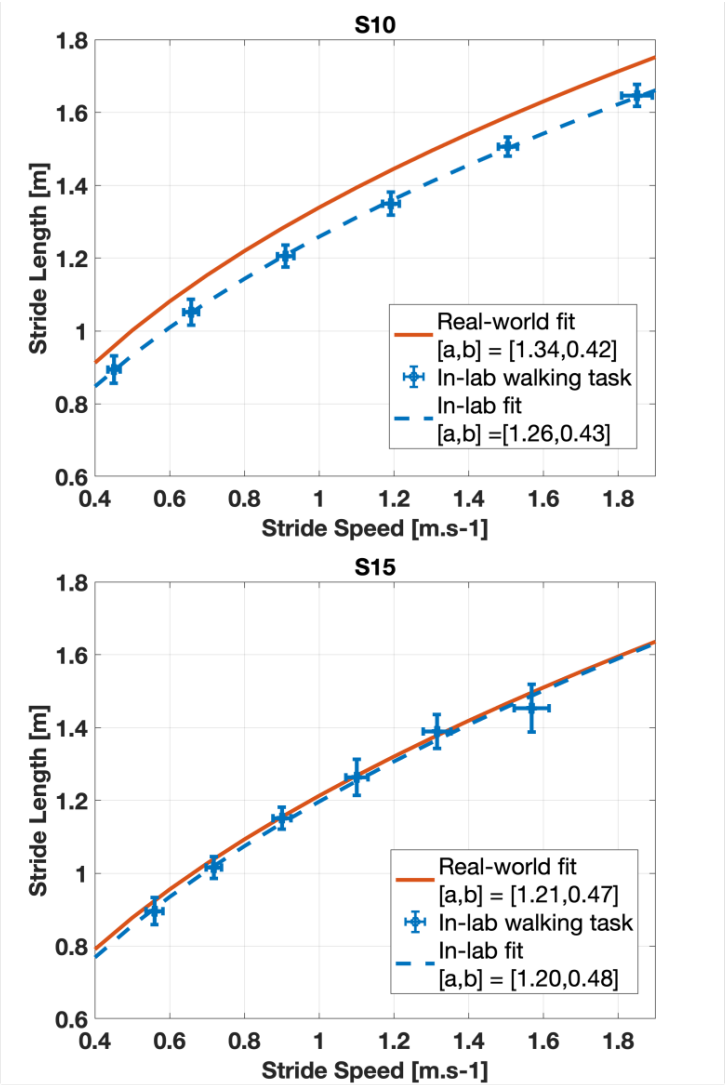

Figure A.1: **Enforcing Walking Strategy** — Power model mapping stride length to stride speed for both the real-world and the in-lab data collection. Each dot represents the average for a given trial on the treadmill and the error bars represent the standard deviation for both stride speed and stride length. We chose to not show the real-world data points to not crowd the plots.

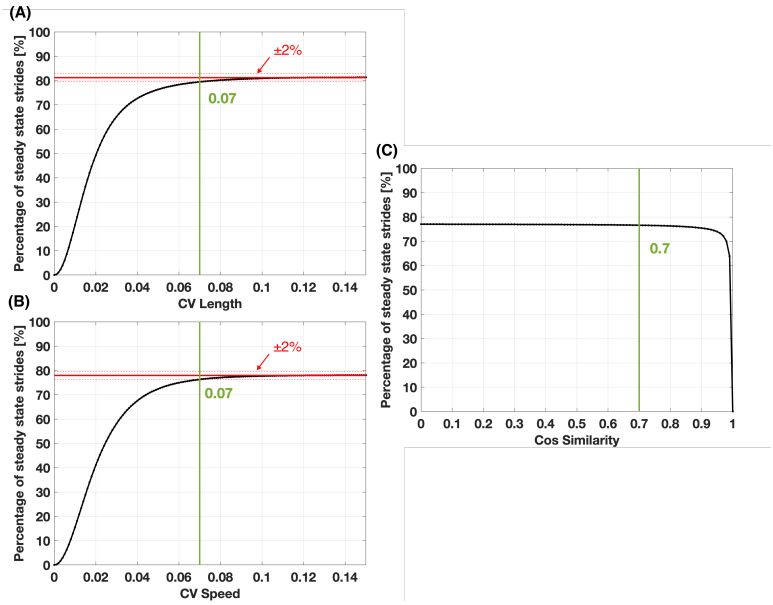

Figure A.2: **Sensitivity Analysis** — Variation of the percentage of steady-state strides based on changes in the parameters CV_{length} (A), CV_{speed} (B), and $cos(\theta)$ (B) for a given subject.

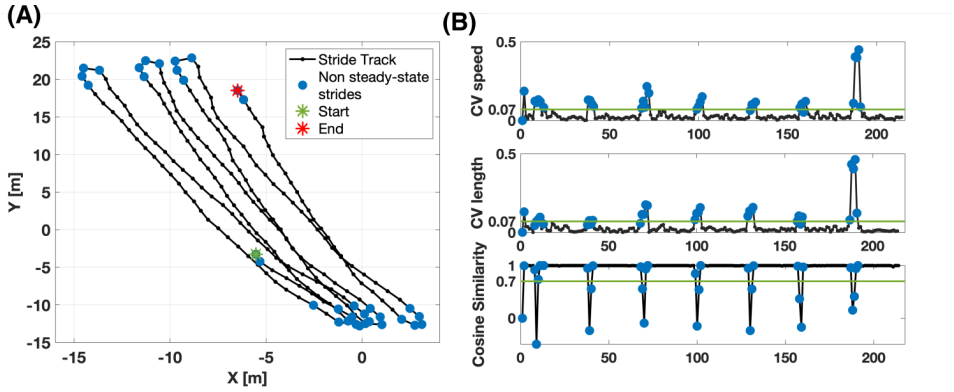

Figure A.3: **In-lab Walk for Validation** — (A) Representative track for S7 during a controlled in-lab walk where participants walked back and forth in a hallway. (B) Parameters variation associated with the track. The green line represents the chosen threshold for each parameter.

APPENDIX B

Chapter 4 - Supplementary Material

B.1 Sensor Wear Time

Overall, wear time for the activPAL was very high, with only 2% of non-wear time recorded for all participants over the 14 days of data collection. Five participants removed the activPAL for short periods during the 14 days of data collection. The cumulative non-wear time varied between 2.1 hours to 69.2 hours among these participants with the longest non-wear time being due to a participant forgetting to place the sensor back after swimming. Only one subject felt discomfort and removed the sensor for 11 hours. Due to a sensor error, only 9 out of the 14 days were extracted for Subject 15. Across participants, the average daily wear time for the Polar OH1 monitor was 7.65 hours between 8 am and 10 pm. Participants with low wear times reported either forgetting to charge the device overnight, or forgetting to put it on in the morning.

B.2 Details on the Extraction of Walking Periods

In section 3.3.2., we explained how we extracted stepping periods from the data labeled by the activPAL. These stepping periods corresponded to a grouping of stepping events based on the duration and type of the activity state in between consecutive stepping events. In this appendix, we detail how, from these stepping periods, we extracted walking periods.

Stride Detection We started by applying a stride detection method to each stepping period. Participants were instructed to place the sensor in a specific orientation such that the x-axis would be pointing inferiorly, the y-axis pointing medially, and the z-axis pointing anteriorly out of the thigh. We observed the data prior to analysis to correct for any orientation errors. To detect strides, we worked with the z-axis acceleration, as it is the axis susceptible to registering the highest peaks of acceleration and changes in direction when an individual is walking or running. We smoothed the raw signal from this axis using a locally weighted scatterplot smoothing (LOWESS) method. This technique allows for the signal to be smoothed without removing the high peaks. To detect strides in each stepping period, we used a peak detection method with a threshold of $5m \cdot s^{-2}$, and a minimum peak prominence of $5m \cdot s^{-2}$. These parameters were determined using a labeled dataset we created specifically for the use of the activPAL. We extracted the distance between consecutive peaks to monitor for any possible outliers, which could correspond to an incorrect stride detection or to a pause in the stepping. Then, we identified sections of consecutive strides that started when a stride was detected and ended whenever an outlier was found or whenever a stepping period ended.

Windowing and Feature Extraction These sections were used to isolate non-overlapping windows of 5 strides (Figure **??** - B). Any section with less than 5 strides was discarded. The window size was chosen based on results from previous studies [114]. Overlapping 5-stride windows were tested but did not perform as well as non-overlapping ones. Thus, each stepping period was divided into a series of 5-stride windows. We extracted an ensemble of 44 features from the time and frequency domain from each window of 5 strides (Figure B.1 - A). The choice of features was based on the literature and on our knowledge of walking gait biomechanics, with an emphasis on features that would allow us to differentiate walking and running [38, 148]. A detailed table of the features extracted, with their formulas (if applicable) and definitions is available in Appendix C.

Principal Component Analysis A principal component analysis (PCA) was applied on the matrix of centered features for each runner. Features were centered using z-scores to obtain a zero mean for each column. The goal was to visualize the 5-stride windows in a 2-dimensional space

to make sure running data was separated from walking data with the set of features we chose. We observed two large separate point clouds for the recreational runners (Figure B.1 - B), and we confirmed the nature of each cloud using heart rate data (Figure B.1 - B - a)), the provided running logs (Figure B.1 - B - b)), and observation of the raw data for a random number of samples from each point cloud. The running logs provided by each runner contained a start time and duration for each run they performed during the study period. We noted that some points logged as running belonged to the cluster of windows identified as walking (Figure B.1 - B - b)). This can be explained by the imprecision of the runs' manual logging, and by the presence of walking instances when one is running. Additionally, some data points appeared far from both clouds. By observing the raw data for these points, we concluded that they correspond to either noise that was mistakenly identified as stepping by the activPAL or bouts with more or less than 5 strides, coming from errors in the stride detection algorithm. The average variance explained by the two first principal components was 48.91% and 8.8% respectively.

Unsupervised Clustering We clustered the data using a method of unsupervised clustering: density-based spatial clustering of applications with noise (DBSCAN). This method marks points in low-density regions as outliers. The parameters for this clustering algorithm were: *epsilon*, which corresponds to the minimum distance between points, and *minPoints*, which corresponds to the minimum of points necessary to form a cluster. These two parameters were manually tuned for each subject to obtain two clusters corresponding to running and walking, as well as the outliers isolation(Figure B.1 - B).

Decision Tree and Classification We built a decision tree for each of the clustering obtained from the runners' data. Decision trees are simple but powerful tools for classification. Their main advantage is their interpretability. In fact, a decision tree can be visualized and the features used, as well as the thresholds can be understood from a biomechanics standpoint. We used the Decision Trees tool from the Statistics and Machine Learning Toolbox™ of MATLAB. We imposed a limit of five branches on the tree for interpretability, and because the results did not change significantly

between a five-branch tree and the bigger ones automatically built by MATLAB (Figure B.1 - C). None of the trees built were identical, but some similarities were observed. Three of the five trees had *mean absolute deviation* for the x-axis acceleration as the top node. The two others had *mean absolute deviation* for the z-axis and *variance* for the x-axis as the top node. All these features are measures of the variability of the signal. Stride time was present at the second level of three of the trees, and stride frequency was present at the third level for two of the trees. We applied each tree to the ensemble of subjects (runners and non-runners). Thus, for each participant, all 5-stride windows were classified into running, walking, or other. The windows were then regrouped back within the stepping period to which they belonged for each subject. Thus, through the classification with the different decision trees, each participant presented an ensemble of stepping periods within which a certain number of windows of 5 strides were labeled as walking, running, or other.

Walking Period Extraction The last step of the walking extraction method relies on establishing a rule to define which stepping period will be kept as a walking period for the analysis, and which ones will be discarded (Figure B.1 – C). This allowed us to keep walking data falsely classified as other within a stepping period, but also to be conservative and discard any stepping period that had a probability of being another activity than walking. We set up a threshold λ, such that, if the percentage of windows labeled walking within a stepping period was superior to λ, we keep the period as a walking period. We chose the parameter λ for each tree that maximized the amount of data labeled run being correctly removed. Finally, we kept the tree that allowed for the highest percentage of runs to be removed.

Performance Evaluation We chose the tree from Subject 14, which allowed for the removal of 99% of the running data overall with a value of λ of 77% (Figure B.2). We also evaluated the performance of this tree using heart rate data and our knowledge of the division between runners and non-runners in our recruited subjects. The average heart rate for the periods we kept as walking was $103bpm$ against $140bpm$ for the discarded stepping periods. This high value of heart rate validates that the discarded periods contained the running data. Additionally, only a small amount

of data was discarded for the 3 non-runners.

B.3 Features

Name	**Formula**	**Meaning**
Jerk	$\int a_t \, dt$	Rate of change of acceleration a with time, related to the smoothness of the signal.
Zero Crossing Mode		Number of time the signal crosses the 0 line.
Norm	$\|a\| = \sqrt{\sum_{t=1}^{T} \|a_t^2\|}$	Captures the signal size.
Stride Frequency	$\frac{1}{stridetime}$	Number of stride per minute
Stride time		Time between two strides
Mean	$\mu = \frac{1}{N} \sum_{t=1}^{N} a_t$	Average of the signal
Variance	$\frac{1}{N-1} \sum_{t=1}^{N} \|a_t - \mu\|^2$	Variance of the signal
Standard Deviation	$\sigma = \sqrt{\frac{1}{N-1} \sum_{t=1}^{N} \|a_t - \mu\|^2}$	Standard deviation of the signal
Skewness	$s = \frac{E(a-\mu)^3}{\sigma^3}$	Measure of the asymmetry of the signal distribution
Kurtosis	$k = \frac{E(a-\mu)^4}{\sigma^4}$	Measure of the weight of the signal distribution tails relative to its center
Mean Absolute Deviation	$mad = \frac{1}{N} \sum_{t=1}^{N} \|a_t - \mu\|$	Measure of the dispersion of signal distribution
Mean Frequency		Mean normalized frequency of the power spectrum of the time-domain signal
Median Frequency		Median normalized frequency of the power spectrum of the time-domain signal
Signal to Noise Ratio		Ratio between signal information and its background undesired noise
Power	$\frac{1}{N} \sum_{t=1}^{N} \|a_t\|^2$	Sum of the absolute squares of its time-domain samples, divided by the signal length, related to the amplitude of the signal
Integral Power Spectral Density		Different measure of power, in the frequency domain, through the power spectral density

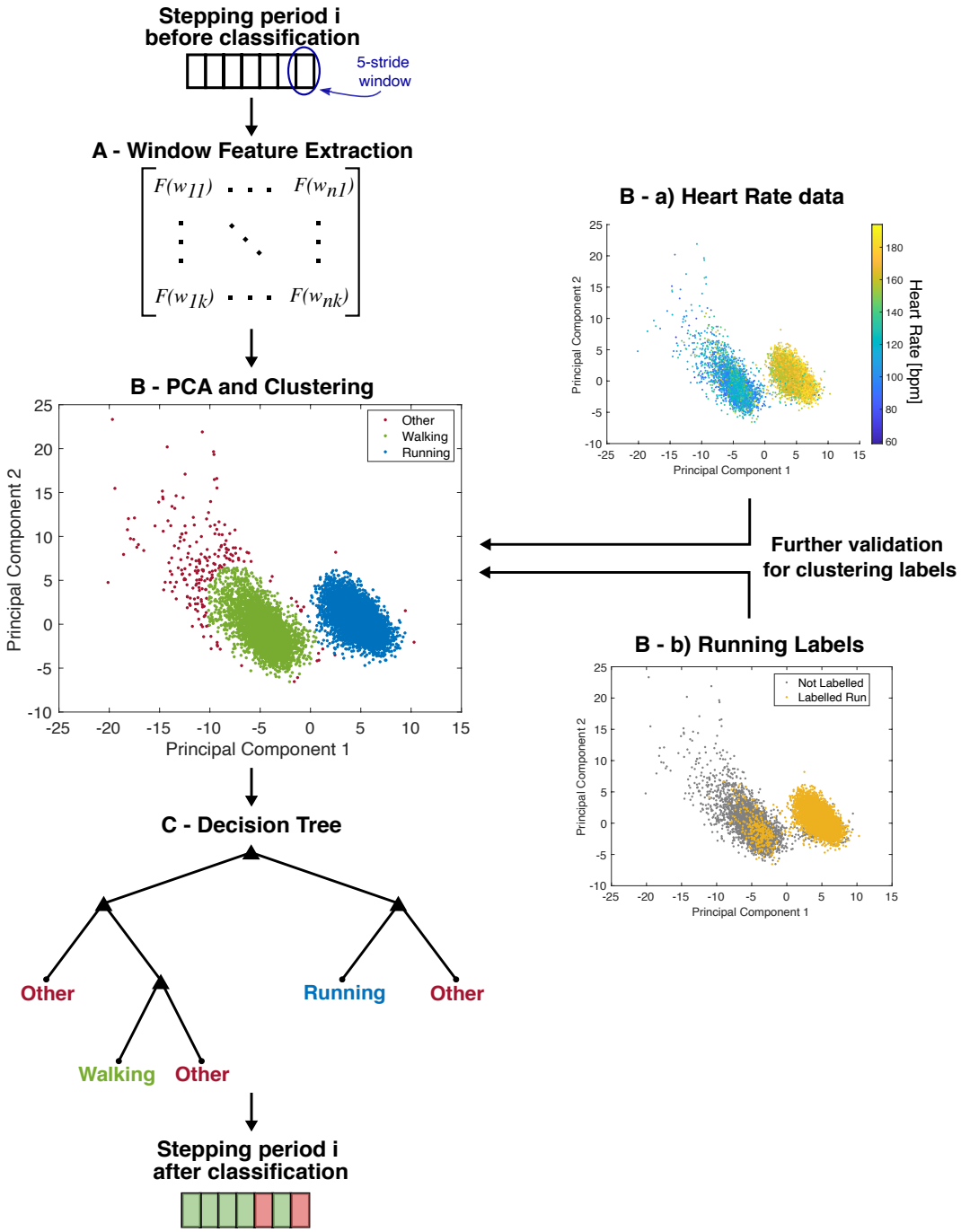

Figure B.1: **Extraction of Walking Periods** — **(A)** From each 5-stride window, an ensemble of 44 features was extracted. **(B)** We applied a principal component analysis to the matrix of features. Then, an unsupervised clustering method was used to isolate the different point clouds. Each point corresponds to a 5-stride window. Using heart rate **(B - a))** and the labels obtained from the runners **(B - b))**, we confirmed the nature of the clusters as walking, running, and others. **(C)** Then, we built a decision tree using the labels from our clustering. Finally, the tree was used to classify each 5-stride window.

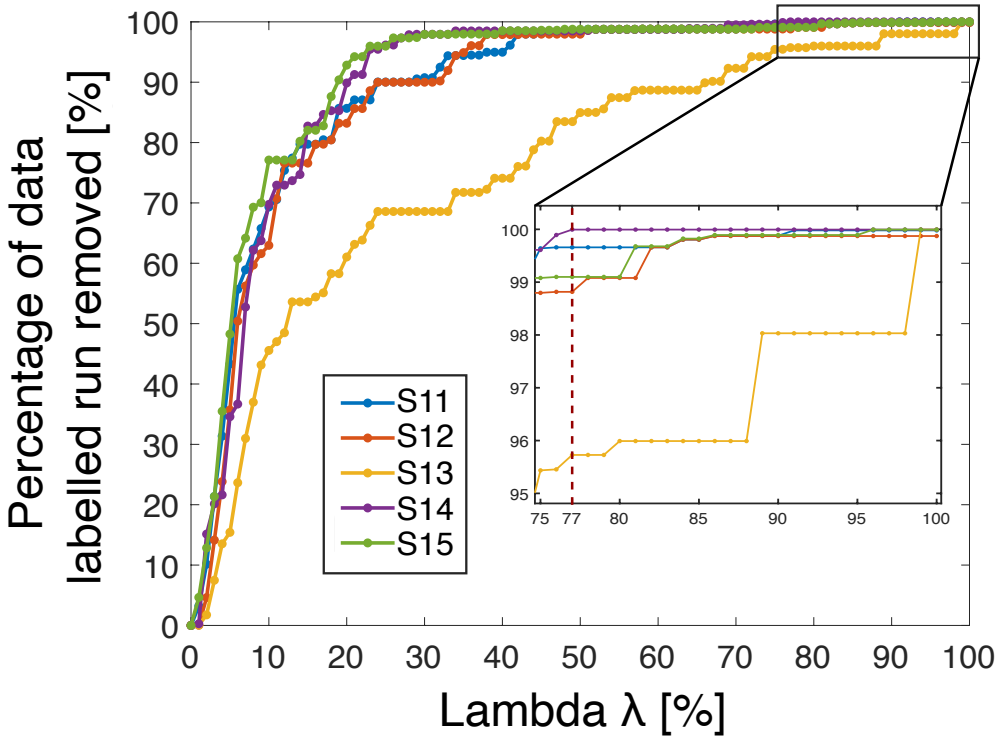

Figure B.2: **Performance Evaluation** — Plot of the percentage of data labeled run being removed against the different values of lambda. Each line represents a runner. We observed the highest percentage of data labeled run being removed for the tree built with Subject 14's data, at a value of λ of 77%, noted by a red dashed line on the zoomed subplot.

APPENDIX C

Chapter 5 - Supplementary Material

C.1 Features

Table C.1: **List of Features**

Signal used	Name	Formula	Meaning
Walking Period	Duration		Duration of walking period
	Continuity	$period\ continuity = \frac{period\ duration - standing\ time}{period\ duration} * 100$	Proportion of standing time in a walking period
Stride Frequency	Average	$\mu = \frac{1}{N}\sum_{t=1}^{N}\frac{1}{stridetime}$	Average of stride frequencies within a walking period
	Standard Deviation	$\sigma = \sqrt{\frac{1}{N-1}\sum_{t=1}^{N}\lvert\frac{1}{stridetime} - \mu\rvert^2}$	Standard deviation of stride frequencies within a walking period
	Kurtosis	$k = \frac{E(\frac{1}{stridetime}-\mu)^4}{\sigma^4}$	Measure of the weight of the distribution of stride frequencies within a walking period tails relative to its center
	Skewness	$s = \frac{E(\frac{1}{stridetime}-\mu)^3}{\sigma^3}$	Measure of the asymmetry of the distribution of stride frequencies within a walking period
	Min		Minimum value for stride frequencies within a walking period
	Max		Maximum value for stride frequencies within a walking period
3-axis Acceleration	Mean	$\mu = \frac{1}{N}\sum_{t=1}^{N} a_t$	Average of the signal
	Standard Deviation	$\sigma = \sqrt{\frac{1}{N-1}\sum_{t=1}^{N}\lvert a_t - \mu\rvert^2}$	Standard deviation of the signal
	Skewness	$s = \frac{E(a-\mu)^3}{\sigma^3}$	Measure of the asymmetry of the signal distribution
	Kurtosis	$k = \frac{E(a-\mu)^4}{\sigma^4}$	Measure of the weight of the signal distribution tails relative to its center
	Min		Minimum signal value
	Max		Maximum signal value
	Variance	$\frac{1}{N-1}\sum_{t=1}^{N}\lvert a_t - \mu\rvert^2$	Variance of the signal
	Mean Jerk	$\frac{1}{N}\sum_{t=1}^{N}\int a_t\, dt$	Average rate of change of signal with time, related to the signal smoothness
	Energy	$Energy = \sum_{t=1}^{N} a_t^2$	Measure of how "strong" the signal is over its duration
	Power	$Energy/N$	Total energy of the signal divided by its length
	Mean Absolute Deviation	$mad = \frac{1}{N}\sum_{t=1}^{N}\lvert a_t - \mu\rvert$	Measure of the dispersion of the signal
	Mean Frequency		Mean normalized frequency of the power spectrum of the time-domain signal
	Median Frequency		Median normalized frequency of the power spectrum of the time-domain signal
	Signal to noise ratio		Ratio between signal information and its background undesired noise
	Squared Root Mean Squared	$\mu = \frac{1}{N}\sum_{t=1}^{N} a_t^2$	Measure of the magnitude of the signal
	Integral of Power Spectral Density		Different measure of power, in the frequency domain, through the power spectral density

BIBLIOGRAPHY

[1] David A. Winter. *Biomechanics and Motor Control of Human Movement: Fourth Edition*. 2009. 1

[2] Tung Wu Lu and Chu Fen Chang. Biomechanics of human movement and its clinical applications. *Kaohsiung Journal of Medical Sciences*, 28(2 SUPPL.), 2012. 1

[3] V. T. Inman. Human locomotion. 1966. *Clinical Orthopaedics and Related Research*, 94(288):3–9, 1993. 1

[4] G A Cavagna and R Margaria. Mechanics of walking. *Journal of Applied Physiology*, 21(1):271–278, jan 1966.

[5] A. Roberts. Gait analysis: normal and pathological function (2nd edition). *The Journal of Bone and Joint Surgery. British volume*, 92-B(8):1184–1184, aug 2010. 1

[6] Jeremy N. Morris and Adrianne E. Hardman. Walking to health. *Sports Medicine*, 23(5):306–332, 1997. 1, 36, 76, 93, 99

[7] Elaine M. Murtagh, Marie H. Murphy, and Janne Boone-Heinonen. Walking: The first steps in cardiovascular disease prevention. *Current Opinion in Cardiology*, 25(5):490–496, 2010. 36

[8] Filipa Matos Wunderlich. Walking and rhythmicity: Sensing urban space. *Journal of Urban Design*, 13(1):125–139, 2008.

[9] I. Min Lee and David M. Buchner. The importance of walking to public health. *Medicine and Science in Sports and Exercise*, 40(7 SUPPL.1):512–518, 2008. 1, 76

[10] Stacy Fritz and Michelle Lusardi. White paper: ”walking speed: The sixth vital sign”. *Journal of Geriatric Physical Therapy*, 32(2):2–5, 2009. 2, 32, 36, 60, 71, 93

[11] Paul L Enright. The Six-Minute Walk Test Introduction Standards and Indications 6-Minute Walk Test Versus Shuttle Walk Test Safety Variables Measured Conducting the Test Ensuring Quality Factors That Influence 6-Minute Walk Distance Interpreting the Results Improving the. *Respiratory Care*, 48(8):783–785, 2003. 2

[12] C. Vaney, H. Blaurock, B. Gattlen, and C. Meisels. Assessing mobility in multiple sclerosis using the Rivermead Mobility Index and gait speed. *Clinical Rehabilitation*, 10(3):216–226, 1996. 2, 36

[13] Catherine M. Dean, Carol L. Richards, and Francine Malouin. Walking speed over 10 metres overestimates locomotor capacity after stroke. *Clinical Rehabilitation*, 15(4):415–421, 2001. 36

[14] Russell T. Johnson, Jocelyn F. Hafer, Ryan D. Wedge, and Katherine A. Boyer. Comparison of measurement protocols to estimate preferred walking speed between sites. *Gait and Posture*, 77(December 2019):171–174, 2020. 2

[15] Kira P. Prahm, Nanna Witting, and John Vissing. Decreased variability of the 6-minute walk test by heart rate correction in patients with neuromuscular disease. *PLoS ONE*, 9(12):1–8, 2014. 2, 36

[16] Grace Wu, Bonnie Sanderson, and Vera Bittner. The 6-minute walk test: How important is the learning effect? *American Heart Journal*, 146(1):129–133, 2003. 2

[17] Alexander M. Aurand, Jonathan S. Dufour, and William S. Marras. Accuracy map of an optical motion capture system with 42 or 21 cameras in a large measurement volume. *Journal of Biomechanics*, 58:237–240, 2017. 2

[18] Patric Eichelberger, Matteo Ferraro, Ursina Minder, Trevor Denton, Angela Blasimann, Fabian Krause, and Heiner Baur. Analysis of accuracy in optical motion capture – A protocol for laboratory setup evaluation. *Journal of Biomechanics*, 49(10):2085–2088, 2016.

[19] Markus Windolf, Nils Götzen, and Michael Morlock. Systematic accuracy and precision analysis of video motion capturing systems-exemplified on the Vicon-460 system. *Journal of Biomechanics*, 41(12):2776–2780, 2008. 2

[20] David J. Clark. Automaticity of walking: Functional significance, mechanisms, measurement and rehabilitation strategies. *Frontiers in Human Neuroscience*, 9(MAY):1–13, 2015. 2, 11

[21] Sabrina J. Abram, Jessica C. Selinger, and J. Maxwell Donelan. Energy optimization is a major objective in the real-time control of step width in human walking. *Journal of Biomechanics*, 91:85–91, 2019. 11, 29

[22] A. E. Minetti and R. Mc N. Alexander. A theory of metabolic costs for bipedal gaits. *Journal of Theoretical Biology*, 186(4):467–476, 1997.

[23] M. Y. Zarrugh, F. N. Todd, and H. J. Ralston. Optimization of energy expenditure during level walking. *European Journal of Applied Physiology and Occupational Physiology*, 33(4):293–306, 1974.

[24] Jeremy D. Wong, Jessica C. Selinger, and J. Maxwell Donelan. Is natural variability in gait sufficient to initiate spontaneous energy optimization in human walking? *Journal of Neurophysiology*, 121(5):1848–1855, 2019. 29

[25] Jessica C. Selinger, Shawn M. O'Connor, Jeremy D. Wong, and J. Maxwell Donelan. Humans Can Continuously Optimize Energetic Cost during Walking. *Current Biology*, 25(18):2452–2456, 2015. 2, 11, 29

[26] Elke Warmerdam, Jeffrey M. Hausdorff, Arash Atrsaei, Yuhan Zhou, Anat Mirelman, Kamiar Aminian, Alberto J. Espay, Clint Hansen, Luc J.W. Evers, Andreas Keller, Claudine Lamoth, Andrea Pilotto, Lynn Rochester, Gerhard Schmidt, Bastiaan R. Bloem, and Walter Maetzler. Long-term unsupervised mobility assessment in movement disorders. *The Lancet Neurology*, 19(5):462–470, 2020. 3, 12, 36, 37, 39

[27] Laura A. Hutchinson, Marcus J. Brown, Kevin J. Deluzio, and Alan R. De Asha. Self-Selected walking speed increases when individuals are aware of being recorded. *Gait and Posture*, 68(November 2018):78–80, 2019. 11

[28] Inbar Hillel, Eran Gazit, Alice Nieuwboer, Laura Avanzino, Lynn Rochester, Andrea Cereatti, Ugo Della Croce, Marcel Olde Rikkert, Bastiaan R. Bloem, Elisa Pelosin, Silvia Del Din, Pieter Ginis, Nir Giladi, Anat Mirelman, and Jeffrey M. Hausdorff. Is every-day walking in older adults more analogous to dual-task walking or to usual walking? Elucidating the gaps between gait performance in the lab and during 24/7 monitoring. *European Review of Aging and Physical Activity*, 16(1):1–12, 2019. 3, 12

[29] Matthew A. Brodie, Milou J. Coppens, Andreas Ejupi, Yves J. Gschwind, Janneke Annegarn, Daniel Schoene, Rainer Wieching, Stephen R. Lord, and Kim Delbaere. Comparison between clinical gait and daily-life gait assessments of fall risk in older people. *Geriatrics and Gerontology International*, 17(11):2274–2282, 2017. 3, 36

[30] Matthew A.D. Brodie, Milou J.M. Coppens, Stephen R. Lord, Nigel H. Lovell, Yves J. Gschwind, Stephen J. Redmond, Michael Benjamin Del Rosario, Kejia Wang, Daina L. Sturnieks, Michela Persiani, and Kim Delbaere. Wearable pendant device monitoring using new wavelet-based methods shows daily life and laboratory gaits are different. *Medical and Biological Engineering and Computing*, 54(4):663–674, 2016. 3, 36

[31] Lauren C. Benson, Christian A. Clermont, Eva Bošnjak, and Reed Ferber. The use of wearable devices for walking and running gait analysis outside of the lab: A systematic review. *Gait and Posture*, 63(March):124–138, 2018. 3, 12

[32] Shanshan Chen, John Lach, Benny Lo, and Guang Zhong Yang. Toward Pervasive Gait Analysis With Wearable Sensors: A Systematic Review. *IEEE Journal of Biomedical and Health Informatics*, 20(6):1521–1537, 2016. 3, 36

[33] Steven S. Coughlin; Jessica Stewart. Use of Consumer Wearable Devices to Promote Physical Activity: A Review of Health Intervention Studies. *Physiology & behavior*, 176(12):139–148, 2017. 3

[34] André Henriksen, Martin Haugen Mikalsen, Ashenafi Zebene Woldaregay, Miroslav Muzny, Gunnar Hartvigsen, Laila Arnesdatter Hopstock, and Sameline Grimsgaard. Using fitness trackers and smartwatches to measure physical activity in research: Analysis of consumer wrist-worn wearables. *Journal of Medical Internet Research*, 20(3), 2018. 3

[35] David R. Bassett, Lindsay P. Toth, Samuel R. LaMunion, and Scott E. Crouter. Step Counting: A Review of Measurement Considerations and Health-Related Applications. *Sports Medicine*, 47(7):1303–1315, 2017. 3

[36] S Koblick, M Yu, Matthew DeMoss, Q Li, CN Nessle, Michelle Rozwadowski, JP Troost, Jennifer A. Miner, A Hassett, Noelle E. Carlozzi, DL Barton, Muneesh Tewari, A Hanauer, and Sung Won Choi. A pilot intervention of using a mobile health app (ONC Roadmap) to enhance health-related quality of life in family caregivers of pediatric patients with cancer. *mHealth*, In Press, 2023.

[37] William E. Kraus, Kathleen F. Janz, Kenneth E. Powell, Wayne W. Campbell, John M. Jakicic, Richard P. Troiano, Kyle Sprow, Andrea Torres, and Katrina L. Piercy. Daily Step Counts for Measuring Physical Activity Exposure and Its Relation to Health. *Medicine and Science in Sports and Exercise*, 51(6):1206–1212, 2019. 3

[38] Angelo M. Sabatini, Chiara Martelloni, Sergio Scapellato, and Filippo Cavallo. Assessment of walking features from foot inertial sensing. *IEEE Transactions on Biomedical Engineering*, 52(3):486–494, 2005. 4, 37, 38, 111

[39] Lauro Ojeda and Johann Borenstein. Non-GPS navigation for security personnel and first responders. *Journal of Navigation*, 60(3):391–407, 2007. 12, 18, 41, 56

[40] John R. Rebula, Lauro V. Ojeda, Peter G. Adamczyk, and Arthur D. Kuo. Measurement of foot placement and its variability with inertial sensors. *Gait and Posture*, 38(4):974–980, 2013. 12, 18, 41

[41] Eric Foxlin. Pedestrian tracking with shoe-mounted inertial sensors. *IEEE Computer Graphics and Applications*, 25(6):38–46, 2005. 4, 37, 38, 41, 56

[42] Silvia Del Din, Alan Godfrey, Brook Galna, Sue Lord, and Lynn Rochester. Free-living gait characteristics in ageing and Parkinson's disease: Impact of environment and ambulatory bout length. *Journal of NeuroEngineering and Rehabilitation*, 13(1):1–12, 2016. 4, 5, 8, 60, 72, 94

[43] Fabio A. Storm, K. P.S. Nair, Alison J. Clarke, Jill M. Van der Meulen, and Claudia Mazzà. Free-living and laboratory gait characteristics in patients with multiple sclerosis. *PLoS ONE*, 13(5):1–15, 2018. 4

[44] Aiden R. Doherty, Paul Kelly, Jacqueline Kerr, Simon Marshall, Melody Oliver, Hannah Badland, Alexander Hamilton, and Charlie Foster. Using wearable cameras to categorise type and context of accelerometer-identified episodes of physical activity. *International Journal of Behavioral Nutrition and Physical Activity*, 10:1–11, 2013. 4, 77

[45] Jean P. Diaz, Rafael L. Da Silva, Boxuan Zhong, He Helen Huang, and Edgar Lobaton. Visual Terrain Identification and Surface Inclination Estimation for Improving Human Locomotion with a Lower-Limb Prosthetic. *Proceedings of the Annual International Conference of the IEEE Engineering in Medicine and Biology Society, EMBS*, 2018-July(1):1817–1820, 2018. 4, 77

[46] F. J. Blaauw, H. M. Schenk, B. F. Jeronimus, L. van der Krieke, P. de Jonge, M. Aiello, and A. C. Emerencia. Let's get Physiqual – An intuitive and generic method to combine sensor technology with ecological momentary assessments. *Journal of Biomedical Informatics*, 63:141–149, 2016. 4

[47] Yue Liao, Stephen S. Intille, and Genevieve F. Dunton. Using Ecological Momentary Assessment to Understand Where and With Whom Adults' Physical and Sedentary Activity Occur. *International Journal of Behavioral Medicine*, 22(1):51–61, 2015. 4

[48] Weixin Wang and Peter Gabriel Adamczyk. Analyzing gait in the real world using wearable movement sensors and frequently repeated movement paths. *Sensors (Switzerland)*, 19(8), 2019. 5, 11, 12, 36, 54, 60, 72

[49] Jay Kim, Natalie Colabianchi, Jeffrey Wensman, and Deanna H. Gates. Wearable Sensors Quantify Mobility in People with Lower Limb Amputation during Daily Life. *IEEE Transactions on Neural Systems and Rehabilitation Engineering*, 28(6):1282–1291, 2020. 5, 11, 12, 60, 72, 77, 101

[50] Ríona Mc Ardle, Silvia Del Din, Paul Donaghy, Brook Galna, Alan J. Thomas, and Lynn Rochester. The impact of environment on gait assessment: Considerations from real-world gait analysis in dementia subtypes. *Sensors (Switzerland)*, 21(3):1–15, 2021. 5, 8, 60, 72

[51] B. Hu, P. C. Dixon, J. V. Jacobs, J. T. Dennerlein, and J. M. Schiffman. Machine learning algorithms based on signals from a single wearable inertial sensor can detect surface- and age-related differences in walking. *Journal of Biomechanics*, 71:37–42, 2018. 5, 9, 78

[52] Zhan Zhang, Yufei Song, Liqing Cui, Xiaoqian Liu, and Tingshao Zhu. Emotion recognition based on customized smart bracelet with built-in accelerometer. *PeerJ*, 2016(7):1–14, 2016. 5, 77, 100

[53] Juan Carlos Quiroz, Elena Geangu, and Min Hooi Yong. Emotion recognition using smart watch sensor data: Mixed-design study. *JMIR Mental Health*, 5(8), 2018. 5, 77, 100

[54] Koren Gast, Rodger Kram, and Raziel Riemer. Preferred walking speed on rough terrain: Is it all about energetics? *Journal of Experimental Biology*, 222(9):1–24, 2019. 7, 12

[55] DB Kowalsky, JR Rebula, LV Ojeda, PG Adamczyk, and AD Kuo. Human walking in the real world: Interactions between terrain type, gait parameters, and energy expenditure. *bioRxiv*, 3:2019.12.29.890434, 2019. 7, 12, 36, 76, 94

[56] Loubna Baroudi, Kira Barton, Stephen M Cain, and K Alex Shorter. Understanding the Influence of Context on Real-World Walking Energetics. *Manuscript Submitted To Journal of Experimental Biology*, page 0, 2023. 7, 77, 80, 85

[57] Loubna Baroudi, Mark W. Newman, Elizabeth A. Jackson, Kira Barton, K. Alex Shorter, and Stephen M. Cain. Estimating Walking Speed in the Wild. *Frontiers in Sports and Active Living*, 2(November):1–14, 2020. 9, 63, 85

[58] Loubna Baroudi, Xinghui Yan, Mark W. Newman, Kira Barton, Stephen M. Cain, and K. Alex Shorter. Investigating walking speed variability of young adults in the real world. *Gait & Posture*, 98(May):69–77, 2022. 9, 11, 12, 17, 80, 81, 85, 93

[59] Muhammad Zeeshan Ul Hasnain Hashmi, Qaiser Riaz, Mehdi Hussain, and Muhammad Shahzad. What lies beneath one's feet? Terrain classification using inertial data of human walk. *Applied Sciences (Switzerland)*, 9(15), 2019. 9, 76, 78, 83, 94

[60] Ugur Dal, Taner Erdogan, Bora Resitoglu, and Hüseyin Beydagi. Determination of preferred walking speed on treadmill may lead to high oxygen cost on treadmill walking. *Gait and Posture*, 31(3):366–369, 2010. 11

[61] Kangneoung Lee, Vishnu Kalyanram, Chuanqi Zheng, Siddharth Sane, and Kiju Lee. Vision-based Ascending Staircase Detection with Interpretable Classification Model for Stair Climbing Robots. pages 6564–6570, 2022.

[62] Kharma C. Foucher, Laura E. Thorp, Diego Orozco, Madelaine Hildebrand, and Markus A. Wimmer. Differences in preferred walking speeds in a gait laboratory compared with the real world after total hip replacement. *Archives of Physical Medicine and Rehabilitation*, 91(9):1390–1395, 2010. 11

[63] Michael S. Orendurff, Jason A. Schoen, Greta C. Bernatz, Ava D. Segal, and Glenn K. Klute. How humans walk: Bout duration, steps per bout, and rest duration. *Journal of Rehabilitation Research and Development*, 45(7):1077–1090, 2008. 11, 60, 66, 73

[64] Patrick Slade, Mykel J. Kochenderfer, Scott L. Delp, and Steven H. Collins. Personalizing exoskeleton assistance while walking in the real world. *Nature*, 610(7931):277–282, 2022. 11, 30, 101

[65] Robert W. Motl, Madeline Weikert, Yoojin Suh, Jacob J. Sosnoff, John Pula, Cristina Soaz, Michaela Schimpl, Christian Lederer, and Martin Daumer. Accuracy of the actibelt ® accelerometer for measuring walking speed in a controlled environment among persons with multiple sclerosis. *Gait and Posture*, 35(2):192–196, 2012. 12, 37

[66] Yanlin Wu, Jennifer L. Petterson, Nick W. Bray, Derek S. Kimmerly, and Myles W. O'Brien. Validity of the activPAL monitor to measure stepping activity and activity intensity: A systematic review. *Gait and Posture*, 97(August):165–173, 2022. 12, 14, 17, 80

[67] Michael V. Potter, Lauro V. Ojeda, Noel C. Perkins, and Stephen M. Cain. Effect of imu design on imu-derived stride metrics for running. *Sensors (Switzerland)*, 19(11), 2019. 12, 18, 41, 56

[68] Ian Cleland, Manhyung Han, Chris Nugent, Hosung Lee, Sally McClean, Shuai Zhang, and Sungyoung Lee. Evaluation of prompted annotation of activity data recorded from a smart phone. *Sensors (Switzerland)*, 14(9):15861–15879, 2014. 12, 77

[69] Yung Ju Chang, Gaurav Paruthi, Hsin Ying Wu, Hsin Yu Lin, and Mark W. Newman. An investigation of using mobile and situated crowdsourcing to collect annotated travel activity data in real-word settings. *International Journal of Human Computer Studies*, 102(November 2016):81–102, 2017. 12, 77

[70] Cormac G. Ryan, P. M. Grant, W. W. Tigbe, and M. H. Granat. The validity and reliability of a novel activity monitor as a measure of walking. *British Journal of Sports Medicine*, 40(9):779–784, 2006. 14, 17, 61, 80

[71] Lauro V. Ojeda, John R. Rebula, Arthur D. Kuo, and Peter G. Adamczyk. Influence of contextual task constraints on preferred stride parameters and their variabilities during human walking. *Medical Engineering and Physics*, 37(10):929–936, 2015. 16

[72] D. W. Grieve and Ruth J. Gear. The relationships between length of stride, step frequency, time of swing and speed of walking for children and adults. *Ergonomics*, 9(5):379–399, 1966. 16, 54, 85

[73] A. D. Kuo. A simple model of bipedal walking predicts the preferred speed-step length relationship. *Journal of Biomechanical Engineering*, 123(3):264–269, 2001. 16, 42, 85

[74] J. M. Brockway. Derivation of formulae used to calculate energy expenditure in man. *Human Nutrition: Clinical Nutrition*, 41(6), 1987. 20

[75] Andy P. Field and Daniel B. Wright. A Primer on Using Multilevel Models in Clinical and Experimental Psychopathology Research. *Journal of Experimental Psychopathology*, 2(2):271–293, 2011. 21, 86

[76] Hirotogu Akaike. Information Theory and an Extension of the Maximum Likelihood Principle. In *Journal of the American Statistical Association*, volume 93, pages 199–213. 1998. 21, 86

[77] Roberto Leo Medrano, Gray Cortright Thomas, and Elliott J. Rouse. Can humans perceive the metabolic benefit provided by augmentative exoskeletons? *Journal of NeuroEngineering and Rehabilitation*, 19(1):1–13, 2022. 31

[78] Talia Y. Moore, Kimberly L. Cooper, Andrew A. Biewener, and Ramanarayan Vasudevan. Unpredictability of escape trajectory explains predator evasion ability and microhabitat preference of desert rodents. *Nature Communications*, 8(1):1–9, 2017. 31

[79] Brian C. Glaister, Greta C. Bernatz, Glenn K. Klute, and Michael S. Orendurff. Video task analysis of turning during activities of daily living. *Gait and Posture*, 25(2):289–294, 2007. 31

[80] L A King, P Carlson-Kuhta, J L Wilhelm, J A Lapidus, M L Dale, L S Talman, N Barlow, M Mancini, and F B Horak. TURN-IT: a novel turning intervention program to improve quality of turning in daily life in people with Parkinson's disease. *BMC neurology*, 22(1):442, 2022. 32

[81] James E. Graham, Glenn V. Ostir, Steven R. Fisher, and Kenneth J. Ottenbacher. Assessing walking speed in clinical research: a systematic review. *Journal of Evaluation in Clinical Practice*, 14(4):552–562, 2008. 32, 36, 60, 93

[82] Michael J. Englesbe, Alisha D. Lussiez, Jeffrey F. Friedman, June A. Sullivan, and Stewart C. Wang. Starting a surgical home. *Annals of Surgery*, 262(6):901–903, 2015. 35

[83] Matteo C. Sattler, Johannes Jaunig, Estelle D. Watson, Mireille N.M. van Poppel, Lidwine B. Mokkink, Caroline B. Terwee, and Pavel Dietz. Physical Activity Questionnaires for Pregnancy: A Systematic Review of Measurement Properties. *Sports Medicine*, 48(10):2317–2346, 2018. 35

[84] Makoto Ayabe, Peter H. Brubaker, Devon Dobrosielski, Henry S. Miller, Akira Kiyonaga, Munehiro Shindo, and Hiroaki Tanaka. Target step count for the secondary prevention of cardiovascular disease. *Circulation Journal*, 72(2):299–303, 2008. 35

[85] Rachel K. Walker, Amanda M. Hickey, and Patty S. Freedson. Advantages and limitations of wearable activity trackers: Considerations for patients and clinicians. *Clinical Journal of Oncology Nursing*, 20(6):606–610, 2016.

[86] Lisa Cadmus-Bertram. Using Fitness Trackers in Clinical Research: What Nurse Practitioners Need to Know. *Journal for Nurse Practitioners*, 13(1):34–40, 2017. 35

[87] Jonathan Afilalo, Sunghee Kim, Sean O'Brien, J. Matthew Brennan, Fred H. Edwards, Michael J. Mack, James B. McClurken, Joseph C. Cleveland, Peter K. Smith, David M. Shahian, and Karen P. Alexander. Gait speed and operative mortality in older adults following cardiac surgery. *JAMA Cardiology*, 1(3):314–321, 2016. 36, 93

[88] Richard W. Bohannon. Comfortable and maximum walking speed of adults aged 20-79 years: Reference values and determinants. *Age and Ageing*, 26(1):15–19, 1997. 36

[89] Young Shin Cho, Seong Ho Jang, Jae Sung Cho, Mi Jung Kim, Hyeok Dong Lee, Sung Young Lee, and Sang Bok Moon. Evaluation of validity and reliability of inertial measurement unit-based gait analysis systems. *Annals of Rehabilitation Medicine*, 42(6):872–883, 2018. 36, 41

[90] Marco Benocci, Laura Rocchi, Elisabetta Farella, Lorenzo Chiari, and Luca Benini. A wireless system for gait and posture analysis based on pressure insoles and inertial measurement units. *2009 3rd International Conference on Pervasive Computing Technologies for Healthcare - Pervasive Health 2009, PCTHealth 2009*, 2009. 37

[91] Lin Shu, Tao Hua, Yangyong Wang, Qiao Li, David Dagan Feng, and Xiaoming Tao. In-shoe plantar pressure measurement and analysis system based on fabric pressure sensing array. *IEEE Transactions on Information Technology in Biomedicine*, 14(3):767–775, 2010. 37

[92] Charlotte L. Edwardson, Elisabeth A.H. Winkler, Danielle H. Bodicoat, Tom Yates, Melanie J. Davies, David W. Dunstan, and Genevieve N. Healy. Considerations when using the activPAL monitor in field-based research with adult populations. *Journal of Sport and Health Science*, 6(2):162–178, 2017. 37, 39

[93] Michaela Schimpl, Christian Lederer, and Martin Daumer. Development and validation of a new method to measure walking speed in free-living environments using the actibelt® platform. *PLoS ONE*, 6(8), 2011. 37, 55

[94] Patima Silsupadol, Kunlanan Teja, and Vipul Lugade. Reliability and validity of a smartphone-based assessment of gait parameters across walking speed and smartphone locations: Body, bag, belt, hand, and pocket. *Gait and Posture*, 58(September):516–522, 2017. 37, 56

[95] Aawesh Shrestha and Myounggyu Won. DeepWalking: Enabling Smartphone-Based Walking Speed Estimation Using Deep Learning. *2018 IEEE Global Communications Conference, GLOBECOM 2018 - Proceedings*, 2018. 37

[96] At L. Hof. Scaling gait data to body size. *Gait and Posture*, 4(3):222–223, 1996. 40, 42, 61, 82, 86

[97] Siddhartha Khandelwal and Nicholas Wickström. Gait Event Detection in Real-World Environment for Long-Term Applications: Incorporating Domain Knowledge Into Time-Frequency Analysis. *IEEE Transactions on Neural Systems and Rehabilitation Engineering*, 24(12):1363–1372, 2016. 41

[98] D.W. Grieve. Gait patterns and the speed of walking. *Bio-medical Engineering*, 3:119–122, 1968. 42

[99] Davide Giavarina. Understanding Bland Altman analysis. *Biochemia Medica*, 25(2):141–151, 2015. 45

[100] L. Lin, A. S. Hedayat, B. Sinha, and M. Yang. Statistical methods in assessing agreement: Models, issues, and tools. *Journal of the American Statistical Association*, 97(457):257–270, 2002. 45

[101] Richard W. Bohannon and Susan S. Glenney. Minimal clinically important difference for change in comfortable gait speed of adults with pathology: A systematic review. *Journal of Evaluation in Clinical Practice*, 20(4):295–300, 2014. 45, 63

[102] Lawrence I-kuei Lin. A Concordance Correlation Coefficient to Evaluate Reproducibility Author (s): Lawrence I-Kuei Lin Published by : International Biometric Society Stable URL : http://www.jstor.org/stable/2532051 REFERENCES Linked references are available on JSTOR for thi. *Biomatrics*, 45(1):255–268, 1989. 45

[103] John E.A. Bertram and Andy Ruina. Multiple walking speed-frequency relations are predicted by constrained optimization. *Journal of Theoretical Biology*, 209(4):445–453, 2001. 54

[104] Lorenzo Chiari, Ugo Della Croce, Alberto Leardini, and Aurelio Cappozzo. Human movement analysis using stereophotogrammetry. Part 2: Instrumental errors. *Gait and Posture*, 21(2):197–211, 2005. 56

[105] Alexandra Pfister, Alexandre M. West, Shaw Bronner, and Jack Adam Noah. Comparative abilities of Microsoft Kinect and Vicon 3D motion capture for gait analysis. *Journal of Medical Engineering and Technology*, 38(5):274–280, 2014. 56

[106] Janusz W. Błaszczyk, Michał Plewa, Joanna Cieślińska-Świder, Bogdan Bacik, Barbara Zahorska-Markiewicz, and Andrzej Markiewicz. Impact of excess body weight on walking at the preferred speed. *Acta Neurobiologiae Experimentalis*, 71(4):528–540, 2011. 58

[107] Joseph A. Jegede, Babatunde O.A. Adegoke, and Oladapo M. Olagbegi. Effects of a Twelve-Week Weight Reduction Exercise Programme on Selected Spatiotemporal Gait Parameters of Obese Individuals. *Journal of Obesity*, 2017, 2017. 58

[108] M. M. Samson, A. Crowe, P. L. de Vreede, J. A.G. Dessens, S. A. Duursma, and H. J.J. Verhaar. Differences in gait parameters at a preferred walking speed in healthy subjects due to age, height and body weight. *Aging Clinical and Experimental Research*, 13(1):16–21, 2001. 58

[109] Atefeh Aboutorabi, Mokhtar Arazpour, Mahmood Bahramizadeh, Stephen William Hutchins, and Reza Fadayevatan. The effect of aging on gait parameters in able-bodied older subjects: a literature review. *Aging Clinical and Experimental Research*, 28(3):393–405, 2016. 58

[110] Kong Y. Chen, Kathleen F. Janz, Weimo Zhu, and Robert J. Brychta. Redefining the roles of sensors in objective physical activity monitoring. *Medicine and Science in Sports and Exercise*, 44(SUPPL. 1):13–23, 2012. 58

[111] Paola Tamburini, Fabio Storm, Chris Buckley, Maria Cristina Bisi, Rita Stagni, and Claudia Mazzà. Moving from laboratory to real life conditions: Influence on the assessment of variability and stability of gait. *Gait and Posture*, 59(October 2017):248–252, 2018. 60

[112] Ralph Jasper Mobbs, Jordan Perring, Suresh Mahendra Raj, Monish Maharaj, Nicole Kah Mun Yoong, Luke Wicent Sy, Rannulu Dineth Fonseka, Pragadesh Natarajan, and Wen Jie Choy. Gait metrics analysis utilizing single-point inertial measurement units: a systematic review. *mHealth*, 8:0–2, 2022. 60

[113] Gillian Barry, Brook Galna, Sue Lord, Lynn Rochester, and Alan Godfrey. Defining ambulatory bouts in free-living activity: Impact of brief stationary periods on bout metrics. *Gait and Posture*, 42(4):594–597, 2015. 62

[114] Lauren C. Benson, Christian A. Clermont, Sean T. Osis, Dylan Kobsar, and Reed Ferber. Classifying running speed conditions using a single wearable sensor: Optimal segmentation and feature extraction methods. *Journal of Biomechanics*, 71:94–99, 2018. 62, 111

[115] Michael O. Leavitt. 2008 Physical Activity Guidelines for Americans. *Health (San Francisco)*, 2008. 63, 99

[116] Mary J. Lindstrom and Douglas M. Bates. Newton—Raphson and EM algorithms for linear mixed-effects models for repeated-measures data. *Journal of the American Statistical Association*, 83(404):1014–1022, 1988. 64

[117] Richard W. Bohannon and A. Williams Andrews. Normal walking speed: A descriptive meta-analysis. *Physiotherapy*, 97(3):182–189, 2011. 66, 73

[118] Stephanie Studenski. Gait Speed and Survival in Older Adults. *JAMA*, 305(1):50, jan 2011. 72

[119] Michaela Schimpl, Carmel Moore, Christian Lederer, Anneke Neuhaus, Jennifer Sambrook, John Danesh, Willem Ouwehand, and Martin Daumer. Association between walking speed and age in healthy, free-living individuals using mobile accelerometry-a cross-sectional study. *PLoS ONE*, 6(8), 2011. 73

[120] Manoj Srinivasan. Optimal speeds for walking and running, and walking on a moving walkway. *Chaos*, 19(2), 2009. 73

[121] Amanda E Paluch, Shivangi Bajpai, David R Bassett, Mercedes R Carnethon, Ulf Ekelund, Kelly R Evenson, Deborah A Galuska, Barbara J Jefferis, William E Kraus, I-Min Lee, Charles E Matthews, John D Omura, Alpa V Patel, Carl F Pieper, Erika Rees-Punia, Dhayana Dallmeier, Jochen Klenk, Peter H Whincup, Erin E Dooley, Kelley Pettee Gabriel, Priya Palta, Lisa A Pompeii, Ariel Chernofsky, Martin G Larson, Ramachandran S Vasan, Nicole Spartano, Marcel Ballin, Peter Nordström, Anna Nordström, Sigmund A Anderssen, Bjørge H Hansen, Jennifer A Cochrane, Terence Dwyer, Jing Wang, Luigi Ferrucci, Fangyu Liu, Jennifer Schrack, Jacek Urbanek, Pedro F Saint-Maurice, Naofumi Yamamoto, Yutaka Yoshitake, Robert L Newton, Shengping Yang, Eric J Shiroma, and Janet E Fulton. Daily steps and all-cause mortality: a meta-analysis of 15 international cohorts. *The Lancet Public Health*, 7(3):e219–e228, 2022. 73

[122] E. Ramanujam, Thinagaran Perumal, and S. Padmavathi. Human Activity Recognition With Smartphone and Wearable Sensors Using Deep Learning Techniques: A Review. *IEEE Sensors Journal*, 21(12):13029–13040, jun 2021. 76

[123] Ong Chin Ann and Lau Bee Theng. Human activity recognition: A review. *Proceedings - 4th IEEE International Conference on Control System, Computing and Engineering, ICCSCE 2014*, (November):389–393, 2014.

[124] Michalis Vrigkas, Christophoros Nikou, and Ioannis A. Kakadiaris. A review of human activity recognition methods. *Frontiers Robotics AI*, 2(NOV):1–28, 2015.

[125] Song Mi Lee, Sang Min Yoon, and Heeryon Cho. Human activity recognition from accelerometer data using Convolutional Neural Network. *2017 IEEE International Conference on Big Data and Smart Computing, BigComp 2017*, pages 131–134, 2017.

[126] Mark V. Albert, Santiago Toledo, Mark Shapiro, and Konrad Kording. Using mobile phones for activity recognition in Parkinson's patients. *Frontiers in Neurology*, NOV(November):1–7, 2012. 76

[127] Erica Twardzik, Kate Duchowny, Amby Gallagher, Neil Alexander, Debra Strasburg, Natalie Colabianchi, and Philippa Clarke. What features of the built environment matter most for mobility? Using wearable sensors to capture real-time outdoor environment demand on gait performance. *Gait and Posture*, 68(September 2018):437–442, 2019. 77

[128] Erica Twardzik, Philippa J. Clarke, Lynda L. Lisabeth, Susan H. Brown, Steven P. Hooker, Suzanne E. Judd, and Natalie Colabianchi. The Relationship Between Environmental Exposures and Post-Stroke Physical Activity. *American Journal of Preventive Medicine*, 63(2):251–261, 2022. 77

[129] Johannes Michalak, Nikolaus F. Troje, Julia Fischer, Patrick Vollmar, Thomas Heidenreich, and Dietmar Schulte. Embodiment of sadness and depression-gait patterns associated with dysphoric mood. *Psychosomatic Medicine*, 71(5):580–587, 2009. 77, 100

[130] Duncan S. Procter, Angie S. Page, Ashley R. Cooper, Claire M. Nightingale, Bina Ram, Alicja R. Rudnicka, Peter H. Whincup, Christelle Clary, Daniel Lewis, Steven Cummins, Anne Ellaway, Billie Giles-Corti, Derek G. Cook, and Christopher G. Owen. An open-source tool to identify active travel from hip-worn accelerometer, GPS and GIS data. *International Journal of Behavioral Nutrition and Physical Activity*, 15(1):1–10, 2018. 77

[131] Ruben Brondeel, Bruno Pannier, and Basile Chaix. Using GPS, GIS, and Accelerometer Data to Predict Transportation Modes. *Medicine and Science in Sports and Exercise*, 47(12):2669–2675, 2015.

[132] Katarzyna Siła-Nowicka, Jan Vandrol, Taylor Oshan, Jed A. Long, Urška Demšar, and A. Stewart Fotheringham. Analysis of human mobility patterns from GPS trajectories and contextual information. *International Journal of Geographical Information Science*, 30(5):881–906, 2016. 77

[133] Corinna Cortes and Vladimir Vapnik. Support-vector networks. *Machine Learning*, 20(3):273–297, sep 1995. 83

[134] Leo Breiman. Random Forests. *Machine Learning*, 45:5–32, 2001. 83

[135] Cha Zhang and Yunqian Ma. *Ensemble machine learning: Methods and applications*. 2012. 83

[136] A. Pedregosa, F. , Varoquaux, G. , Gramfort, A. , Michel, V., Thirion, B. , Grisel, O. , Blondel, M., Prettenhofer, P., Weiss, R. , Dubourg, V. , Vanderplas, J. , Passos, M. Cournapeau, D. , Brucher, M. , Perrot, and E. Duchesnay. Scikit-learn: Machine Learning in Python. *Journal of Machine Learning Research*, 12:2825–2830, 2011. 83

[137] José Pinheiro, Douglas Bates, and R Core Team. nlme: Nonlinear Mixed Effects Models. 2022. 86

[138] Marta Karas, Jacek K. Urbanek, Vittorio P. Illiano, Guy Bogaarts, Ciprian M. Crainiceanu, and Jonas F. Dorn. Estimation of free-living walking cadence from wrist-worn sensor accelerometry data and its association with SF-36 quality of life scores. *Physiological Measurement*, 42(6), 2021. 93

[139] Anisoara Paraschiv-Ionescu, Christopher J. Newman, Lena Carcreff, Corinna N. Gerber, Stephane Armand, and Kamiar Aminian. Correction: Locomotion and cadence detection using a single trunk-fixed accelerometer: Validity for children with cerebral palsy in daily

life-like conditions (Journal of NeuroEngineering and Rehabilitation DOI: 10.1186/s12984-019-0494-z). *Journal of NeuroEngineering and Rehabilitation*, 16(1):1–11, 2019.

[140] Benedikt Fasel, Cyntia Duc, Farzin Dadashi, Flavien Bardyn, Martin Savary, Pierre André Farine, and Kamiar Aminian. A wrist sensor and algorithm to determine instantaneous walking cadence and speed in daily life walking. *Medical and Biological Engineering and Computing*, 55(10):1773–1785, 2017. 93

[141] Elaine M. Murtagh, Jacqueline L. Mair, Elroy Aguiar, Catrine Tudor-Locke, and Marie H. Murphy. Outdoor Walking Speeds of Apparently Healthy Adults: A Systematic Review and Meta-analysis. *Sports Medicine*, 51(1):125–141, 2021. 94

[142] Kleverton Krinski, Daniel G.S. Machado, Luciana S. Lirani, Sergio G. DaSilva, Eduardo C. Costa, Sarah J. Hardcastle, and Hassan M. Elsangedy. Let's walk outdoors! self-paced walking outdoors improves future intention to exercise in women with obesity. *Journal of Sport and Exercise Psychology*, 39(2):145–157, 2017.

[143] Kathleen Fuegen and Kimberly H. Breitenbecher. Walking and being outdoors in nature increase positive affect and energy. *Ecopsychology*, 10(1):14–25, 2018. 94

[144] Krishnaji Parvataneni, Leone Ploeg, Sandra J. Olney, and Brenda Brouwer. Kinematic, kinetic and metabolic parameters of treadmill versus overground walking in healthy older adults. *Clinical Biomechanics*, 24(1):95–100, 2009. 104

[145] Pamela A. Macfarlane and Marilyn A. Looney. Walkway length determination for steady state walking in young and older adults. *Research Quarterly for Exercise and Sport*, 79(2):261–267, 2008. 104, 106

[146] Gerda Strutzenberger, Lisa Claußen, and Hermann Schwameder. Analysis of sloped gait: How many steps are needed to reach steady-state walking speed after gait initiation? *Gait and Posture*, 83:167–173, 2021.

[147] U. Lindemann, B. Najafi, W. Zijlstra, K. Hauer, R. Muche, C. Becker, and K. Aminian. Distance to achieve steady state walking speed in frail elderly persons. *Gait and Posture*, 27(1):91–96, 2008. 104

[148] Ervin Sejdic, Kristin A. Lowry, Jennica Bellanca, Mark S. Redfern, and Jennifer S. Brach. A Comprehensive Assessment of Gait Accelerometry Signals in Time, Frequency and Time-Frequency Domains. *IEEE Transactions on Neural Systems and Rehabilitation Engineering*, 22(3):603–612, may 2014. 111